Journal of Computer Networks and Communications

Trends and Applications for Cognitive Radio

Guest Editors: Enrico Del Re, Torleiv Maseng, and Luca Simone Ronga

Trends and Applications for Cognitive Radio

Journal of Computer Networks and Communications

Trends and Applications for Cognitive Radio

Guest Editors: Enrico Del Re, Torleiv Maseng,
and Luca Simone Ronga

Editorial Board

Contents

Hindawi Publishing Corporation
Journal of Computer Networks and Communications
Volume 2012, Article ID 643604, 2 pages
doi:10.1155/2012/643604

Editorial
Trends and Applications for Cognitive Radio

Enrico Del Re,[1] Torleiv Maseng,[2] and Luca Simone Ronga[3]

[1] *Department of Electronics and Telecommunications, University of Florence, Via di Santa Marta 3, 50139 Florence, Italy*
[2] *Forsvarets Forskningsinstitutt, P.O. Box 25, 2027 Kjeller, Norway*
[3] *Italian National Consortium for Telecommunications (CNIT), Via di Santa Marta 3, 50139 Firenze, Italy*

Correspondence should be addressed to Enrico Del Re, enrico.delre@cnit.it

Received 27 July 2012; Accepted 27 July 2012

After a decade of cognitive radio, it is time to check the level of maturity and the real gains attained by this technology. Born with many expectations, which is the real status of its deployment? From one side a sensible slowing down of the standardization process is perceived, probably due to economical reasons rather than technical issues. On the other side the demand of spectral efficiency for boosting performances lowering energy consumption is rapidly increasing. The feeling is that the latter driver prevails against the former, and this is proven by an increased scientific and industrial interest on efficient CR solutions.

The special issue describes some of the most relevant technological trends and promising applications of the CR idea.

The paper entitled "*The SS-SCR scheme for dynamic spectrum access*" describes an interesting connection between a sense-based resource allocation and a cooperation scheme for a multihop, multichannel, and multi PU cognitive environment. The scheme can be implemented in a cloud-computing environment, relevant to a consolidated technological trend for future urban deployments.

The paper entitled "*Cognitive code-division channelization with admission control*" combines a resource allocation strategy with an admission control procedure, revealing all the inner complexity this process owns. The proposed solution is interesting also for its energy efficiency, proving that a satisfactory compromise between efficiency and performance is one of the achievements of CR.

The paper entitled "*Optimizing cooperative cognitive radio networks with opportunistic access*" deeply explores the adoption of cooperation for opportunistic radio access. Several configurations of relays and direct accesses are studied and compared, giving a complete view of the capability of the cooperative paradigm.

The paper entitled "*Optimal pricing of spectrum resources in wireless opportunistic access*" represents here a wide class of relevant studies for CR, that is, the adoption of Game Theory to model the selfish behavior of secondary nodes only partially aware of the complete spectral environment. The paper provides an in-depth study of the advantages of the taxation of used resources in terms of local and global throughput.

The paper entitled "*Hybrid experiential-heuristic cognitive radio engine architecture and implementation*" implements the resources decision process by integrating the two main approaches, an heuristic one with a learning-based one. The resulting scheme is studied and experimented on a real HW platform to prove its capabilities in terms of flexibility and spectral efficiency.

The paper entitled "*On spectrum sensing for TV white space in china*" enters the details of a possible exploitation of TV white spaces. The paper reports an experimental HW implementation of the spectrum sensing module for the Chinese context, revealing the global applicability of TVWS concept.

The paper entitled "*Cognitive scout node for communication in disaster scenarios*" presents an interesting application of CR in emergency scenarios. The proposal is based on a scout node with two main functions: the establishment of a detailed radio spectrum map in the theatre of operations and a cooperative base-station aiding the primary network during emergency.

The selected papers show recent theoretical advances toward CR adoption, but also real experimental setups that prove the high degree of maturity of this technology for mass

deployment. The negative energy balance due to increased complexity in the CR receivers is compensated by the improved spectral efficiency attained by recent CR schemes.

Enrico Del Re
Torleiv Maseng
Luca Simone Ronga

Hindawi Publishing Corporation
Journal of Computer Networks and Communications
Volume 2012, Article ID 510942, 9 pages
doi:10.1155/2012/510942

Research Article

Cognitive Code-Division Channelization with Admission Control

Kanke Gao,[1] Onur Ozdemir,[2] Dimitris A. Pados,[1] Stella N. Batalama,[1] Tommaso Melodia,[1] and Andrew L. Drozd[2]

[1] *Department of Electrical Engineering, The State University of New York at Buffalo, Buffalo, NY 14260, USA*
[2] *ANDRO Computational Solutions, 7902 Turin Road Bldg. 2, Rome, NY 13440, USA*

Correspondence should be addressed to Kanke Gao, kgao@buffalo.edu

Received 14 February 2012; Revised 9 May 2012; Accepted 9 May 2012

Academic Editor: Enrico Del Re

We consider the problem of joint resource allocation and admission control in a secondary code-division network coexisting with a narrowband primary system. Our objective is to find the maximum number of admitted secondary links and then find the optimal transmitting powers and code sequences of those secondary links such that the total energy consumption of the secondary network is minimized subject to the conditions that primary interference temperature constraints, secondary signal-to-interference-plus-noise ratio (SINR) constraints and secondary peak power constraints are all satisfied. This is an NP-hard optimization problem which motivates the development of suboptimal algorithms. We propose a novel iterative algorithm to solve this problem in a computationally efficient manner. Numerical results demonstrate that the proposed algorithm provides excellent solutions that result in high energy efficiency and large admitted percentage of secondary links.

1. Introduction

With the explosive demand in wireless service in recent years, radio spectrum has become the scarcest resource for the modern wireless communication industry. Therefore, both spectrum regulation makers and wireless technology specialists endeavor to seek solutions that would increase the amount of available frequency spectrum. With the FCC's report that much of the licensed radio spectrum is highly underutilized [1], the concept of *cognitive radio* was proposed as a solution to the spectrum scarcity problem, where secondary (unlicensed) users can opportunistically access the licensed spectrum provided that they do not cause any "harmful" interference to the primary (licensed) network. From the realization point of view, cognitive radio networking can be realized using two approaches: underlay and overlay [2]. Conventional cognitive radio proposals utilize the overlay approach where secondary users (SUs) detect *spectrum holes* (frequency bands not used by primary users) by sensing the whole spectrum and then transmit over them. In contrast, under the underlay approach, SUs can coexist with the primary users (PUs) as long as interference from SUs does not exceed the tolerable *interference temperature* at the primary receivers. Spread spectrum technology has been proposed as the most promising technology to maximize frequency reuse by exploiting the underlay approach [3]. Spread spectrum technology allows cognitive code-division users to coexist in parallel in frequency and time with primary users. The major challenge is to admit the maximum number of secondary users to access the spectrum and efficiently allocate power and signature to each secondary user.

Admission control and resource allocation problem can be traced back to the 90's. In [4, 5], Foschini and Miljanic proposed a distributed asynchronous power control algorithm under predefined signal-to-interference-plus-noise constraints in conventional cellular systems, which converges to the optimal power allocation solution that minimizes the total transmission power. Furthermore, a distributed power control problem under user-specific signal-to-interference-plus-noise ratio (SINR) and power budget constraints was considered in [6], where distributed constrained power control (DCPC) and asynchronous distributed constrained power control (ADCPC) schemes were developed to maximize the minimum SINR of all users under synchronous and asynchronous power updates, respectively. In [7, 8], admission control problem was studied, and a number of single

or multiple transmitter removal algorithms were reported. Among them, stepwise maximum interference removal algorithm (SMIRA) is the most effective one resulting in the smallest outage probability. Recently, interesting research works on admission and power control under the framework of cognitive code-division networks were reported in [9–11]. A centralized algorithm combining geometric programming and tree-pruning method [9] was presented to allow secondary users to share the spectrum under secondary quality of service (QoS) constraints and a primary interference temperature constraint. In [10], a gradient descent algorithm was proposed to solve admission control and power allocation jointly. More recently, in [11], a spectrum underlay cognitive radio network (CRN) was considered, and a low-complexity suboptimal algorithm named interference constraint-aware SMIRA (I-SMIRA) was proposed to maximize the number of admitted SUs. In all the above literature of cognitive code-division networks, no optimization was carried out with respect to code channels (signatures) of secondary users. In contrast, code design for secondary code-division links was considered in [12–14], where SUs coexist with a wideband primary code-division multiple access (CDMA) system. In [12], a single secondary code-divison link is designed such that it achieves the maximum SINR subject to primary SINR requirements [12]. The extension to the design of multiple secondary code-division links is studied in [13, 14]. In practice, there exist many scenarios where the primary (legacy) users communicate with modulated narrowband signals. Under these scenarios, the design of secondary underlay code-division links still remains an open problem.

To the best of our knowledge, this paper presents the first research work on the problem of establishing secondary code-division links coexisting with a primary narrowband system. Since the wideband transmissions of secondary users generally experience multipath fading, the RAKE matched filter is utilized at the secondary receivers (SRs). Our objective is to maximize the number of admitted secondary links and minimize the total power consumption of active secondary links under the following constraints: (1) SINR constraints at secondary RAKE receivers, (2) interference constraints at the primary receivers (PRs), and (3) peak transmission power constraints at secondary transmitters (STs). This optimization problem is an NP-hard problem, which motivates the development of efficient suboptimal algorithms that provide good solutions. We propose an iterative algorithm to solve this problem which produces a suboptimal solution with excellent cognitive networking performance characteristics in terms of the number of admitted SUs and network energy consumption. We provide numerical results to demonstrate that our proposed algorithm outperforms existing signature design and admission control algorithms previously proposed in the literature.

1.1. Contributions. Within this context, our main contributions in this paper can be outlined as the following.

(i) *Uncoordinated Code-Division Spectrum Management.* Unlike traditional frequency division operations, we consider multiple secondary wideband code-division links coexisting with a primary narrowband system, a scenario which has not been previously addressed.

(ii) *Joint Power and Code-Channel Allocation.* Our optimization framework incorporates code sequence design as an additional optimization dimension/resource. This additional dimension is expected to improve spectrum utilization compared to conventional power optimization approaches considered in [6, 9–11].

(iii) *New Removal Criterion.* For the admission control problem, we define a new metric that aggregates only the effective violation (both primary interference and secondary SINR violation) from STs, which is different from and more effective than the one proposed in [11].

The rest of the paper is organized as follows. We present the cognitive code-division network model and formulate the admission control and resource allocation problem in Section 2. The proposed iterative algorithm is described in detail in Section 3. We provide computational complexity analysis in Section 4. In Section 5, simulation results are presented to demonstrate the performance of our proposed algorithm. Concluding remarks are presented in Section 6.

2. System Model and Problem Statement

We consider a primary narrowband system where each primary user holds the license for one of N subbands of the spectrum. We assume that K of N primary users, $1 \leq K \leq N$, are active to transmit from primary transmitters PT_j to primary receivers PR_j, $j = 1, 2, \ldots, K$ in each time slot. A secondary network with M requesting links between secondary transmitters ST_i and secondary receivers SR_i, $i = 1, 2, \ldots, M$, shares the spectrum with the primary system in a spectrum underlay manner. For notational convenience, we number each secondary and primary transmitter-receiver pair by the indices $i \in \mathcal{M} \triangleq \{1, \ldots, M\}$ and $j \in \mathcal{K} \triangleq \{1, \ldots, K\}$, respectively, and refer to them as users. All secondary users are equipped with spread spectrum devices and are expected to simultaneously communicate over the whole spectrum without causing any harmful interference to primary users. Due to the dispersion characteristics of the wireless channel, secondary wideband spread spectrum signals with processing gain L are assumed to propagate over multipath (frequency-selective) fading channels with R resolvable paths.

After carrier demodulation, chip-matched filtering and sampling at the chip rate over the duration of a multipath extended symbol (bit) period of $L + R - 1$ chips, the received signal at SR_i can be represented as

$$\mathbf{r}_i = \sum_{m=1}^{M} \sqrt{E_m} b_m \mathbf{H}_{i,m} \mathbf{s}_m + \mathbf{i}_i + \mathbf{n}, \tag{1}$$

where $E_m > 0$ is the bit energy, $b_m \in \{\pm 1\}$ is the information bit, and $\mathbf{s}_m \in \mathbb{R}^L$ ($\|\mathbf{s}_m\| = 1$) is the normalized signature

vector of secondary link m, $m \in \mathcal{M}$; $\mathbf{i}_i$ represents interference induced by all active PUs; $\mathbf{n}$ is additive white Gaussian noise (AWGN) at SR_i with mean $\mathbf{0}$ and covariance $\xi^2\mathbf{I}$. In (1), $\mathbf{H}_{i,m}$ is the multipath channel matrix from ST_m to SR_i given in the form of

$$\mathbf{H}_{i,m} \triangleq \begin{bmatrix} h_{i,m}^{(1)} & 0 & \cdots & 0 \\ h_{i,m}^{(2)} & h_{i,m}^{(1)} & \cdots & 0 \\ \vdots & \vdots & & \vdots \\ h_{i,m}^{(R)} & h_{i,m}^{(R-1)} & \cdots & h_{i,m}^{(1)} \\ 0 & h_{i,m}^{(R)} & \cdots & h_{i,m}^{(2)} \\ \vdots & \vdots & & \vdots \\ 0 & 0 & \cdots & h_{i,m}^{(R)} \end{bmatrix}_{L+R-1\times L}, \tag{2}$$

where $h_{i,m}^{(r)}$ represents rth resolvable path coefficient modeled as a Rayleigh-distributed random variable. In order to exploit the multipath diversity, we assume that each SR uses a normalized RAKE-matched filter that collects the signal energy from all the received signal paths for the user of interest, that is,

$$\mathbf{w}_{R-MF,i} = \frac{\mathbf{H}_{i,i}\mathbf{s}_i}{||\mathbf{H}_{i,i}\mathbf{s}_i||}. \tag{3}$$

The receiver in this manner achieves the performance of an Rth order diversity communications system. The output of the RAKE filter is given by

$$y_i = \frac{\sqrt{E_i}\mathbf{s}_i^T\mathbf{H}_{i,i}^T\mathbf{H}_{i,i}\mathbf{s}_i b_i}{||\mathbf{H}_{i,i}\mathbf{s}_i||} + \sum_{m=1,m\neq i}^{M} \frac{\sqrt{E_m}\mathbf{s}_i^T\mathbf{H}_{i,i}^T\mathbf{H}_{i,m}\mathbf{s}_m b_m}{||\mathbf{H}_{i,i}\mathbf{s}_i||} + \widetilde{n}, \tag{4}$$

where $\widetilde{n}$ is the "despread" signal of the narrowband primary interference plus noise, which can be seen as zero-mean AWGN with variance σ^2 [15]. The assumption of AWGN is due to the fact that after despread processing, the power of narrowband primary interference is evenly spread across the broad band of secondary spread spectrum system. The output SINR of the filter $\mathbf{w}_{R-MF,i}$ can be calculated as

$$\begin{aligned} \mathrm{SINR}_i &= \frac{E_i\left(\mathbf{s}_i^T\mathbf{H}_{i,i}^T\mathbf{H}_{i,i}\mathbf{s}_i\right)}{\sum_{m=1,m\neq i}^{M} E_m\left(\left|\mathbf{s}_i^T\mathbf{H}_{i,i}^T\mathbf{H}_{i,m}\mathbf{s}_m\right|^2/||\mathbf{H}_{i,i}\mathbf{s}_i||^2\right)+\sigma^2} \\ &= \frac{\widetilde{E}_i}{\sum_{m=1}^{M}\widetilde{E_m}A_{i,m}+\sigma^2}, \end{aligned} \tag{5}$$

where $\widetilde{E}_i \triangleq E_i||\mathbf{H}_{i,i}\mathbf{s}_i||^2$ denotes the received bit energy at SR_i after its receiver filter and

$$A_{i,m} = \begin{cases} \dfrac{\left|\mathbf{s}_i^T\mathbf{H}_{i,i}^T\mathbf{H}_{i,m}\mathbf{s}_m\right|^2}{||\mathbf{H}_{i,i}\mathbf{s}_i||^2||\mathbf{H}_{m,m}\mathbf{s}_m||^2}, & i\neq m, \\ 0, & i=m. \end{cases} \tag{6}$$

At the primary narrowband receivers, secondary spread spectrum signals are seen as white noise at each licensed narrowband with constant spectral densities [15]. They are also assumed to experience flat fading on each licensed narrow band. In the spirit of cognitive radio, causing no harmful interference can be evaluated by a metric called *interference temperature*, which is defined to be the interference from all SUs measured at PRs.

Here, we consider joint maximization of the number of admitted SUs and minimization of total energy consumption in the secondary cognitive radio network (CRN). The objective is to find a joint admission control and resource (i.e., power and signature) allocation scheme that maximizes the number of SUs accessing the spectrum and minimizes the total energy consumption. Minimizing total network energy is an important problem especially when the network has a constraint on the interference it can cause to other neighboring networks. Since our goal is to admit as many users as possible and minimize the energy consumption of the network, we initially formulate the problem as a multiobjective optimization problem with three sets of constraints: (1) SINR constraints at the SRs, (2) interference temperature constraints at PRs, and (3) power budget constraints at the STs. We can now formulate problem, referred to as P, as follows:

$$\text{Find} \quad \mathbf{E}, \mathbf{S}$$

$$\text{Maximize } \{||\mathbf{E}||_0\}, \qquad \left\{-\sum_{m=1}^{M} E_m\right\} \tag{7}$$

$$\text{Subject to} \quad \sum_{i=1}^{M} g_{j,i}E_i \leq I_j, \quad \forall j \in \mathcal{K}, \tag{8}$$

$$\mathrm{SINR}_i \geq \mathbf{I}(E_i)\gamma, \quad \forall i \in \mathcal{M}, \tag{9}$$

$$0 < E_i < E_{\max}, \quad \forall i \in \mathcal{M}. \tag{10}$$

In P, $\mathbf{S} \triangleq [\mathbf{s}_1, \mathbf{s}_2, \ldots, \mathbf{s}_M]$, $\mathbf{E} \triangleq [E_1, \mathbf{s}_2, \ldots, E_M]$, $||\mathbf{E}||_0$ is the zero norm of $\mathbf{E}$ which denotes the number of admitted users, $\mathbf{I}(\cdot)$ is the indicator function for positive real numbers $\mathbb{R}_+$, and $g_{j,i}$ is the path coefficient from ST_i to PR_j. Inequality (8) represents a set of K interference temperature constraints for the PUs. Inequality (9) represents a set of M SINR constraints for the SUs. The SU i will transmit, if and only if the SINR of that link is greater than or equal to the threshold SINR. If the link is not active, that is, if the user is not admitted, the SINR constraint is automatically satisfied.

The problem P is a multiobjective optimization problem (MOP) for which the solution space is represented by a set of Pareto optimal (trade-off) solutions (non-dominated by any other solution) between the two objectives [16]. One technique for solving MOPs is to maximize a (normalized) weighted sum of the objectives where a larger weight represents the objective with higher importance (or priority). However, in our problem, the two objective functions are of different nature, that is, the number of users can only take integer values whereas the total energy can take real values, hence a weighted objective will not be well defined. There are

other techniques in the literature to solve MOPs such as evolutionary algorithms [17], but they may be computationally expensive and are not the focus of this work. Our goal in this work is not to find a set of Pareto optimal solutions. Instead, similar to the weighted objective approach, we prioritize our objectives. Let us consider a scenario where the priority is to minimize the energy consumption of the network. Let $\mathcal{S} \triangleq \{(O_1, O_2) | O_1 \in \mathbb{N}, O_2 \in \mathbb{R}_-\}$ denote the set of objective value pairs corresponding to Pareto optimal solutions obtained by solving P. It is easy to see that $(0,0)$ is a trivial Pareto optimal objective pair, that is, $(0,0) \in \mathcal{S}$, since it corresponds to zero (minimum) energy consumption in the network. However, our main goal here is to find a solution that corresponds to a large number of admitted SUs that consume the minimum energy possible. In other words, we assign the first objective in (7) higher importance over the other. Therefore, we divide the problem P into two separate single objective optimization problems and solve them in an iterative manner until convergence is obtained. In the next section and subsections therein, we provide the details of our proposed admission control and resource allocation algorithm.

3. Proposed Admission Control and Resource Allocation Algorithm

Since the objective corresponding to the number of admitted users has higher priority, we start the problem by assuming that all M requesting secondary links are supported. (A set of secondary links is supported if and only if there exists at least one nontrivial (i.e., power greater than zero) resource allocation solution such that all corresponding constraints in (9)-(10) are satisfied.) In this case, the problem is a single-objective joint power and signature allocation problem. Note that this first problem may or may not admit any feasible solutions. After the first problem is attempted to be solved, we define a new single-objective optimization problem for admission control. This second problem is solved only if the previously obtained power and signature allocation solution viloates the constraints of P or if there is no feasible solution to the first problem. We explain the details of our approach in the next subsections.

3.1. Joint Power and Code-Channel Allocation. Under the assumption that there are M SUs that are supported, let P1 denote the new single-objective optimization problem formulated as

$$\begin{aligned} &\text{Find} && \mathbf{E}, \mathbf{S} \\ &\text{Minimize} && \sum_{m=1}^{M} E_m \\ &\text{Subject to} && \text{Constraints in (9) and (10).} \end{aligned} \tag{11}$$

We note that P1 is a nonconvex optimization problem. Our approach in solving P1 starts with optimizing the secondary signature set assuming that the energy associated with each SU, that is, $\mathbf{E}$ is fixed and unknown. The signature set optimization does not require the knowledge of $\mathbf{E}$. We notice that the secondary SINR constraints in (9) can be equivalently written in the form of

$$(\mathbf{I} - \gamma \mathbf{A})\widetilde{\mathbf{E}} \geq \mathbf{b}, \tag{12}$$

where $\mathbf{b} \triangleq \gamma\sigma^2\mathbf{1}$, $\widetilde{\mathbf{E}} = [\widetilde{E_1}, \widetilde{E_2}, \ldots, \widetilde{E_M}]^T$, and $\mathbf{A}$ is the matrix of entries $A_{i,j}$ defined in (6), $i, j \in \mathcal{M}$. By the Perron-Frobenius theorem [18], it is well known that there exists a positive vector $\widetilde{\mathbf{E}} > \mathbf{0}$ such that (12) is satisfied with equality if and only if $\rho(\mathbf{A}) < 1/\gamma$, where $\rho(\mathbf{A})$ is the Perron root of $\mathbf{A}$. Note that $\rho(\mathbf{A})$ is an implicit function of secondary signature set $\mathbf{S}$. For a given $\rho(\mathbf{A}) < 1/\gamma$, when (12) is satisfied with equality, it means that the system is using the lowest energy $\widetilde{\mathbf{E}} > \mathbf{0}$ possible to satisfy its SINR constraint. Moreover, smaller $\rho(\mathbf{A})$ means that the system can support a higher SINR requirement. Therefore, intuitively, if we minimize $\rho(\mathbf{A})$, we provide more room to further reduce $\widetilde{\mathbf{E}}$ to satisfy the given SINR requirement in (12) with equality. Therefore, the signature set $\mathbf{S}$ can be optimized to minimize $\rho(\mathbf{A})$ to maximize the energy efficiency of the secondary network. Now, we explain our optimization approach as follows. We note that it is difficult to minimize $\rho(\mathbf{A})$ directly. However, from matrix theory on induced norm, we can write the following:

$$\frac{1}{\sqrt{M}}\sum_{i,j} A_{i,j} \leq \rho(\mathbf{A}) \leq \max_i \sum_j A_{i,j} \leq \sum_{i,j} A_{i,j}. \tag{13}$$

Based on the fact that $\rho(\mathbf{A})$ is lower and upper bounded by multiples of $\sum_{i,j} A_{i,j}$, we define a new cost function $J \triangleq \sum_{i,j} A_{i,j}$ and we optimize the secondary signature by minimizing J using a block coordinate descent algorithm, that is, by iteratively updating one secondary signature at a time. Although J is not a tight bound for $\rho(\mathbf{A})$ in general, it is utilized here for two reasons: (1) minimization of J can be carried out in a tractable manner, (2) the solutions obtained by minimizing J provide good solutions (in fact better solutions than the ones proposed in the literature) as shown by numerical results in Section 5. The signature for secondary link i that minimizes J is given by

$$\mathbf{s}_i^* = \arg\min_{\mathbf{s}_i} \frac{\mathbf{s}_i^T \mathbf{Q}_i \mathbf{s}_i}{\left\|\mathbf{H}_{i,i}\mathbf{s}_i\right\|^2} + \widetilde{Q}_i, \tag{14}$$

where $\widetilde{Q}_i = \sum_{j \neq i} \sum_{m \neq i} A_{j,m}$ and

$$\begin{aligned} \mathbf{Q}_i \triangleq \mathbf{H}_{i,i}^T &\left(\sum_{j \neq i} \frac{\mathbf{H}_{i,j}\mathbf{s}_j\mathbf{s}_j^T\mathbf{H}_{i,j}^T}{\left\|\mathbf{H}_{j,j}\mathbf{s}_j\right\|^2} \right) \mathbf{H}_{i,i} \\ &+ \sum_{m \neq i} \frac{\mathbf{H}_{m,i}^T\mathbf{H}_{m,m}\mathbf{s}_m\mathbf{s}_m^T\mathbf{H}_{m,m}^T\mathbf{H}_{m,i}}{\left\|\mathbf{H}_{m,m}\mathbf{s}_m\right\|^2}. \end{aligned} \tag{15}$$

Let $\mathbf{z} \triangleq \mathbf{\Lambda}^{1/2}\mathbf{U}^T\mathbf{s}_i$ where $\mathbf{U}$ and $\mathbf{\Lambda}$ denote eigenvector matrix and diagonal eigenvalue matrix of $\mathbf{H}_{i,i}^T\mathbf{H}_{i,i}$, respectively. If we treat other secondary signatures as fixed parameters, then the optimization (14) takes the equivalent form

$$\mathbf{z}^* = \arg\min_{\mathbf{z}} \frac{\mathbf{z}^T\mathbf{\Lambda}^{-1/2}\mathbf{U}^T\mathbf{Q}_i\mathbf{U}\mathbf{\Lambda}^{-1/2}\mathbf{z}}{\mathbf{z}^T\mathbf{z}}. \tag{16}$$

It is well known that the optimal solution $\mathbf{z}^*$ is the eigenvector of $\mathbf{\Lambda}^{-1/2}\mathbf{U}^T\mathbf{Q}_i\mathbf{U}\mathbf{\Lambda}^{-1/2}$ with minimum eigenvalue. Therefore, the signature $\mathbf{s}_i^*$ that minimizes (14) is given by

$$\mathbf{s}_i^* = \frac{\mathbf{U}\mathbf{\Lambda}^{-1/2}\mathbf{z}^*}{\left(\mathbf{z}^{*T}\mathbf{\Lambda}^{-1}\mathbf{z}^*\right)^{1/2}}. \tag{17}$$

It is straightforward to see that the updated objective J at $\mathbf{s}_i^*$ is no larger than its value evaluated at $\mathbf{s}_i$. In general, repeating the update iteratively for all the signature sets, the secondary signature set converges because the objective function J reduces monotonically after each update and it is lower bounded. In order to deal with ill-conditioned cases where there are multiple stationary (local minimum) points of J with the same value, we stop the iterations if there is no significant improvement in the cost function after a certain number of iterations.

After computing the secondary signature set, we consider the constraints in (10) and (12) together and follow the ADCPC algorithm proposed in [6] to update the transmission bit energy for each secondary link in an iterative manner. The energy update at each iteration t is given by

$$E_i(t) = \min\left\{E_{\max}, \frac{\gamma E_i(t-1)}{\mathrm{SINR}_i(t-1)}\right\}. \tag{18}$$

Following [6], it can be shown that the iterative update in (18) converges to a unique vector determined by the fixed-point solution

$$\mathbf{E}^{\mathcal{M}} = \min\left\{E_{\max}\mathbf{1}, \gamma\mathbf{W}^{-1}\mathbf{A}\mathbf{W}\mathbf{E}^{\mathcal{M}} + \mathbf{W}^{-1}\mathbf{b}\right\}, \tag{19}$$

where $\mathbf{W} \triangleq \mathrm{diag}(\|\mathbf{H}_{1,1}\mathbf{s}_1\|^2, \|\mathbf{H}_{2,2}\mathbf{s}_2\|^2, \ldots, \|\mathbf{H}_{M,M}\mathbf{s}_M\|^2)$, $\mathcal{M}$ is the set of active secondary links and $\mathbf{E}^{\mathcal{M}}$ is the solution of (19), referred to as *stationary bit-energy vector*. In [6], it was also shown that if the stationary bit-energy vector $\mathbf{E}^{\mathcal{M}}$ by (18) meets all secondary SINR constraints in (9), then the secondary SINR constraints are satisfied with equality. The solution $\mathbf{E}^{\mathcal{M}}$ of (19) is optimal in terms of energy efficiency provided that all the constraints in (9), (10) of the problem P1 are satisfied.

We should note here that there is a possibility of not having a feasible solution for P1, since it may not be feasible for all M secondary links to transmit at the same while satisfying their SINR constraints. In this case, the fixed energy point $\mathbf{E}^{\mathcal{M}}$ in (19) will have at least one SU that uses its maximum energy $E_{\max}$. Whether there is a feasible solution for P1 or not, the admission control procedure which is explained in the next section needs to be followed, since P1 does not incorporate primary interference temperature constraints.

3.2. Admission Control. When the network is dense and the number of requesting secondary links is high, it becomes difficult to support all requesting secondary links simultaneously, that is, the constraints in (8), (9), and (10) may not be simultaneously satisfied for all requesting secondary links. In this case, the problem becomes an admission control problem where the objective is to find the subset of requesting secondary links with the maximum size while satisfying all the constraints in (8), (9), and (10). We now attempt to solve the admission control problem denoted by P2 formulated as

$$\begin{aligned} \text{Find} \quad & \mathbf{E}, \mathbf{S} \\ \text{Maximize} \quad & \|\mathbf{E}\|_0 \\ \text{Subject to} \quad & \text{Constraints in (8), (9) and (10).} \end{aligned} \tag{20}$$

The problem of admission control, that is, maximizing the number of admitted SUs was shown to be NP-hard in [11]. The NP-hardness of this problem motivates the development of effective and computationally efficient heuristic algorithms that provide good suboptimal solutions. In fact, not surprisingly, all the admission control algorithms developed in the literature so far are based on such heuristics [7–11]. For P2, rather than using the conventional admission control procedure proposed in [8], we propose a new removal criterion that effectively incorporates primary interference temperature constraints. We start with following the notations originally proposed in [8]. For every bit-energy vector $\mathbf{E}$ and subset $\mathcal{M}_0 \subseteq \mathcal{M}$, let us define

$$\alpha_i(\mathbf{E}) \triangleq \frac{\gamma\left(\widetilde{E}_i \sum_{j\neq i} A_{j,i} + \sigma^2\right)}{\|\mathbf{H}_{i,i}\mathbf{s}_i\|^2} - E_i, \tag{21}$$

$$\beta_i(\mathbf{E}) \triangleq \frac{\gamma\left(\sum_{j\neq i} A_{i,j}\widetilde{E}_j + \sigma^2\right)}{\|\mathbf{H}_{i,i}\mathbf{s}_i\|^2} - E_i, \tag{22}$$

$$D^{\mathcal{M}_0}(\mathbf{E}) \triangleq \sum_{i\in\mathcal{M}_0} \beta_i(\mathbf{E}). \tag{23}$$

We note that $\alpha_i(\mathbf{E})$ indicates the excess interference power caused by ST_i; $\beta_i(\mathbf{E})$ indicates the excess interference power measured at SR_i; $D^{\mathcal{M}_0}(\mathbf{E})$ indicates the total excess interference power which all the SRs in the subset $\mathcal{M}_0$ experience. From the results in [8], we note that

$$\begin{aligned} &\beta_i(\mathbf{E}) \geq 0, \quad i \in \mathcal{M}, \\ &D^{\mathcal{M}}(\mathbf{E}) = \sum_{i\in\mathcal{M}} \beta_i(\mathbf{E}) = \sum_{i\in\mathcal{M}} \alpha_i(\mathbf{E}) \geq 0. \end{aligned} \tag{24}$$

We also see that $D^{\mathcal{M}}(\mathbf{E}^{\mathcal{M}}) = 0$ if and only if all M secondary links are supported.

The basic idea behind our admission control algorithm is that we iteratively remove the link which violates the constraints in (8), (9), and (10) the most until all the constraints are satisfied. We now explain the algorithm more formally. Due to the fact that the stationary bit-energy vector $\mathbf{E}^{\mathcal{M}}$ already satisfies power budget constraints in (10), we consider admission control in three different scenarios.

Scenario 1. The stationary bit-energy vector $\mathbf{E}^{\mathcal{M}}$ satisfies all the primary interference constraints in (8), whereas it violates some of the secondary SINR constraints in (9).

Scenario 2. The stationary bit-energy vector $\mathbf{E}^{\mathcal{M}}$ satisfies all the secondary SINR constraints in (9), whereas it violates some of the primary interference constraints in (8).

Scenario 3. The stationary bit-energy vector $\mathbf{E}^{\mathcal{M}}$ violates some of the primary interference constraints in (8) and some of the secondary SINR constraints in (9), simultaneously.

In Scenario 1, the admission control problem can be equivalently converted into the problem considered in [8]. In this case, SMIRA in [8] can be used to remove the most violated secondary link one after one until all the constraints in (8), (9), and (10) are satisfied. According to the definition of violation measure in (21), (22), and (23), the removal criterion of SMIRA is to reduce $D^{\mathcal{M}}(\mathbf{E})$ the most by removing the secondary link indexed by i_{remove} given as

$$i_{\text{remove}} = \arg \max_{i \in \mathcal{M}} \{\max(\alpha_i(\mathbf{E}), \beta_i(\mathbf{E}))\}. \tag{25}$$

Intuitively, secondary link i_{remove} is the one that causes the most interference to other secondary links or receives the most interference from other links.

For Scenarios 2 and 3, we define a new metric that quantifies the excess interference power caused by ST_i and measured at PRs as

$$\eta_i(\mathbf{E}) \triangleq \sum_{j \in \mathcal{M}} \left[E_i - \frac{1}{g_{j,i}} \left(I_j - \sum_{k \neq i} g_{j,k} E_k \right) \right] x_{j,i}, \tag{26}$$

where

$$x_{j,i} = \begin{cases} 1, & \sum_{k \in \mathcal{M}} g_{j,k} E_k - I_j > 0, \\ 0, & \text{otherwise.} \end{cases} \tag{27}$$

We note that $\eta_i(\mathbf{E})$ represents aggregate effective violation caused by ST_i at the PRs for which the primary interference constraints are violated. Note that this metric different than the one proposed in [11] which incorporates all the effects (even including negative (non)violation effects) from primary transmitters. In Scenario 2, some of the primary interference temperature constraints are violated. Therefore, we remove the secondary link in Scenario 2 as follows:

$$i_{\text{remove}} = \arg \max_{i \in \mathcal{M}} \{\eta_i(\mathbf{E}) E_i\}. \tag{28}$$

In the last scenario (Scenario 3), we have to aggregate the violation effects of both secondary SINR constraints and primary interference constraints. We propose the following removal criterion for Scenario 3:

$$i_{\text{remove}} = \arg \max_{i \in \mathcal{M}} \{[\max(\alpha_i(\mathbf{E}), \beta_i(\mathbf{E})) + \eta_i(\mathbf{E})] E_i\}. \tag{29}$$

In fact, $[\max(\alpha_i(\mathbf{E}), \beta_i(\mathbf{E})) + \eta_i(\mathbf{E})] E_i$ denotes the comprehensive excess interference power of secondary link i weighted by its transmitting power. By using this criterion, intuitively, the network would potentially reserve the maximum number of secondary links that consume the minimum total energy.

After removing one link at a time, we return to P1 again and attempt to solve P1 and repeat the procedure in an alternating manner. We note that removing one link at a time does not necessarily solve P2, but the whole iterative algorithm solves P1 and P2 jointly as explained in the next section.

3.3. Joint Admission Control and Resource Allocation. The steps of our iterative joint admission control and resource allocation algorithm are summarized as follows.

(1) At iteration $t = 0$, set $\mathbf{E}(0) = c\mathbf{1}$ (c is a small constant).

(2) Solve P1 using the proposed method in Section 3.1 and go to step 3. If there is no feasible solution for P1, go to step 3 (Note that the number of admitted SUs M is updated at each iteration (see Section 3.1).).

(3) If the constraints of P (or P2) are violated, remove one link using the proposed method in Section 3.2, set $t = t + 1$, set $M = M - 1$ and go to step 2. Else stop.

Note that the convergence of this iterative algorithm is guaranteed, because, at step 3, the SUs that were previously removed are not reconsidered. In this case, the solution will be suboptimal, however the iterations will eventually converge in the worst case to the point corresponding to the objective pair $(0, 0)$, that is, the solution that has zero admitted users. Therefore, the maximum number of iterations required for convergence is M. The details regarding the steps of our proposed joint admission control and resource allocation algorithm are explained in Algorithm 1.

4. Computational Complexity

The computational cost is evaluated in terms of "FLOP", which is defined by an additive or a multiplicative operation. The computational complexity of the signature set optimization is dominated by the complexity of the eigendecomposition for Q_i, $i \in \mathcal{M}$, which is $\mathcal{O}(ML^3)$. Given the optimized signature set, the power allocation is carried out by the iterative procedure in (18) using DCPC and ADCPC algorithms. The complexity of this procedure is of order $\mathcal{O}(M^2L^2)$. Then, we test whether the constraints (9) and (8) (equivalently, (12) and (8)) are satisfied. If the constrains are all met, this pair $(\mathbf{E}, \mathbf{S})$ is output as the optimal solution. Otherwise, the admission control procedure is followed, whose complexity is of order $\mathcal{O}(ML)$. We repeat the procedure of joint power and code-channel allocation and the procedure of admission control in an alternating manner until all the aforementioned constraints are satisfied (see Algorithm 1). As noted, the maximum number of iterations required for convergence of Algorithm 1 is at M. This is due to the greedy nature of the algorithm. At each iteration, one secondary user is removed from the network and that user is not admitted again in the following iterations. Therefore, the total complexity of Algorithm 1 is of order $\mathcal{O}(M^2L^3 + M^3L^2)$. For comparison purposes, consider the alternative algorithms that use our optimized signature set along with SMIRA and I-SMIRA. The former and the latter have computational complexities of order $\mathcal{O}(M^3L^2)$ and

1: Select an arbitrary initial signature set for M requesting secondary links.
2: Calculate $\mathbf{Q}_i$ by (15).
3: Obtain $\mathbf{U}$ and $\mathbf{\Lambda}$ through eigendecomposition of $\mathbf{H}_{i,i}^T\mathbf{H}_{i,i}$.
4: Update $\mathbf{s}_i$ using (17).
5: Repeat Step 2–4 until the secondary signature set converges.
6: Calculate the matrix $\mathbf{A}$ by (6).
7: $t = 0$; initialize $\mathbf{E}(0)$ with $c\mathbf{1}$, where c is a small constant.
8: $t = t + 1$.
9: **for** $i = 1, 2, \ldots$ **do**
10: Update $E_i(t) \leftarrow \min\{E_{\max}, \gamma E_i(t-1)/\mathrm{SINR}_i(t-1)\}$
11: **end for**
12: Repeat Step 6–11 until $\mathbf{E}$ converges to a stationary bit-energy vector.
13: Calculate $\alpha_i(\mathbf{E})$, $\beta_i(\mathbf{E})$ and $\eta_i(\mathbf{E})$ by (21), (22) and (26), respectively.
14: **if** $\sum_{i\in\mathcal{M}} g_{j,i}E_i \le I_j \quad \forall\, j = 1, 2, \ldots, K$ **then**
15: **if** $(\mathbf{I} - \gamma\mathbf{A})\widetilde{\mathbf{E}} \ge \mathbf{b}$ **then**
16: Flag_constraints_satisfied $\leftarrow 1$
17: **else**
18: Remove the secondary link $i_{\text{remove}} = \arg\max_{i\in\mathcal{M}}\{\max(\alpha_i(\mathbf{E}), \beta_i(\mathbf{E}))\}$.
19: **end if**
20: **else**
21: **if**$(\mathbf{I} - \gamma\mathbf{A})\widetilde{\mathbf{E}} \ge \mathbf{b}$ **then**
22: Remove the secondary link $i_{\text{remove}} = \arg\max_{i\in\mathcal{M}}\{\eta_i(\mathbf{E})E_i\}$.
23: **else**
24: Remove the secondary link $i_{\text{remove}} = \arg\max_{i\in\mathcal{M}}\{[\max(\alpha_i(\mathbf{E}), \beta_i(\mathbf{E})) + \eta_i(\mathbf{E})]E_i\}$.
25: **end if**
26: **end if**
27: Repeat Step 1–26 until Flag_constraints_satisfied = 1.

Algorithm 1: Proposed joint admission control and resource allocation algorithm.

$\mathcal{O}(M^3L^2 + M^2L)$, respectively. This suggests that if M is equal or close to L, then both three algorithms have the same order of computational complexity.

5. Simulation Results

In this section, we provide some simulation results to evaluate the performance of the proposed algorithm. We consider a primary narrowband system with $K = 5$ active transmission links and a secondary code-division network with M requesting links and processing gain $L = 16$. We assume that each secondary transmission between secondary transmitters and receivers propagates over a multipath channel with $R = 3$ resolvable paths where the corresponding channel coefficients are taken to be the magnitude of independent complex Gaussian random variables with mean 0 and variance 1. The channels between secondary transmitters and primary receivers follow a path loss model with the path-loss exponent of 4, that is, $g_{j,i} = C/d_{j,i}^4$, where $d_{j,i}$ denotes the distance between ST_i and PR_j drawn i.i.d. from a uniform distribution over $[2, 2.5]$, and C is a constant set to 1/3 [10]. The SINR threshold and maximum allowable bit energy for secondary links are set to $\gamma = 10$ dB and $E_{\max} = 17$ dB, respectively. The maximum tolerable interference temperatures at the K primary receivers are all set to $I_j = 3$, $j = 1, \ldots, K$. The variance ξ of AWGN in (1) is set to 1. We assume that each primary transmitter creates 5 dB (≈ 3.2) interference on their corresponding (narrow)bands at the secondary receivers. Furthermore, each primary user is assumed to occupy $1/L$ of the whole available bandwidth. Under these assumptions, the total primary interference power at a given secondary receiver equals 1. As a result, the total primary interference plus noise after RAKE filtering ("despreading") becomes zero-mean AWGN with variance $\sigma^2 = 2$ [15]. Our simulations are based on 1000 Monte Carlo random channel realizations.

We compare the performance of the proposed joint resource allocation and admission control algorithm (Section 4) with the following benchmarks. (i) Proposed optimized secondary signature set by (17) with SMIRA; (ii) Proposed optimized secondary signature set by (17) with I-SMIRA; (iii) Karystinos-Pados (KP) bound equality binary signature set [19–21] with I-SMIRA (The binary signature set that achieves KP bound is minimum total-squared correlation optimal. For $L = 16$, when $M \le L$ the KP-optimal sequences coincide with the familiar Walsh-Hadamard signature codes.).

In Figure 1, we plot the admitted percentage of secondary links as a function of the SINR threshold γ of secondary links. We assume that there are $M = 16$ requesting secondary links in the network. It is clear from the figure that the proposed optimized secondary signature set results in significant performance improvement with respect to the KP bound equality signature set. Furthermore, the proposed joint resource allocation and admission control algorithm outperforms other three algorithms including the ones using

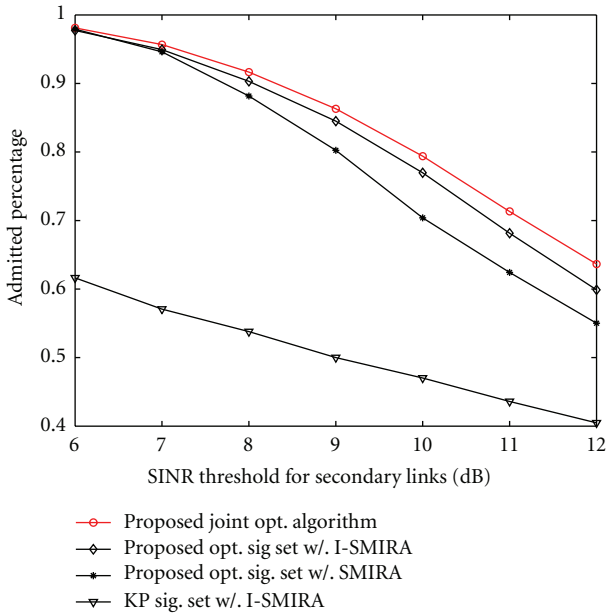

Figure 1: Admitted percentage of secondary links as a function of the SINR threshold for secondary links.

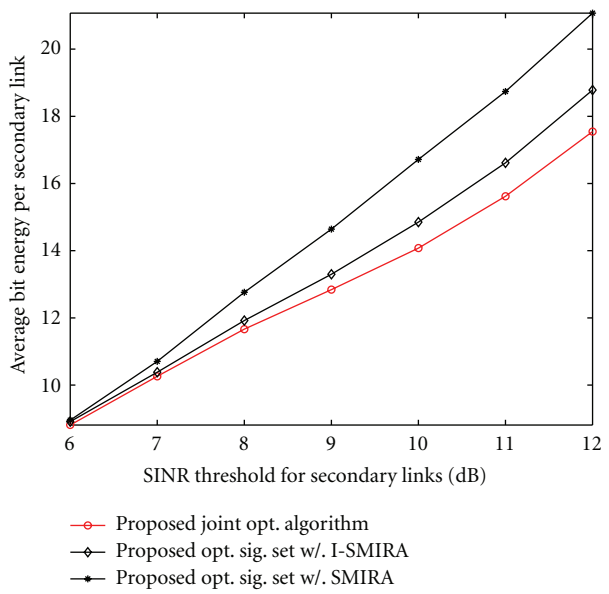

Figure 2: Average bit energy per secondary link as a function of the SINR threshold for secondary links.

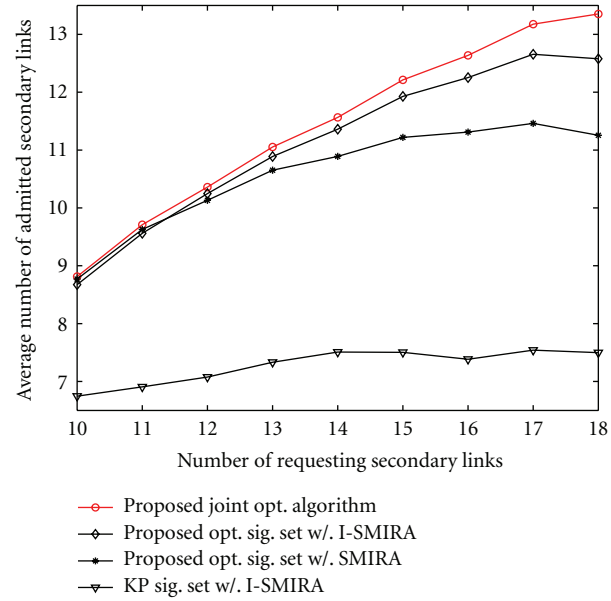

Figure 3: Average number of admitted secondary links versus the number of requesting secondary links averaged over 1000 random channel realizations.

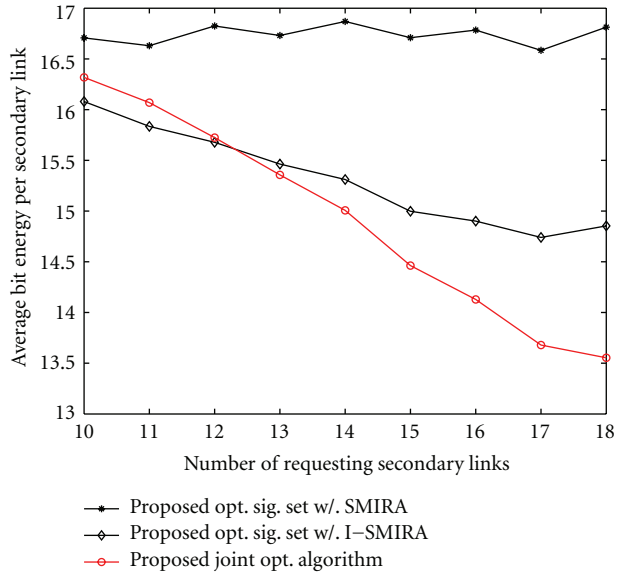

Figure 4: Average bit energy per secondary link versus the number of requesting secondary links.

our optimized signature sets with SMIRA and I-SMIRA admission control strategies. The improvement achieved by the proposed algorithm becomes more significant as secondary SINR threshold increases, that is, as secondary QoS requirement becomes more stringent. In Figure 2, we investigate the energy efficiency of the secondary network. Here, we do not include the KP bound equality signature set with I-SMIRA in the comparison due to its relatively low admission rate of secondary links. The proposed algorithm again achieves the highest energy efficiency compared to its counterparts.

Figures 3 and 4 demonstrate the impact of the number of requesting secondary links on the secondary network performance. We fix the secondary SINR threshold to 10 dB and vary the number of requesting secondary links from 10 to 18. Figures 3 and 4 show the average number of admitted secondary links and the average bit energy per secondary link, respectively, versus the number of requesting secondary links. Similarly, the proposed joint resource allocation and

admission control algorithm achieves visible improvement against the other two algorithms. We should mention that, when the number of requesting secondary links is small, the performance of the optimized signature set with I-SMIRA is slightly better than the proposed algorithm in terms of average bit energy consumption as seen in Figure 4. This is due to the fact that the proposed algorithm supports more secondary links than I-SMIRA which in turn increases the relative average energy cost when the number of requesting secondary links is small. As the number of secondary requests increases, it is clear that the proposed joint algorithm results in better energy efficiency outperforming other algorithms.

6. Conclusions

We studied the problem of cognitive code-division networking where secondary users coexist with a narrowband primary system. We formulated the problem as the search for the powers and signatures of secondary links to maximize the number of admitted secondary links and minimize the total power consumption of secondary links under primary interference temperature constraints, secondary SINR constraints, and maximum peak power constraints. We proposed an iterative joint admission control and resource allocation algorithm for this NP-hard optimization problem which provides excellent results by allowing a large number of active secondary links while improving the energy efficiency of the network as shown in the simulation results.

Depending on the operation mode of the primary system (narrowband or wideband), the proposed solution in this paper can be combined with a primary system identification technique followed by an adaptive selection of secondary operation mode between the proposed solution herein and the solution proposed in [12]. Such an adaptive operation mode will ensure that the secondary links can efficiently and effectively share the licensed band in a dynamically changing environment.

Acknowledgments

This material is based on research sponsored by the Air Force Research Laboratory, under Agreement no. FA8750-11-C-0124. The views and conclusions contained herein are those of the authors and should not be interpreted as necessarily representing the official policies or endorsements, either expressed or implied, of the Air Force Research Laboratory or the USA Government.

References

[1] Federal Communications Commission, "Spectrum policy task force," Report ET Docket 02-135, 2002.

[2] Q. Zhao and B. M. Sadler, "A survey of dynamic spectrum access," *IEEE Signal Processing Magazine*, vol. 24, no. 3, pp. 79–89, 2007.

[3] K. Gao, S. N. Batalama, and D. A. Pados, "Bounds on the maximum SINR of binary and quaternary code-division," *IEEE Transactions on Communications*, vol. 60, pp. 14–18, 2012.

[4] G. J. Foschini and Z. Miljanic, "Simple distributed autonomous power control algorithm and its convergence," *IEEE Transactions on Vehicular Technology*, vol. 42, no. 4, pp. 641–646, 1993.

[5] G. J. Foschini and Z. Miljanic, "Distributed autonomous wireless channel assignment algorithm with power control," *IEEE Transactions on Vehicular Technology*, vol. 44, no. 3, pp. 420–429, 1995.

[6] S. A. Grandhi, J. Zander, and R. Yates, "Constrained power control," *Wireless Personal Communications*, vol. 1, no. 4, pp. 257–270, 1994.

[7] J. C. Lin, T. H. Lee, and Y. T. Su, "Power control algorithm for cellular radio systems," *Electronics Letters*, vol. 30, no. 3, pp. 195–197, 1994.

[8] M. Andersin, "Gradual removals in cellular PCS with constrained power control and noise," *Wireless Networks*, vol. 2, no. 1, pp. 27–43, 1996.

[9] Y. Xing, C. N. Mathur, M. A. Haleem, R. Chandramouli, and K. P. Subbalakshmi, "Dynamic spectrum access with QoS and interference temperature constraints," *IEEE Transactions on Mobile Computing*, vol. 6, no. 4, pp. 423–433, 2007.

[10] L. Zhang, Y. C. Liang, and Y. Xin, "Joint admission control and power allocation for cognitive radio networks," in *Proceedings of the IEEE International Conference on Acoustics, Speech and Signal Processing (ICASSP '07)*, pp. 673–676, Honolulu, Hawaii, USA, April 2007.

[11] L. Le and E. Hossain, "Resource allocation for spectrum underlay in cognitive radio networks," *IEEE Transactions on Wireless Communications*, vol. 7, no. 12, pp. 5306–5315, 2008.

[12] K. Gao, S. N. Batalama, D. A. Pados, and J. D. Matyjas, "Cognitive code-division channelization," *IEEE Transactions on Wireless Communications*, vol. 10, no. 4, pp. 1090–1097, 2011.

[13] A. Elezabi, M. Kashef, M. Abdallah, and M. Khairy, "CDMA underlay network with cognitive interference-minimizing code assignment and semi-blind interference suppression," *Wireless Communications and Mobile Computing*, vol. 9, no. 11, pp. 1460–1471, 2009.

[14] M. Li, S. N. Batalama, D. A. Pados, T. Melodia, M. J. Medley, and J. D. Matyjas, "Cognitive code-division links with blind primary-users identification," *IEEE Transaction on Wireless Communications*, vol. 10, pp. 3743–3753, 2011.

[15] J. G. Proakis, *Digital Communications*, McGraw-Hill, New York, NY, USA, 4th edition, 2001.

[16] S. Boyd and L. Vandenberghe, *Convex Optimization*, Cambrige University Press, Cambridge, UK, 2004.

[17] K. Deb, *Multi-Objective Optimization Using Evolutionary Algorithms*, Wiley, New York, NY, USA, 2001.

[18] E. Seneta, *Non-Negative Matrices*, G. Allen, London, UK, 1973.

[19] G. N. Karystinos and D. A. Pados, "New bounds on the total squared correlation and optimum design of DS-CDMA binary signature sets," *IEEE Transactions on Communications*, vol. 51, no. 1, pp. 48–51, 2003.

[20] C. Ding, M. Golin, and T. Kløve, "Meeting the Welch and Karystinos-Pados bounds on DS-CDMA binary signature sets," *Designs, Codes, and Cryptography*, vol. 30, no. 1, pp. 73–84, 2003.

[21] V. P. Ipatov, "On the Karystinos-Pados bounds and optimal binary DS-CDMA signature ensembles," *IEEE Communications Letters*, vol. 8, no. 2, pp. 81–83, 2004.

Hindawi Publishing Corporation
Journal of Computer Networks and Communications
Volume 2012, Article ID 851204, 12 pages
doi:10.1155/2012/851204

Research Article

The SS-SCR Scheme for Dynamic Spectrum Access

Vinay Thumar,[1] Taskeen Nadkar,[1] U. B. Desai,[2] and S. N. Merchant[1]

[1] *Department of Electrical Engineering, Indian Institute of Technology, Bombay 400076, India*
[2] *Indian Institute of Technology Hyderabad, Yeddumailaram 502205, India*

Correspondence should be addressed to Vinay Thumar, vinay_thumar@ee.iitb.ac.in

Received 16 December 2011; Revised 24 April 2012; Accepted 1 May 2012

Academic Editor: Torleiv Maseng

We integrate the two models of *Cognitive Radio (CR)*, namely, the conventional *Sense-and-Scavenge (SS) Model and Symbiotic Cooperative Relaying (SCR)*. The resultant scheme, called *SS-SCR*, improves the efficiency of spectrum usage and reliability of the transmission links. *SS-SCR* is enabled by a suitable cross-layer optimization problem in a multihop multichannel CR network. Its performance is compared for different PU activity patterns with those schemes which consider *SS* and *SCR* separately and perform disjoint resource allocation. Simulation results depict the effectiveness of the proposed *SS-SCR* scheme. We also indicate the usefulness of cloud computing for a practical deployment of the scheme.

1. Introduction

1.1. Cognitive Radio/Dynamic Spectrum Access. The emerging *Cognitive Radio (CR)* technology is an attempt to alleviate the inefficient utilization of the spectrum, created by the current *Command-and-Control* spectrum access policy. It temporarily allows unused portions of the spectrum (*spectrum holes* or *white-spaces*), owned by the licensed users, known as *primary users (PUs)*, to be accessed by unlicensed users, known as *secondary users (SUs)*, without causing intrusive interference to the former's communication [1]. This is the *Sense-and-Scavenge (SS)* Model of conventional CR. A CR node is characterized by an adaptive, multi-dimensionally aware, autonomous radio system empowered by advanced intelligent functionality, which interacts with its operating environment and learns from its experiences to *reason*, *plan*, and *decide* future actions to meet various needs [2].

In the *SS* model of CR, the temporal PU activity patterns have a significant influence on the opportunities for the SUs. The source traffic for the PU alternates between ON (busy) and OFF (idle) periods. The ON/OFF activity is characterized by suitable statistical models, for predictive estimation of the patterns. Exponential [3–6] and log-normal [3–5] distributions are popularly used in the literature to model the ON (and OFF) times of the PU activity. Measurements have also revealed that successive ON and OFF periods are independent, though in some cases long-term correlations exist [4].

1.2. Symbiotic Cooperative Relaying. An interesting paradigm that has surfaced in the research surrounding CR is a symbiotic architecture, which improves the efficiency of spectrum usage and reliability of the transmission links [7–12]. According to this model, which we refer to as *Symbiotic Cooperative Relaying (SCR)*, the PU seeks to enhance its own communication by leveraging other users in its vicinity, having better channel conditions, as cooperative relays for its transmission and in return provides suitable remuneration to them. The SU nodes, being scavengers of the licensed PU spectrum, are potential candidates as relays, since they are idling when the PU transmission is in progress. Besides, they have cognitive capabilities, which give a large amount of flexibility of reconfiguration and resource allocation during the cooperative relaying process. The cooperation from the SU network results in enhanced transmission rate of the PU, which translates into reduced transmission time for the same amount of information bits of the PU as that transmitted on its direct link. Then, the time saved can be offered to the SUs for their own communication as a reward for cooperating with the PU (with a fixed rate demand). The SUs can achieve

their communication in the *time incentive* without the need for spectrum sensing. In our previous work, we have formulated a cross-layer design to enable the *SCR* scheme, called *Cognitive Relaying with Time Incentive (CRTI)*, for an Orthogonal Frequency Division Multiplexing-(OFDM-) based multi-hop CR network, with special emphasis on the MAC layer coordination protocol [13]. We have also proposed that it is possible to reward the SUs with incentive frequency bands, that is, *Cognitive Relaying with Frequency Incentive (CRFI)* [12, 14]. Some unique challenges are faced when the *SCR* scheme is enabled on the spectra of multiple PUs; we have addressed these in prior work as well [15, 16].

In case of *SCR*, the PU is assumed to have a constant occupancy state throughout the frame duration (in a frame-based communication); that is, it does not exhibit intermittent ON/OFF periods. During those frames when *SCR* is enabled, the PU should definitely be ON.

1.3. The SS-SCR Scheme. In this paper, we integrate the two aforementioned models of CR, namely, the *Sense-and-Scavenge (SS)* model of conventional CR and *Symbiotic Cooperative Relaying (SCR)*. We refer to this composite scheme as *SS-SCR*. *SS-SCR* entails a multiple PU scenario, with each PU having its own distinct bandwidth of operation. On the PUs' spectra having a weak direct link, *SCR* is enabled, while, on the rest of the PUs' bands, *SS* is enabled. Since most present day wireless technologies such as IEEE 802.16 [17] and 802.22 [18] are based on OFDM, the multichannel multi-hop networks, thus created, pose a more challenging environment for deployment of the *SS-SCR* scheme, as opposed to simplistic two-hop or single-channel scenarios addressed in the literature (discussed in *Related Literature*). Optimum resource (time, bandwidth, power) allocation, which can be achieved by leveraging the channel diversity abundantly available in a multichannel network, will improve spectral efficiency and in turn maximize the transmission opportunities for both the PUs and SUs. With this objective, we present our original contributions in this paper, which are summarized as follows.

(1) We propose a scheme for enabling *SS-SCR* by means of a suitable cross-layer optimization problem which addresses power control, scheduling, and routing. Though the work can readily be extended to any number of PUs, currently a simple scenario with two PUs is assumed—on the spectrum of one we enable *SS*, while on the other we enable *SCR*. The *SS-SCR* scheme jointly considers the resource allocation on both the PUs' bands to maximize the overall spectral efficiency and mutual benefits of both entities under concern, namely, the PU and SU.

(2) For comparison, we also describe two schemes which consider the *SS* and *SCR* separately, and the resource allocation on each of the PUs' bands is disjoint. All the schemes are investigated under various PU ON/OFF traffic models.

(3) We propose the use of cloud computing to enhance the performance of *SS-SCR* in practical CR networks.

To detail our work, the paper has been organized as follows. Section 2 presents related background literature. Section 3 describes the system model and communication scenario. Section 4 methodically explains the generalized cross-layer optimization problem. In Section 5 we propose the *SS-SCR* scheme, while in Section 6 we describe the problems for the *SS* and *SCR* schemes separately considered. Section 7 provides a note on the practical implementation. Section 8 illustrates the use of *cloud computing* for *SS-SCR*. In Section 9, we present simulation results and their detailed analysis. Section 10 concludes the paper.

2. Related Literature

Conventionally, there are two approaches to spectrum sharing in CR [19]: *underlay approach*, in which the SUs and the PU access the same frequency band by the use of sophisticated spread spectrum techniques, and *overlay approach*, in which the SUs access the licensed spectra when the PU is not using it. The *SS* model pertains to the *overlay approach*—the SUs sense the spectrum to detect a white space and utilize it for their own communication.

Surrounding the concept of *SCR* for CR, many schools of thought have evolved to accommodate substantially different technologies and solutions. Simeone et al. [7, 8] have used game theoretic tools to analyze the performance of cooperation in a CR network, wherein the PU leases the owned spectrum to an ad hoc network of SUs in exchange for cooperation in the form of transmission power from the SUs. The model proposed by J. Zhang and Q. Zhang [9] is more rational; when the PU's demand is satisfied, it is willing to enhance its benefit in any other format, for instance, by collecting a higher revenue from the SU. Xue et al. [10] have considered a single full-duplex amplify-and-forward (AF) SU relay to assist the PU transmission. Gong et al. [11] have analyzed the power and diversity gains obtained by AF relaying of the PU's data by multiple cooperating SUs. All of the aforementioned works in the literature have considered either a single-relay node or single-channel CR networks. The authors have also contributed significantly towards *SCR* schemes for multichannel multi-hop networks [12–16]. The cross-layer formulations in this work are inspired by those of Shi and Hou [20], Zhang et al. [21], and some references therein. While Shi et al. aim at maximizing the sum throughput of the SUs in a multi-hop multichannel CR network, in the proposed *SS-SCR* scheme, the objective is to perform a joint resource allocation on both the PUs band (*SS* and *SCR*) for maximizing the net spectral efficiency. As far as the previous works of the authors are concerned, the concept of *CRTI* [13] involves a cross-layer optimization problem for a single source, that is, PU Tx, for throughput maximization. The approaches to *CRFI* [13, 14] are totally different in their objective—that of achieving a specified throughput for the PU while using the least number of frequency bands. Techniques for *CRTI* for multiple PUs [15, 16] describe the maximization of the time incentive for the SUs, while utilizing multiple PUs spectra optimally. Two methods have been proposed for the same, the formulations for which are distinct, and different from those in the literature [20, 21].

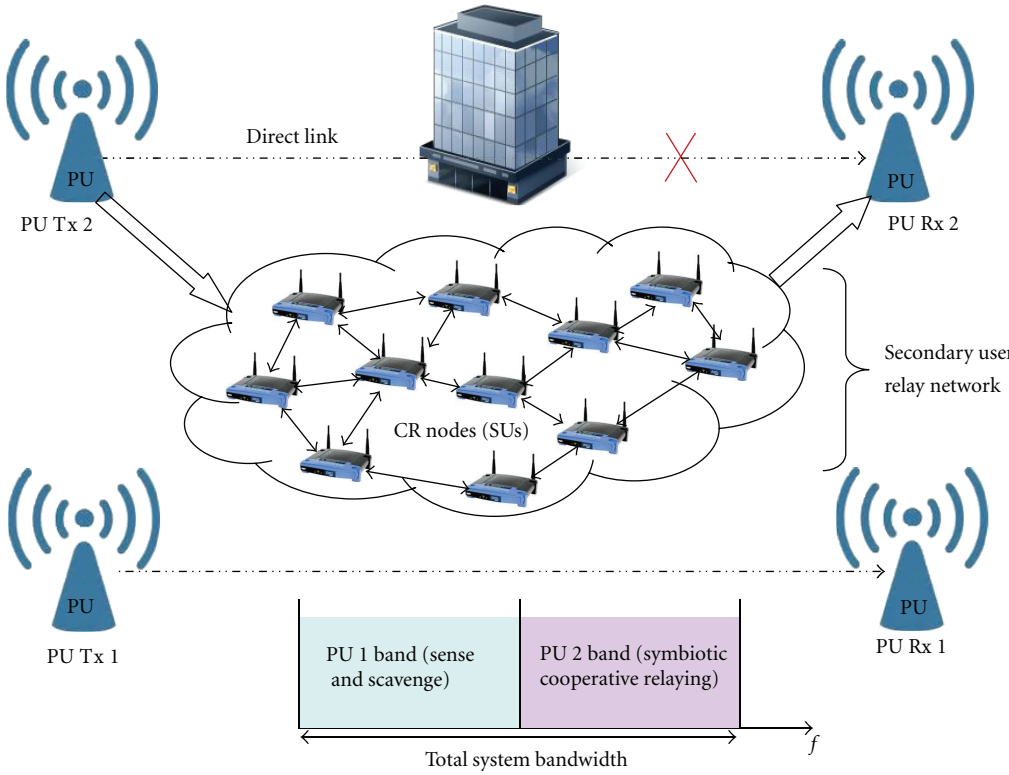

Figure 1: System model.

This work differs from the above in the fact that it is a *hybrid* architecture: it integrates the conventional *SS* model with *SCR*, for a multiple PU scenario.

3. System Description

We consider a CR system with a network of cognitive SUs and two PU transceivers (Figure 1). Each PU has its own distinct bandwidth of operation. The available bandwidth is divided into frequency flat subchannels by deploying OFDM. The band-sets of the two PUs are denoted by $\mathbb{M}_1$ and $\mathbb{M}_2$, respectively. On the band-set of PU 1, conventional CR mode of operation, that is, *SS*, is enabled. The SUs are continuously sensing the spectrum for a transmission opportunity; when PU 1 is OFF, the SUs use its spectrum for their own communication. The activity of PU Tx 1 is detected by all the SU nodes by cooperative spectrum sensing [22]. Band-set $\mathbb{M}_1$ is also referred to as the *SS* band.

On the other hand, on the band-set of PU 2, *SCR* is enabled. Rather than using the direct link, the PU Tx 2 relays its data through the SU network and in return rewards them with a *time incentive* λ_t for their own communication. If C_{dir} is the throughput (bits/sec/Hz) obtained on the direct link, C_{rel} is the maximized throughput (bits/sec/Hz) obtained through the SU relay network, then the incentive in a time frame normalized to unity is $\lambda_t = 1 - C_{\text{dir}}/C_{\text{rel}}$, $0 \le \lambda_t \le 1$. On band-set $\mathbb{M}_2$ (also referred to as the *SCR* band), PU Tx 2 acts as the source, PU Rx 2 as the destination, and the SU nodes act as the relays in the multi-hop relay network (Figure 1). Decode-and-forward multihopping is assumed at each node.

The fading gains for various links are mutually independent and are modeled as zero mean complex circular Gaussian random variables. The protocol interference model is assumed [20]. The channel gains are invariant within a frame but vary over frames (i.e., block-fading channels). We assume that the channel gains from the PU Tx 2 to SUs, the SUs to the PU Rx 2, and those among the SUs are good enough to provide a significantly higher end-to-end throughput as compared to the direct link of PU 2, resulting in performance gains for both the PU and the SUs on band-set $\mathbb{M}_2$.

4. Problem Formulation: Cross-Layer Optimization

In the subsequent sections we will be describing the proposed *SS-SCR* scheme which considers joint resource allocation on both PUs' bands, as well as the schemes which are disjoint in their resource allocation on the two bands. Each scheme will involve solving a sequence of optimization problems, their objective being maximization of the sum throughput of the users under consideration (PU or SUs or both) within the given resources (time slot, frequency bands, power). To efficiently exploit the channel diversities available in the multi-hop multichannel SU network, we allow flow splitting and spatial reuse of frequencies outside the interference range

of nodes. Each optimization problem involves a cross-layer view for power allocation, frequency band scheduling, and routing. A relay with poor channel conditions on all its links will be eliminated from the routes which strive to achieve maximum throughput; thus relay selection is automatically achieved by the problem. We describe the basic structure of such a cross-layer optimization problem which will be suitably adapted for the various schemes to be described subsequently.

Optimization Problem (P1):

$$\max_{\left(x_{ij}^{(m)},P_{ij}^{(m)},f_{ij}(l)\right)} \sum_{l\in\mathbb{L}} \sum_{j\in T_i} f_{ij}(l) \quad i = s(l). \tag{1}$$

It is subject to the constraints which are described as follows.

Flow Constraints:

$$\sum_{j\in T_i}^{j\neq s(l)} f_{ij}(l) = \sum_{k\in T_i}^{k\neq d(l)} f_{ki}(l) \quad \forall i \in \mathbb{N},\ l \in \mathbb{L},\ i \neq s(l),\ i \neq d(l), \tag{2}$$

$$f_{ij}(l) \geq 0 \quad \forall (i,j) \in \mathbb{E},\ l \in \mathbb{L}, \tag{3}$$

$$\sum_{l\in\mathbb{L}} f_{ij}(l) - \sum_{m\in M} \log_2\left(1 + \frac{h_{ij}^{(m)} P_{ij}^{(m)}}{\sigma^2}\right) \leq 0 \quad \forall (i,j) \in \mathbb{E}. \tag{4}$$

Frequency Domain Scheduling Constraints:

$$\sum_{j\in T_i} x_{ij}^{(m)} + \sum_{k\in T_i} x_{ki}^{(m)} \leq 1 \quad \forall i \in \mathbb{N},\ m \in \mathbb{M}, \tag{5}$$

$$x_{ij}^{(m)} = \{0,1\} \quad \forall (i,j) \in \mathbb{E},\ m \in \mathbb{M}. \tag{6}$$

Power Constraints:

$$\begin{aligned} P_{ij}^{(m)} - P_{T_{ij}}^{(m)} x_{ij}^{(m)} &\geq 0 \quad \forall (i,j) \in \mathbb{E},\ m \in \mathbb{M}, \\ P_{ij}^{(m)} - P_{\text{peak}} x_{ij}^{(m)} &\leq 0 \quad \forall (i,j) \in \mathbb{E},\ m \in \mathbb{M}, \end{aligned} \tag{7}$$

$$\sum_{j\in T_i, m\in\mathbb{M}} P_{ij}^{(m)} \leq P_{\text{avl}_i} \quad \forall i \in \mathbb{N}. \tag{8}$$

Interference Constraints:

$$P_{kh}^{(m)} + \left(\sum_{k\in I_j^m} P_{kh}^{(m)} h_{kj}^{(m)} - P_I + P_{\text{peak}} - P_{kh}^{(m)}\right) x_{ij}^{(m)} \leq P_{\text{peak}}, \tag{9}$$

$$\forall i \in \mathbb{N},\ m \in \mathbb{M},\ j \in T_i,\ k \in I_j^m,\ k \neq i.$$

Since our objective (1) is to maximize the throughput, it is sufficient to maximize the sum of outgoing flows from the source node [23]. We denote the communication between each unique transmitter-receiver pair as a session. $s(l)$ and $d(l)$ represent the source and destination of the session l, $l \in \mathbb{L}$, where $\mathbb{L}$ denotes the set of the sessions.

Bidirectional links are assumed; that is, in the network graph each node i has an transmit/receive set of nodes T_i. $f_{ij}(l)$ is the data flow (bits/sec) from node i to node j for session l. Equation (2) indicates that, except for the source and destination nodes, the inflow into a node is equal to the outflow. Equation (3) ensures that all the flows are non-negative. Equation (4) refers to the fact that the sum of the flows on a link cannot exceed the capacity of a link according to Shannon's channel capacity theorem [24]. Each link has $|\mathbb{M}|$ orthogonal frequency bands, and the net achievable throughput is the sum throughput of the individual bands. $h_{ij}^{(m)}$ denotes the channel power gain on band m, and $P_{ij}^{(m)}$ denotes the corresponding power allocation. We have assumed unit bandwidth of each band. In (4), the log function contains only σ^2 in the denominator due to the use of an interference model, which ensures that when node i is transmitting to node j on band m, the interference from all other nodes in this band must remain negligible due to the frequency domain scheduling and interference constraints. $\mathbb{N}$ denotes the node set of the network and $\mathbb{E}$ denotes the edge set.

Equation (5) suggests that if a node i has used a band m for transmission or reception, it cannot be used by node i again for any other transmission or reception. Note that $x_{ij}^{(m)}$ is a binary variable which takes the value 1 if and only if band m is active on link (i, j).

Equation (7) ensure that $P_{ij}^{(m)} \in [P_{T_{ij}}^{(m)}, P_{\text{peak}}]$ if the band m is selected and $P_{ij}^{(m)} = 0$ if the band is not selected. The data transmission from node i to node j is successful only if the received transmission power exceeds a power threshold P_T, from which we can calculate the minimum required transmission power on a band m at node i as $P_{T_{ij}}^{(m)} = P_T/h_{ij}^{(m)}$. P_{peak} denotes the maximum power that can be allocated to any band m, under which we compute the interference set I_j^m of a receiving node j. Equation (8) is to ensure that the total power transmitted on all the active bands at node i does not exceed the power available at the node P_{avl_i}.

Equation (9) ensures that for a successful transmission on link i to j, on an interfering link k to h, the transmit power on any band m cannot exceed a threshold P_{peak} if $x_{ij}^{(m)} = 0$, and if $x_{ij}^{(m)} = 1$, then $\sum_{k\in I_j^m} P_{kh}^{(m)} h_{kj}^{(m)} \leq P_I$. The complete list of symbols with their description is given in Table 1.

In the above optimization problem $h_{ij}^{(m)}$, σ^2, P_T, P_I, P_{peak}, and P_{avl_i} are all constants, while $x_{ij}^{(m)}$, $P_{ij}^{(m)}$, and $f_{ij}(l)$ are the optimization variables. The formulation is a *mixed integer nonlinear programming problem (MINLP)*. Based on the discussion on similar problems in [20, 21] and the references therein, we conjecture that the given problem is NP-hard. We are thus motivated to investigate a linear formulation, which will greatly simplify the problem (which is observed in terms of reduced computation time during simulation). This entails employing three tangential supports to the log term in (4), as its approximation [20]. The tangential supports are drawn at points 1, 2, and 3 on the *log* curve (Figure 2), namely, $(0, 0)$, $(\beta, f(\beta))$, and $(P_{\text{peak}}, f(P_{\text{peak}}))$. β denotes the x-coordinate of the point of intersection of the tangents drawn at points 1 and 3. The solution to the log relaxed

Table 1: Notations.

Symbol	Definition
PU Tx, PU Rx	PU transmitter, PU receiver
(i, j)	Edge between nodes i and j
T_i	The set of nodes that node i can transmit to and receive from
$h_{ij}^{(m)}$	Channel gain on edge (i, j) and band m
$x_{ij}^{(m)}$	Band assignment on edge (i, j) and band m
$P_{ij}^{(m)}$	Power allocation on edge (i, j) and band m (W)
$P_{T_{i,j}}^{(m)}$	Detection threshold of band m on edge (i, j) (W)
P_I	Interference threshold of a node (W)
P_{peak}	Maximum power that can be transmitted on a frequency band (W)
$P_{\text{node}_i}/P_{\text{avl}_i}$	Power available at node i (W)
I_j^m	Set of nodes that can interfere with node j on band m
σ^2	Additive white Gaussian noise (AWGN) variance (W)
$\mathbb{N}$	Node set of the entire network
$\mathbb{M}$	Band set of the entire network
$\mathbb{E}$	Edge set of the entire network
$\mathbb{L}$	Set of SU sessions in the entire network
$s(l)$, $d(l)$	Source of session l, destination of session l
$f_{ij}(l)$	Flow on edge (i, j) and band m for session l (bps)

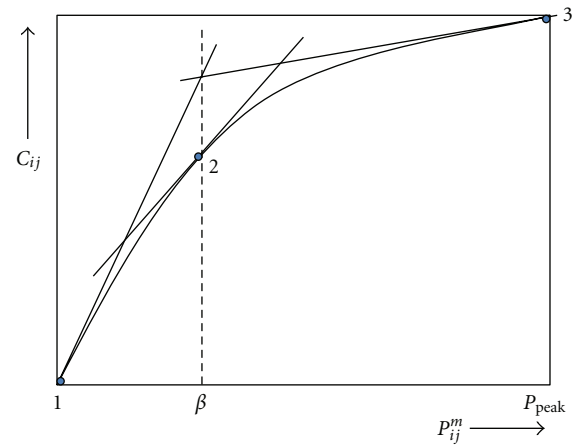

Figure 2: Approximating the log function.

problem provides an upper bound to the original maximization problem P1.

A Feasible Centralized Solution. We suggest an approach to obtain a feasible suboptimum solution to the original problem by decoupling the operations of power allocation and band scheduling and that of flow computation. The solution consists of two steps.

(1) The power allocation and band scheduling (P_{ij}^m, x_{ij}^m) are obtained from the log relaxed problem with tangential supports. This solution, however, may violate the flow constraints.

(2) The above (P_{ij}^m, x_{ij}^m) are substituted in the original problem, which is then solved only with respect to f_{ij} as the optimization variable. The overall result represents a feasible solution to the original problem P1.

5. The SS-SCR Scheme

As described earlier, PU 1's activity is changing on band-set $\mathbb{M}_1$ (*SS* band), providing intermittent periods for the SUs to communicate; on band-set $\mathbb{M}_2$ (*SCR* band), PU 2 is ON and relaying its data through the SU network. It is on this band that a *time incentive* will be offered to the SUs in return for their cooperation. In *SS-SCR*, we solve a joint resource allocation problem on both the PUs' bands; that is, $\mathbb{M}_1 \cup \mathbb{M}_2$, in every such time interval that PU 1's activity changes. There are totally four possibilities (Figure 3): PU 1 is OFF and PU 2 is relaying on $\mathbb{M}_2$, PU 1 is ON and PU 2 is relaying on $\mathbb{M}_2$, PU 1 is OFF and SUs are using the *time incentive* on $\mathbb{M}_2$, and PU 1 is ON and SUs are using the *time incentive* on $\mathbb{M}_2$. Cross-layer optimization problems are formulated for the aforementioned possibilities, as follows.

(Ia) PU 1 is OFF and PU 2 is relaying on $\mathbb{M}_2$. In this case, the joint problem entails maximizing the sum throughput of the SUs and PU 2; the SUs want to make the best utilization of the OFF time of PU 1, while PU 2 wants to maximize its throughput through the SU network so that in turn it can maximize the *time incentive* offered to the cooperating SUs. The complete band-set $\mathbb{M}_1 \cup \mathbb{M}_2$ and the total node power budget P_{node_i} are available for the problem.

(Ib) PU 1 is ON and PU 2 is relaying on $\mathbb{M}_2$. PU 2 can maximize its throughput through the SU network only on $\mathbb{M}_2$ with the total node power budget P_{node_i}.

(Ic) PU 1 is OFF and SUs are using the *time incentive* on $\mathbb{M}_2$. The SUs can now use the complete band-set $\mathbb{M}_1 \cup \mathbb{M}_2$ with the total node power budget P_{node_i} to maximize their sum throughput.

(Id) PU 1 is ON and SUs are using the *time incentive* on $\mathbb{M}_2$. The SUs can only use $\mathbb{M}_2$ with the total node power budget P_{node_i} to maximize their sum throughput.

To enable *SS-SCR*, the following parameters should be set in problem P1 (Table 2).

6. Disjoint Resource Allocation for SS and SCR

In this section, we describe schemes based on disjoint resource allocation on the *SS* and *SCR* bands, considering them as separate problems.

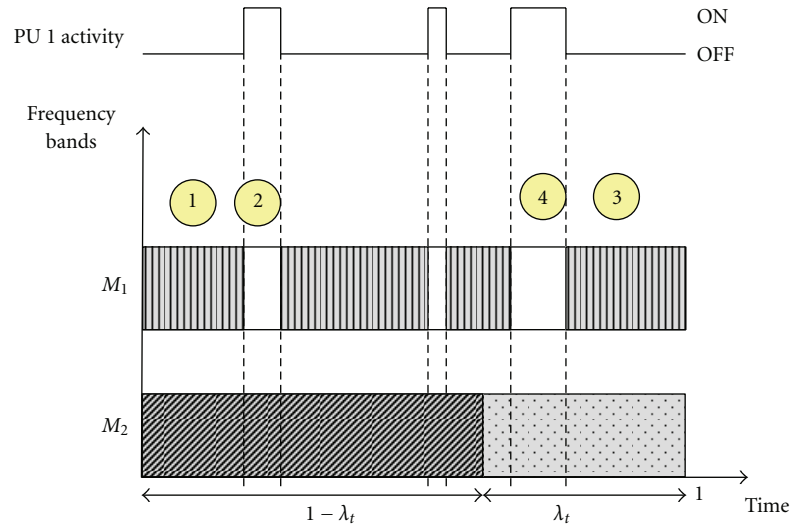

1. PU1 is OFF and PU2 is relaying through SU network
2. PU1 is ON and PU2 is relaying through SU network
3. PU1 is OFF and SUs are communicating in time incentive
4. PU1 is ON and SUs are communicating in time incentive

Figure 3: SS-SCR scheme.

Table 2: SS-SCR.

	Node set ($\mathbb{N}$)	Band-set ($\mathbb{M}$)	Session set ($\mathbb{L}$)	$P_{\text{avl}_i}(W)$
(Ia)*	All SUs PU Tx 2, PU Rx 2	$\mathbb{M}_1 \bigcup \mathbb{M}_2$	SUs, PU 2	P_{node_i}
(Ib)	All SUs PU Tx 2, PU Rx 2	$\mathbb{M}_2$	PU 2	P_{node_i}
(Ic)	All SUs	$\mathbb{M}_1 \bigcup \mathbb{M}_2$	SUs	P_{node_i}
(Id)	All SUs	$\mathbb{M}_2$	SUs	P_{node_i}

*Note: A provision should be made to prevent the SUs from relaying their data through PU Tx 2 and PU Rx 2 by means of additional constraints: $x_{ij}^{(m)} = 0$, j = PU Tx 2 and $x_{ij}^{(m)} = 0$, i = PU Rx 2.

Table 3: Scheme A.

	Node set ($\mathbb{N}$)	Band-set ($\mathbb{M}$)	Session set ($\mathbb{L}$)	$P_{\text{avl}_i}(W)$
(IIa)	All SUs	$\mathbb{M}_1$	SUs	P_{node_i}
(IIb)	All SUs, PU Tx 2, PU Rx 2,	$\mathbb{M}_2$	PU 2	$P_{\text{node}_i} - P_{\text{cons}_i}$
(IIc)	All SUs	$\mathbb{M}_3$	SUs	$P_{\text{node}_i} - P_{\text{cons}_i}$

6.1. Scheme A. This scheme gives priority to the activity on the *SS* band and second preference to the *SCR* band. It is devised for that situation in which the OFF periods of PU 1 are high. The following steps are adopted (Figure 4(a)).

(IIa) First, the SUs' sum throughput maximization problem is solved on band-set $\mathbb{M}_1$ (*SS* band). The SUs will be sensing for a spectrum opportunity on this band. In the OFF time of PU 1, they will utilize this band for their own communication. The total node power budget P_{node_i} is available for them at each node i.

(IIb) Secondly, on band-set $\mathbb{M}_2$ (*SCR* band), PU Tx 2 will relay its data through the SU network with maximized throughput. Since the communication happens concurrently with the SU's communication on $\mathbb{M}_1$, now the power available at each node i is the node power budget minus the power consumed in step (IIa), that is, $P_{\text{node}_i} - P_{\text{cons}_i}$. The channel diversity and consequently the higher throughput obtained from the SU network will diminish the transmission time for the same number of bits as those transmitted on the direct link of PU 2. The time saved is offered as an incentive to the SUs for their own communication.

(IIc) In the *time incentive* obtained from PU 2, the SUs maximize their sum throughput on $\mathbb{M}_2$. The power available at each node i is $P_{\text{node}_i} - P_{\text{cons}_i}$.

To enable Scheme A, the following parameters should be set in problem *P1* (Table 3).

6.2. Scheme B. This scheme gives priority to the activity on the *SCR* band and second preference to the *SS* band. It is devised for that situation in which the ON periods of PU 1 are high. The following steps are adopted (Figure 4(b)).

(IIIa) First, on band-set $\mathbb{M}_2$ (*SCR* band), PU Tx 2 will relay its data through the SU network with maximized throughput. The total node power budget P_{node_i} is available for its communication. The higher throughput achieved, as compared to the direct link of PU 2, will generate a *time incentive* for the SUs on $\mathbb{M}_2$.

(IIIb) Next, in the *time incentive* obtained from PU 2, the SUs maximize their sum throughput on band-set $\mathbb{M}_2$. The power available at each node i is P_{node_i}.

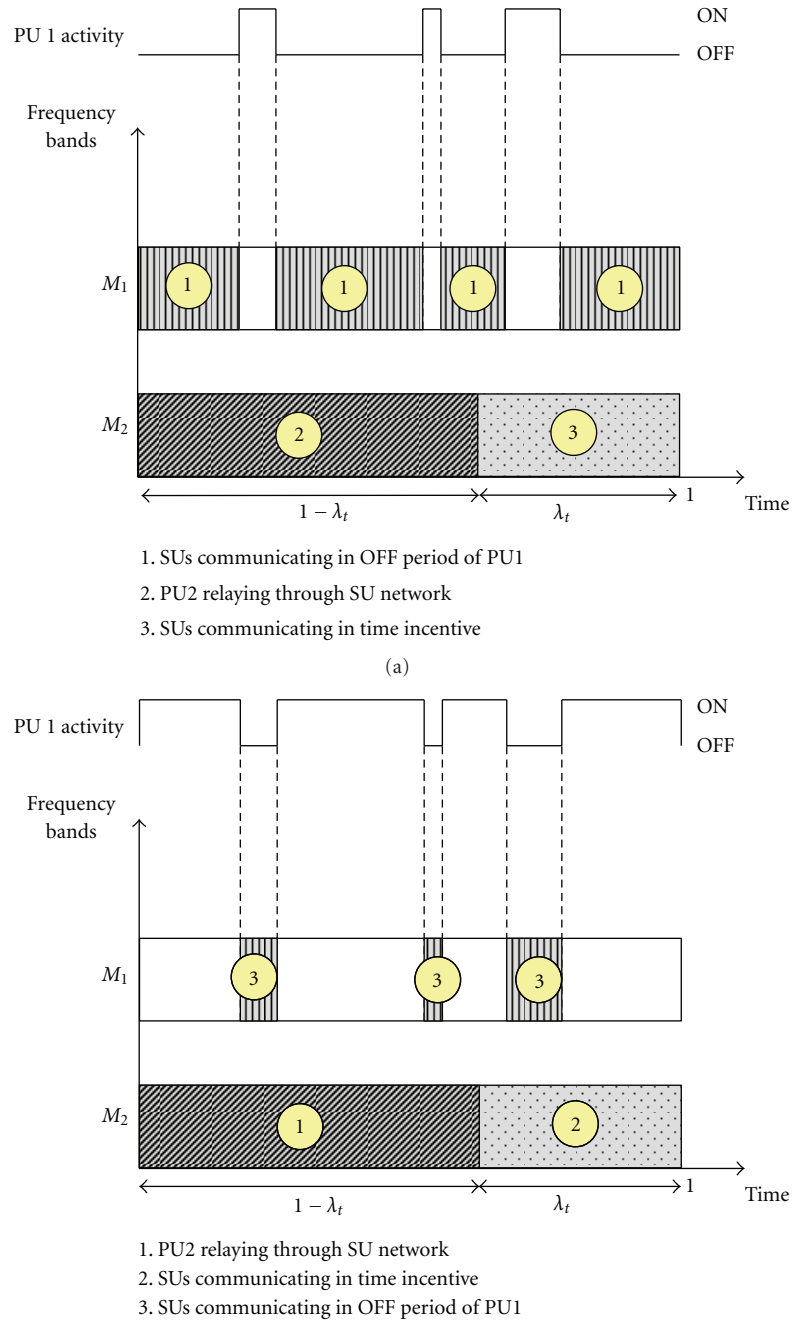

Figure 4: Separate SS and SCR: (a) Scheme A (b) Scheme B.

(IIIc) Lastly, the SUs' sum throughput maximization problem is solved on band-set $\mathbb{M}_1$ (*SS* band). The SUs will be sensing for a spectrum opportunity on this band. In the OFF time of the PU, they will utilize this band for their own communication. Since this transmission is concurrent with that on $\mathbb{M}_2$, the power available for them at each node i is minimum of that left after consumption in the relaying interval and the incentive period, that is, $\min(P_{\text{node}_i} - P_{\text{cons}_{\text{III}ai}}, P_{\text{node}_i} - P_{\text{cons}_{\text{III}bi}})$.

To enable Scheme B, the following parameters should be set in problem P1 (Table 4).

7. A Note on the Practical Implementation

To make the *SS-SCR* scheme a practical reality, a MAC schedule is needed to coordinate all the operations. The MAC frame consists of a control interval in which estimation of the channel states, prediction of PU activity, solving the optimization problems at a centralized controller, and

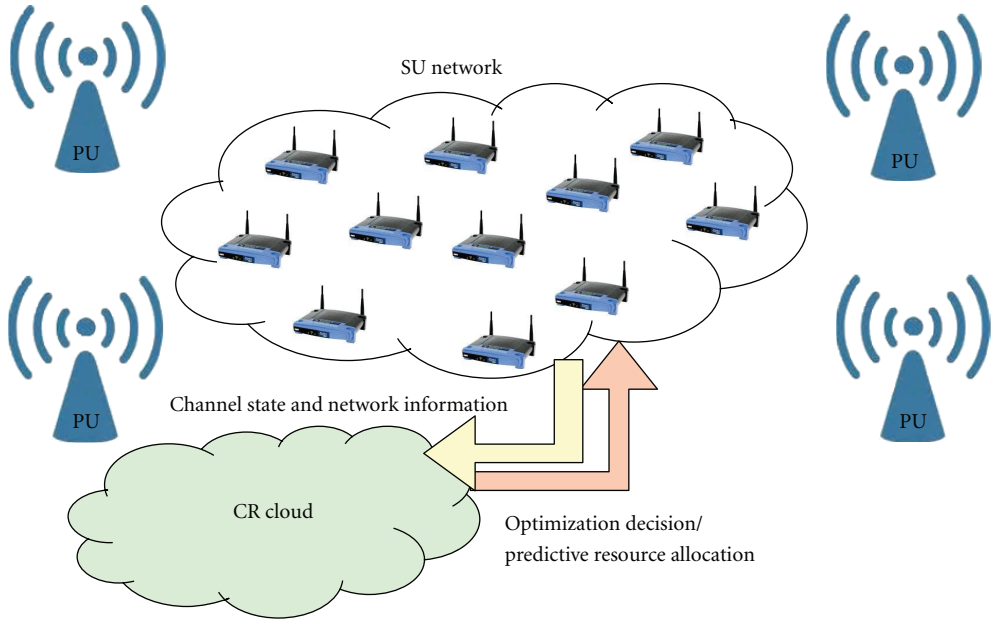

Figure 5: Cloud computing for SS-SCR.

Table 4: Scheme B.

	Node set ($\mathbb{N}$)	Band-set ($\mathbb{M}$)	Session set ($\mathbb{L}$)	$P_{\text{avl}_i}(W)$
(IIIa)	All SUs, PU Tx 2, PU Rx 2	$\mathbb{M}_2$	PU 2	P_{node_i}
(IIIb)	All SUs	$\mathbb{M}_2$	SUs	P_{node_i}
(IIIc)	All SUs	$\mathbb{M}_1$	SUs	Min $P_{\text{node}_i} - P_{\text{cons}_{\text{IIIa}i}}$, $P_{\text{node}_i} - P_{\text{cons}_{\text{IIIb}i}}$

dissemination of the decision throughout the network, are conducted [13]. It is followed by the data interval in which the PUs and SUs communicate using the designated resources. Based on the predicted PU activity, it can be decided when the different solutions of the joint resource allocation are to be applied. The prediction may be corroborated with spectrum sensing to protect the PU 1 from the SU's interference. The *time incentive* can be computed in the control interval itself, to determine when the SUs can access the *SCR* band. An important underlying assumption for the successful execution of the SS-SCR scheme, as well as Schemes A and B (included for comparison), is that the solution time for the optimization problem on the available spectrum is less than the spectrum hole created by the inactivity of PU 1.

Discontiguous OFDM (D-OFDM) is used at the physical layer, which allows the relays to decode only a fraction of the total subcarriers. A control channel is dedicated for all the signalling that enables and coordinates the entire SS-SCR scheme.

8. Cloud Computing for SS-SCR

In *SS-SCR*, the SU nodes are involved with the following tasks, (i) spectrum sensing, (ii) collaborative spectrum sensing decision algorithms, (iii) machine learning algorithms for PU activity prediction based on recorded history, (iv) solving the cross-layer optimization problems for resource allocation and (v) software defined radio (SDR) technologies for reconfiguration. Most of these operations involve both processing vast volume of data (depending on the network size and parameters) and processing it fast. The cognitive SU nodes may have limited computing and storage capability, which may prevent them from realizing their full potential. In such a situation, shifting some of the operations to the *cloud* may drastically improve the performance of the system [25–27]. *Cloud computing* is a recent technology revolution that is shaping the world. However, the decision to exploit the vast computational resources of the *cloud* should be governed by the volume of data and computational complexity, as well as time sensitivity. Primarily for the tasks of PU activity prediction and solving the cross-layer optimization (especially in a large network), the *cloud* may be of great use in *SS-SCR* (Figure 5). A low latency, high-bandwidth, reliable link is needed between the SU network and the *cloud*; else the connectivity may become a performance bottleneck.

9. Simulation Results and Discussion

We have simulated a network with the nodes randomly distributed in an area of 10 square units (Figure 8). Nodes 1 and 9 represent PU Tx 1-PU Rx 1, on the band-set of which *Sense-and-Scavenge (SS)* takes place. Nodes 10 and 11 represent PU Tx 2-PU Rx 2, on the band-set of which

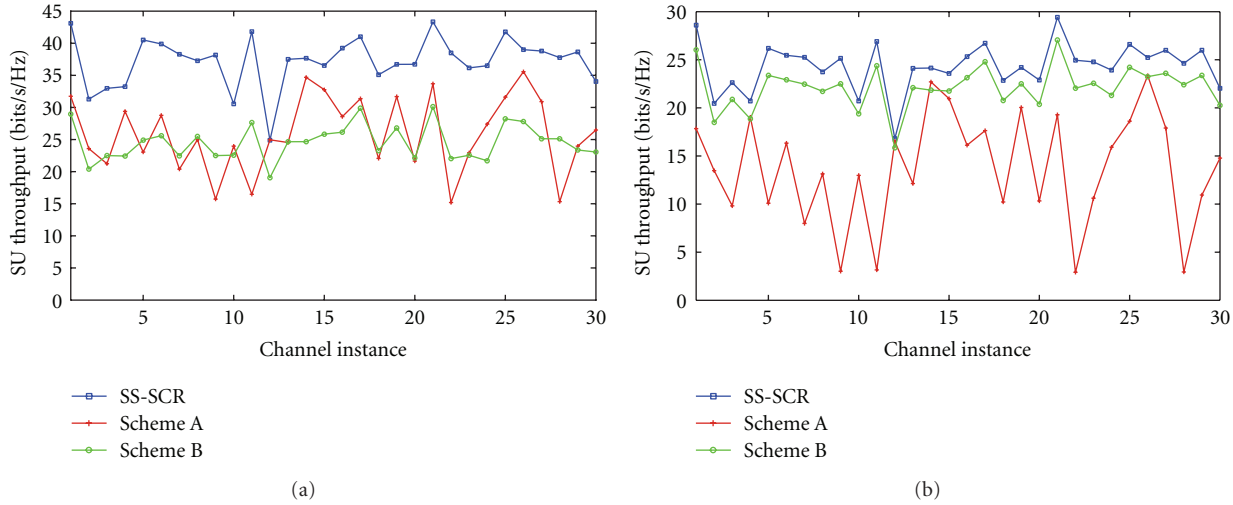

Figure 6: SU throughput versus channel instance (log-normal): (a) high mean OFF time, (b) high mean ON time.

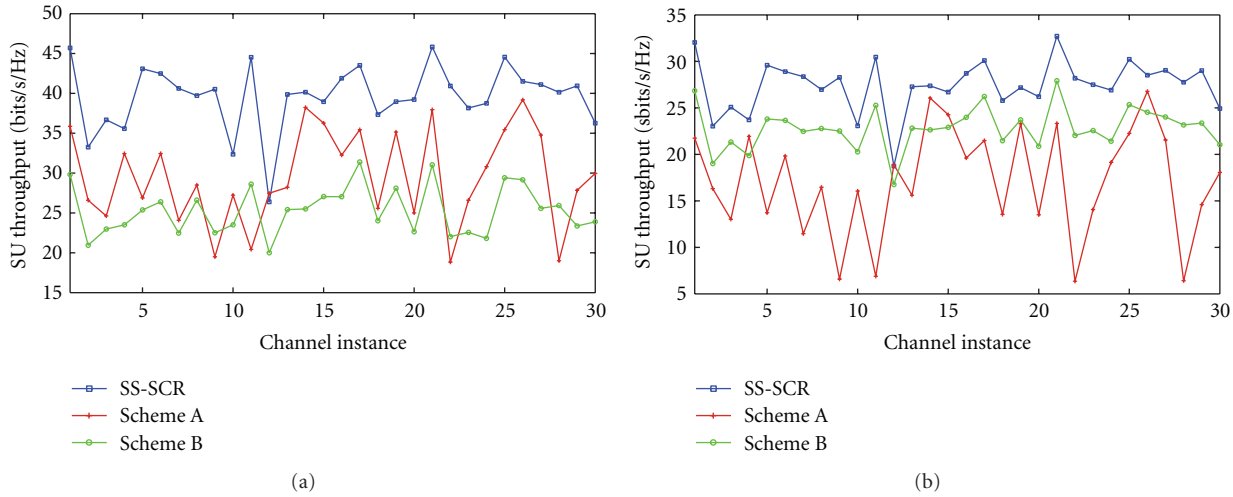

Figure 7: SU throughput versus channel instance (exponential): (a) high mean OFF time, (b) high mean ON time.

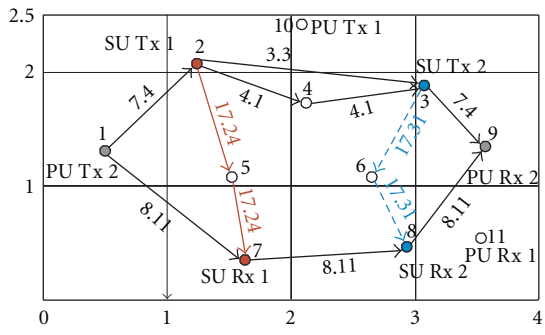

Figure 8: Flow allocation.

Symbiotic Cooperative Relaying (SCR) takes place. Nodes 2 to 8 represent the SU relay nodes.

All the links undergo the Rayleigh multipath fading, defined in the time domain by $\sum_{l=0}^{L-1} h_l \delta(t - lT)$ where h_l is the complex amplitude of path l and L is the number of channel taps. The lth channel coefficient between two nodes with a distance d between them is distributed as $N(0, 1/d^{\eta})$, and the frequency domain channel is given by its Fourier transform. The path loss exponent $\eta = 2.5$. The AWGN variance $\sigma^2 = 1e-4$. A 16 band OFDM system is considered on each link. Bands 1–8 are the *SS* bands, while 9–16 are the *SCR* bands. The OFDM subcarrier bandwidth is unit Hz.

The detection threshold is $P_T = 0.01$ W, the interference threshold is $P_I = 0.001$ W, the peak power constraint on each frequency band is $P_{\text{peak}} = 0.5$ W, and the node power constraint is $P_{\text{node}_i} = 3$ W (it is the same on each node i).

The environment has been simulated in MATLAB, while the LINGO [28] software has been used to solve the MINLP problem.

Figures 6(a) and 6(b) depict the sum SU throughput (bits/sec/Hz) for the proposed *SS-SCR* scheme with respect to 30 independent channel instances. It is compared with Schemes A and B, which consider *SS* and *SCR* separately, on

Table 5: Results for SS-SCR.

Edge (i, j)	Frequency band $*$ power (W) $x_{ij}^{(m)} * P_{ij}^{(m)}$
(1,2)	[0 0 0 0 0 0 0 0 0 0 0.08 0.5 0.5 0 0 0 0]
(1,7)	[0 0 0 0 0 0 0 0 0 0 0 0 0 0 0.5 0.412 0.5 0.5]
(2,3)	[0 0 0 0 0 0.5 0.486 0 0 0 0 0 0 0 0 0 0]
(2,4)	[0 0 0 0 0 0 0 0 0 0.380 0 0 0 0 0.5 0 0 0]
(2,5)	[0 0.017 0.023 0.053 0.073 0 0 0 0 0 0 0 0 0 0.053 0.023 0.389]
(3,6)	[0.495 0.240 0.028 0.021 0 0 0 0 0 0 0 0 0 0.081 0.029 0.5 0.028 0.075]
(3,9)	[0 0 0 0 0 0 0 0 0 0.5 0.5 0.5 0 0 0 0 0]
(4,3)	[0 0 0 0 0 0.5 0 0 0 0.5 0 0 0 0 0 0 0 0]
(5,7)	[0 0 0 0 0 0 0.0522 0.5 0.5 0.5 0.5 0.5 0.5 0.447 0 0 0 0]
(6,8)	[0 0 0 0 0 0.5 0.5 0.5 0.471 0.028 0.5 0.5 0 0 0 0 0]
(8,9)	[0 0 0 0 0 0 0 0 0 0 0 0 0 0 0.215 0.5 0.5 0.5 0.5]

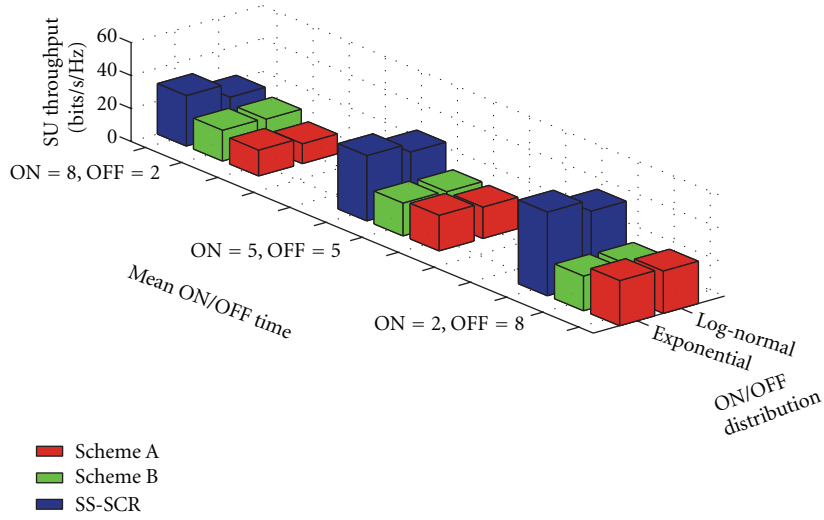

Figure 9: SU throughput versus mean ON/OFF time: log-normal and exponential.

their respective bands. Each of the values are averaged over 100 time frames, each of 10 sec duration. Two SU sessions are assumed, with nodes 2–7 forming the first pair and nodes 3–8 forming the second pair. The ON and OFF periods of PU 1 are each assumed to follow a log-normal distribution. In Figure 6(a), the mean ON time of PU 1 (μ_{ON}) is 2 and the mean OFF time (μ_{OFF}) is 8, while the variance of each distribution ($\sigma^2_{\text{ON}} = \sigma^2_{\text{OFF}}$) is 10. It is observed that Scheme A performs better (on an average) than Scheme B since it gives preference to the SUs to communicate on the *SS* band, which is free most of the time (mean OFF time of PU 1 is higher). In Figure 6(b), the mean ON time of PU 1 (μ_{ON}) is 8 and the mean OFF time (μ_{OFF}) is 2, while the variance of each distribution ($\sigma^2_{\text{ON}} = \sigma^2_{\text{OFF}}$) is 10. It is observed that Scheme B performs better (on an average) than Scheme A because it gives preference to PU 2's relaying and consequently creates a higher *time incentive* for the SUs to communicate, while PU 1 provides few opportunities for the SUs to communicate on its band (mean OFF time of PU 1 is lower). *SS-SCR* consistently performs better than the disjoint *SS* and *SCR* schemes, since the complete band-set, $\mathbb{M}_1 \cup \mathbb{M}_2$, is available in every time interval for the SU's communication with the total node power budget. Figures 7(a) and 7(b) depict a similar trend for the exponential distribution of PU 1. In Figure 7(a), $\mu_{\text{OFF}} = \sigma_{\text{OFF}} = 8$ and $\mu_{\text{ON}} = \sigma_{\text{ON}} = 2$, while in Figure 7(b), $\mu_{\text{OFF}} = \sigma_{\text{OFF}} = 2$ and $\mu_{\text{ON}} = \sigma_{\text{ON}} = 8$.

To illustrate the results of the cross-layer optimization problems, the band assignment and power allocation for a particular channel instance for *SS-SCR* (Case Ia) are shown in Table 5. The corresponding flow (bits/sec/Hz) is shown in Figure 8.

Figure 9 demonstrates the average sum SU throughput with different mean ON and OFF times of the log-normal and exponential distributions (fixed variance $\sigma^2_{\text{ON}} = \sigma^2_{\text{OFF}} = 10$). It is observed that when the mean OFF time is higher and ON time is lower, Scheme A performs better than Scheme B, for reasons described earlier. But as the OFF time reduces and the ON time increases, the trend reverses. For equal mean ON and OFF times, both Schemes A and B perform similarly. *SS-SCR* is consistently better than the previous two schemes, but its performance degrades and approaches that of Scheme B as the mean ON time increases. This is because

the band-set of PU 1 is available for too short a duration for it to exploit the channel diversity. The above discussion holds true for log-normal and exponentially distributed ON/OFF periods of PU 1.

10. Conclusion

We have proposed a novel *SS-SCR* scheme to be deployed in CR networks with multiple PUs, some of which have weak direct links. On the spectra of such licensed users *SCR* is enabled, while on the other PUs' spectra conventional *SS* is implemented. The hybrid *SS-SCR* scheme results in a better utilization of the available resources (time, bandwidth, power) by means of the formulated cross-layer optimization problems. Its performance is compared, for different PU activity patterns on the *SS* bands, with those schemes which consider *SS* and *SCR* separately and perform disjoint resource allocation. Simulation results depict that the *SS-SCR* scheme with joint resource allocation gives a higher net SU throughput as compared to the other schemes. Further, the usefulness of *cloud computing* is illustrated to realize the full potential of *SS-SCR*.

Appendix

If D_{off} is the random variable which describes the OFF period of the PU activity and if it follows the log-normal distribution, its probability density function (PDF) is given by

$$f_{\text{off}}(t;\mu,\sigma) = \frac{1}{t\sigma\sqrt{2\pi}} e^{-(\ln t-\mu)^2/2\sigma^2}, \quad t > 0. \tag{A.1}$$

μ and σ denote the mean and standard deviation, respectively.

In case of the exponential distribution,

$$f_{\text{off}}(t;\lambda) = \lambda e^{-\lambda t}, \quad t \geq 0. \tag{A.2}$$

The mean and standard deviation are both given by $1/\lambda$.

Acknowledgments

This work has been supported in part by the Ministry of Communication and Information Technology, Government of India, New Delhi. The work has also been supported by Microsoft Corporation and Microsoft Research India under the Microsoft Research India PhD Fellowship Award 2009.

References

[1] S. Haykin, "Cognitive radio: brain-empowered wireless communications," *IEEE Journal on Selected Areas in Communications*, vol. 23, no. 2, pp. 201–220, 2005.

[2] H. Zhang, "Cognitive Radio Networking for Green Communications and Green Spectrum," http://www.comnets.org/keynote.html.

[3] K. W. Sung, S. L. Kim, and J. Zander, "Temporal spectrum sharing based on primary user activity prediction," *IEEE Transactions on Wireless Communications*, vol. 9, no. 12, pp. 3848–3855, 2010.

[4] J. Riihijärvi, J. Nasreddine, and P. Mähönen, "Impact of primary user activity patterns on spatial spectrum reuse opportunities," in *Proceedings of the European Wireless Conference (EW '10)*, pp. 962–968, ita, April 2010.

[5] M. Wellens, J. Riihijärvi, and P. Mähönen, "Empirical time and frequency domain models of spectrum use," *Physical Communication*, vol. 2, no. 1-2, pp. 10–32, 2009.

[6] F. Bouali, O. Sallent, J. Pérez-Romero, and R. Agustí, "Strengthening radio environment maps with primary-user statistical patterns for enhancing cognitive radio operation," in *Proceedings of the 6th International ICST Conference on Cognitive Radio Oriented Wireless Networks and Communications (CROWNCOM '11)*, pp. 256–260, 2011.

[7] O. Simeone, Y. Bar-Ness, and U. Spagnolini, "Cooperative cognitive radio," in *Cooperative Wireless Communications*, Y. Zhang, H. Chen, and M. Guizani, Eds., pp. 209–230, Auerbach, CRC Press, 2009.

[8] O. Simeone, I. Stanojev, S. Savazzi, Y. Bar-Ness, U. Spagnolini, and R. Pickholtz, "Spectrum leasing to cooperating secondary ad hoc networks," *IEEE Journal on Selected Areas in Communications*, vol. 26, no. 1, pp. 203–213, 2008.

[9] J. Zhang and Q. Zhang, "Stackelberg game for utility-based cooperative cognitive radio networks," in *Proceedings of the 10th ACM International Symposium on Mobile Ad Hoc Networking and Computing (MobiHoc '09)*, pp. 23–31, May 2009.

[10] P. Xue, P. Gong, N. Cao, and D. K. Kim, "Symbiotic Architecture for the cognitive radio networks with amplify-and-forward relaying cooperation," in *Proceedings of the 18th Joint Conference on Communications and Information (JCCI '09)*, pp. 49–54, Jeju, Korea, 2009.

[11] P. Gong, J. H. Park, J. M. Yoo, B. S. Yu, and D. K. Kim, "Throughput maximization with multiuser non-selfish cognitive relaying in CR networks," in *Proceedings of the 4th International Symposium on Wireless and Pervasive Computing (ISWPC '09)*, February 2009.

[12] T. Nadkar, V. Thumar, U. B. Desai, and S. N. Merchant, "Symbiotic cooperative relaying in cognitive radio networks with time and frequency incentive," *Springer Telecommunications System Journal*.

[13] T. Nadkar, V. Thumar, G. Shenoy, A. Mehta, U. B. Desai, and S. N. Merchant, "A cross-layer framework for symbiotic relaying in cognitive radio networks," in *Proceedings of the IEEE International Symposium on Dynamic Spectrum Access Networks (DySPAN '11)*, pp. 498–509, deu, May 2011.

[14] T. Nadkar, V. Thumar, G. Shenoy, U. B. Desai, and S. N. Merchant, "Cognitive relaying with frequency incentive," in *Proceedings of the 54th Annual IEEE Global Telecommunications Conference (GLOBECOM '11)*, 2011.

[15] T. Nadkar, V. Thumar, G. Shenoy, U. B. Desai, and S. N. Merchant, "Cognitive relaying with time incentive: protocol design for multiple primary users," in *Proceedings of the IEEE 22nd International Symposium on Personal, Indoor and Mobile Radio Communications (PIMRC '11)*, pp. 577–582, 2011.

[16] V. Thumar, T. Nadkar, G. Shenoy, U. B. Desai, and S. N. Merchant, "Cognitive relaying with time incentive: multiple primary users," in *Proceedings of the IEEE 74th Vehicular Technology Conference (VTC '11)*, 2011.

[17] IEEE 802.16 WiMax, http://www.ieee802.org/16/.

[18] IEEE 802.22 WRAN, http://www.ieee802.org/22/.

[19] I. F. Akyildiz, W. Y. Lee, M. C. Vuran, and S. Mohanty, "NeXt generation/dynamic spectrum access/cognitive radio wireless networks: a survey," *Computer Networks*, vol. 50, no. 13, pp. 2127–2159, 2006.

[20] Y. Shi and Y. T. Hou, "A distributed optimization algorithm for multi-hop cognitive radio networks," in *Proceedings of the 27th IEEE Communications Society Conference on Computer Communications (INFOCOM '08)*, pp. 1966–1974, April 2008.

[21] J. Zhang, Z. Zhang, H. Luo, and A. Huang, "A column generation approach for spectrum allocation in cognitive wireless mesh network," in *Proceedings of the IEEE Global Telecommunications Conference (GLOBECOM '08)*, pp. 3091–3095, December 2008.

[22] Y. Zeng, Y. C. Liang, A. T. Hoang, and R. Zhang, "A review on spectrumsensing for cognitive radio: challenges and solutions," *Eurasip Journal on Advances in Signal Processing*, vol. 2010, Article ID 381465, 2010.

[23] P. Dimitri Bertsekas, *Network Optimization—Continuous and Discrete Models*, Athena Scientific, Belmont, Mass, USA, 1998.

[24] T. M. Cover and J. A. Thomas, *Elements of Information Theory*, Wiley-Interscie, New York, NY, USA, 2nd edition, 2006.

[25] F. Ge, H. Lin, A. Khajeh et al., "Cognitive radio rides on the cloud," in *Proceedings of the IEEE Military Communications Conference (MILCOM '10)*, pp. 1448–1453, November 2010.

[26] C. H. Ko, D. H. Huang, and S. H. Wu, "Cooperative spectrum sensing in TV white spaces: when cognitive radio meets cloud," in *Proceedings of the IEEE Conference on Computer Communications Workshops (INFOCOM WKSHPS '11)*, pp. 672–677, April 2011.

[27] H. Harada, H. Murakami, K. Ishizu et al., "A software defined cognitive radio system cognitive wireless clouds," in *Proceedings of the 50th Annual IEEE Global Telecommunications Conference (GLOBECOM '07)*, pp. 294–299, November 2007.

[28] "LINGO: User's guide," LINDO Systems Inc., 2006.

Hindawi Publishing Corporation
Journal of Computer Networks and Communications
Volume 2012, Article ID 794572, 14 pages
doi:10.1155/2012/794572

Research Article

Optimal Pricing of Spectrum Resources in Wireless Opportunistic Access

Hanna Bogucka

Chair of Wireless Communications, Poznan University of Technology, ul. Polanka 3, 60-965 Poznan, Poland

Correspondence should be addressed to Hanna Bogucka, hbogucka@et.put.poznan.pl

Received 8 February 2012; Accepted 23 April 2012

Academic Editor: Luca Ronga

We consider opportunistic access to spectrum resources in cognitive wireless networks. The users equipment, or the network nodes in general are able to sense the spectrum and adopt a subset of available resources (the spectrum and the power) individually and independently in a distributed manner, that is, based on their local channel quality information and not knowing the Channel State Information (CSI) of the other nodes' links in the considered network area. In such a network scenery, the competition of nodes for available resources is observed, which can be modeled as a game. To obtain spectrally efficient and fair spectrum allocation in this competitive environment with the nodes having no information on the other players, taxation of resources is applied to coerce desired behavior of the competitors. In the paper, we present mathematical formulation of the problem of finding the optimal taxation rate (common for all nodes) and propose a reduced-complexity algorithm for this optimization. Simulation results for these derived optimal values in various scenarios are also provided.

1. Introduction

Opportunistic spectrum access and flexible and efficient spectrum allocation procedures as well are considered as measures to increase the utilization of the scarce radio resources in future wireless communication networks. Apart from the spectral efficiency, the Quality of Experience (QoE), and the associated fairness in resources distribution are in the focus of research towards the cognitive, opportunistic, and dynamic spectrum access. The spectrum allocation procedures are usually centralized, require the Channel State Information (CSI) of all links in the network, and involve the overhead traffic, which in turn occupies the scarce radio resources. For the future communication concepts, such as cognitive or opportunistic radio, the nodes are expected to take intelligent decisions on the amount of resources to be utilized in a distributed way, thus minimizing or eliminating the overhead traffic.

In this paper, we consider opportunistic acquisition of orthogonal frequency channels by the network nodes. An example of the multiple-access technique using such orthogonal channels is the well-known Orthogonal Frequency Division Multiple Access (OFDMA). In the opportunistic OFDMA, the network nodes are able to adopt a subset of accessible subcarriers (SCs) individually, as well as the transmission rate and power allocated to these SCs [1]. Below, we consider a more general scenario of the opportunistic access to frequency channels of any bandwidth, limited centralized management, and very limited control traffic, that is, there is no central frequency-channel scheduler, and no CSI exchange between the network nodes. Our approach to opportunistic spectrum allocation is related to noncooperative game theory and to the concept of pricing.

The game-theoretic scheduling for OFDMA has been considered in the literature as centralized and distributed SCs allocation. The centralized schemes allow for more efficient and fair spectrum utilization; however they require centralized management and a considerable amount of control traffic related to the CSI of all possible links in all considered frequency channels and to the information on the allocated channels. This information has to be exchanged or to be available at a central unit (e.g., at a base station of a cellular network) every time the channels qualities change for the nodes in the network area. Newest results for such centralized solutions based on cooperative complete information game models have been presented in [2–4]. Distributed decision

making, on the contrary, deploys noncooperative games and seeks for Nash Equilibrium (NE) as a game solution. However, for the spectrum allocation, only the complete-information games have been considered in the literature so far. We believe that such models cannot be considered for practical applications in dynamically changing wireless networks, since the complete knowledge of the CSI related to all links to be available at every other node would require a lot of control traffic between the nodes in dedicated control channels. This information would have to be sent every time the channels change, so in mobile environment, the control traffic would be comparable to the information-data traffic. Thus, noncooperative complete-information game models are only suitable for multicell environment, where the players are the base stations, which have the CSI of all links in their cell areas [5, 6], or in static wireless scenarios.

The concept of resource pricing (or coercive taxation) has been considered in the literature extensively for power allocation, for example, for OFDM and OFDMA in [7–9]. There, the resource that is taxed is the power used by the network nodes, and the goal is to maximize the sum throughput given the total allowable transmission power in the network. In these papers however, it has been assumed that the SCs distribution among the users has already been done somehow centrally.

Pricing has been also applied for distributed power and interference management in the network, for example, in [10] for the code-division multiple access. For this purpose the complete-information noncooperative game models have been formulated. Such game-theoretic problem formulation has practical application for interference management, due to the fact that the complete information on the interference level can be available for each player, since the nodes can measure it locally. However, for the spectrum management the problem is different.

Some papers, for example, [11–13] consider distributed allocation of resources based on pricing in a multicell scenario, where the base stations act as players. The pricing concepts developed for the multicell scenario, cannot be considered for the distributed resource allocation in decentralized networks, because contrary to a base station that may have the CSI of all links, a network node may only have the CSI of its own link. Another approach to price based spectrum management is based on iterative water filling, which allows all players to use the same frequency channels and adjust their power levels in these channels based on pricing function [14]. Definition of the pricing function for each player requires the CSI knowledge and exchange between the neighboring players, as well as the number of iterations. Similarly, in [15] the information exchange between the secondary and primary users is assumed for the spectrum leasing. In [16] the spectrum sharing is modeled as the oligopoly competition between the primary users and the Bertrand game model, which again requires the knowledge of the secondary users' CSI by the players (primary users). Although the above-mentioned works have contributed to significant advance in the game-theoretic price-based models for spectrum sharing, they all make an assumption on the complete information available for all players that relate to their links CSI or they narrow to the power and interference management.

In our earlier work [17], we have presented distributed SCs allocation interference-free method in a network of the OFDMA-based opportunistic radios. It aimed at rational and efficient spectrum utilization in both the uplink or downlink transmission. Rationality in our case means that apart from maximizing the spectral efficiency, the network and each individual node aim at lowering the cost of this efficiency (resulting from taxation of resources) and at increasing the QoE (resulting from the number of served nodes). These rationality measures have been reflected in the definition of the noncooperative game model with complete information, and in the utility function defined for each player (the network node). The definition of this game involved aggregation of the players, in such a way that each player (the network node) can view all other players as one, named the network-nodes community (NNC). The complete information required in this game does not include the individual CSI of the other network nodes, but only the local (single-link) CSI and the taxation rate. This way noncooperative game with full information is reasonable and practically applicable in the dynamically changing network scenarios.

Here, in this paper, we present a generalized framework for the taxation-based allocation of orthogonal frequency channels in the opportunistic radio. First, we show inappropriateness of the complete-information game models in the considered framework. Then, we consider selfish and social behavior of the players by appropriate definitions of the utility functions reflecting such behaviors. These utility functions include the linear-taxation summand dependent on the amount of the acquired spectrum resources. We aim at finding the optimal taxation rate to come up with a high overall network efficiency defined in two ways. We provide the mathematical description of the problem of finding the optimal tax rate, show that the problem complexity is NP hard, and present and examine the reduced-complexity algorithm for solving it.

In Section 2, we present the main idea of the proposed game-theoretic approach to distributed spectrum allocation and provide formal definitions of the considered games. In Section 3, we mathematically derive the amount of bandwidth each player is inclined to acquire. In Section 4, we present the reduced-complexity algorithm to obtain the optimal taxation, where the optimality is defined in a number of ways. The simulation results are presented in Section 5, and the work is concluded in Section 6.

2. Taxation-Based Models of Distributed Spectrum Allocation

We consider the scenery of multiple cognitive-radio nodes (or users) appearing in the opportunistic network area, that make use of the orthogonal frequency channels, for example, OFDMA subcarriers. It implies that the nodes do not have to apply any guard frequency bands to limit the out-of-band interference. The frequency correction at the

receiver is also assumed to be perfect. This scenery of the opportunistic and cognitive radio network is presented in Figure 1. The nodes are able to sense the radio environment, detect the parameter called tax rate available in a given area, detect available spectrum resources, and acquire a subset of these resources usable for their intended transmission, for example, peer-to-peer communication, an access to a cellular network or to any wireless network in general. The goal of each node is to make the best use of these resources, that is, obtain high data rate at the lowest cost. As a proof of our concept, we consider the freedom in the spectrum allocation, that is, theoretically even the smallest part of the spectrum can be used by a player. This theoretical assumption can be refined for practical applications, if we assume that the nodes demand the spectrum only if they can make use of it, that is, if there is a minimal contiguous part of the spectrum available for their intended communication (such as one OFDM subcarrier band) that may include the protection band to mitigate the interference to other transmissions.

Let us consider the resource acquisition procedure as a game, which each network node plays against the other nodes (the players). Let us assume that there are K players, and the available bandwidth is B. (For the simplicity of our considerations, in the remainder of this paper, we assume that B and K are fixed, although in dynamically changing network environment, the number of players, their demands, and the available bandwidth vary.) A single player decides what portion of the available bandwidth she is going to use. (Note that such a personification and female pronouns are established in the game-theoretic convention.) Selfish player aiming at her throughput maximization would occupy the whole available spectrum; however, such a behavior decreases the spectral efficiency and the capacity of the network, as well as the QoE of other players who cannot access the network. The problem is known as the Tragedy of Commons described in [18].

As a countermeasure for the problem of commons sharing and utilization, taxation of the resources is introduced. In our network scenery presented in Figure 1, the taxation rate is the same for all network nodes or users (the players). This tax rate is known in the considered area. It can be stored in an area database (among other parameters, required for the efficient operation of the cognitive or opportunistic users, e.g., the spectrum masks for available bands in a given location and time, primary-users detection thresholds, etc.) or transmitted by the elected master node in case, when the considered network operates independently from the area database in an ad hoc manner. It is being updated periodically and broadcasted in this area as one parameter among many other ones in a typical Broadcast Control CHannel (BCCH), or specifically defined Cognitive Pilot Channel (CPC) [19]. Let us stress that this broadcast transmission of a single parameter occupies really minor resources, contrary to the situation of transmitting full CSI of all links in the considered frequency band using dedicated channels.

2.1. Inappropriateness of the All Links Complete-Information Game Model. Let us first show that the complete-information game model which makes use of the CSI of all involved links is not suitable for our scenario. The utility function for player k in such a game, in which the concept of resource taxation is applied, reflects her throughput (revenue) and its related cost, and is defined as (Note that from this point, the mathematical analysis in this paper is performed in a continuous space for the sake of generality, however it can be easily translated into a discrete orthogonal channel scenario.)

$$\varsigma(w_k(f)) = \int_{B_1}^{B_2} \log_2[1 + \delta_k P_k(f)\gamma_k(f)w_k(f)]df - r_0 b_k, \tag{1}$$

where $w_k(f)$ is the function indicating the occupancy of the frequencies by player k ($w_k(f) = 1$ if frequency f is assigned to user k and $w_k(f) = 0$ otherwise), B_1 and B_2 are the lower and the upper bounds of the available spectrum ($B_2 - B_1 = B$), b_k is the amount of bandwidth the player acquires, $\gamma_k(f) = |H_k(f)|^2/\mathcal{N}_0$ is the Carrier-to-Noise Ratio (CNR) measured at the frequency f, $H_k(f)$ and $P_k(f)$ are the kth user's channel characteristic and the power spectral density allocated to this frequency, respectively, and $\mathcal{N}_0$ is the noise power spectral density. Let us note that for the case of orthogonal channels, interference that is usually added to noise equals zero. Moreover, in (1), δ_k is the factor (often called the Signal-to-Noise Ratio (SNR)-gap) depending on the assumed player's Bit Error Probability (BEP) P_{e_k}. (In case of M-QAM, $\delta_k = -1,5/\ln(0,5\,P_{e_k})$, while for $M \geq 4$ and the SNR in the range of 0–30 dB it can be set more precisely as $\delta_k = -1,5/\ln(5\,P_{e_k})$ [20].) Finally, in the above equation, r_0 is a linear tax rate.

Since every channel can be used by a sole player:

$$\begin{aligned} &\forall f \exists! k : w_k(f) = 1, \\ &b_k = \int_{B_1}^{B_2} w_k(f)df. \end{aligned} \tag{2}$$

To find the NE in such a game, we shall be solving this problem numerically. This numerical representation of finding the NE is the binary linear programming problem, that is, for a given set of $\gamma_k(f)$ values for all K nodes and for a considered number of available channels we shall find binary values $w_k(f)$ for a given r_0. Then, looking for optimum r_0 to maximize some goal function, for example, the network sum throughput, would be even more complex. Note, that solution of such a defined problem would require the knowledge of all $\gamma_k(f)$ by every node, and thus, as mentioned before such a model for resource allocation is not practical.

2.2. Game Models Using Only the Local CSI. To narrow the space of this analysis and to eliminate the necessity for complete information concerning other players' strategies and payoffs, we propose to treat the rest of the players as a whole (the NNC). Note that NNC is not formally organized

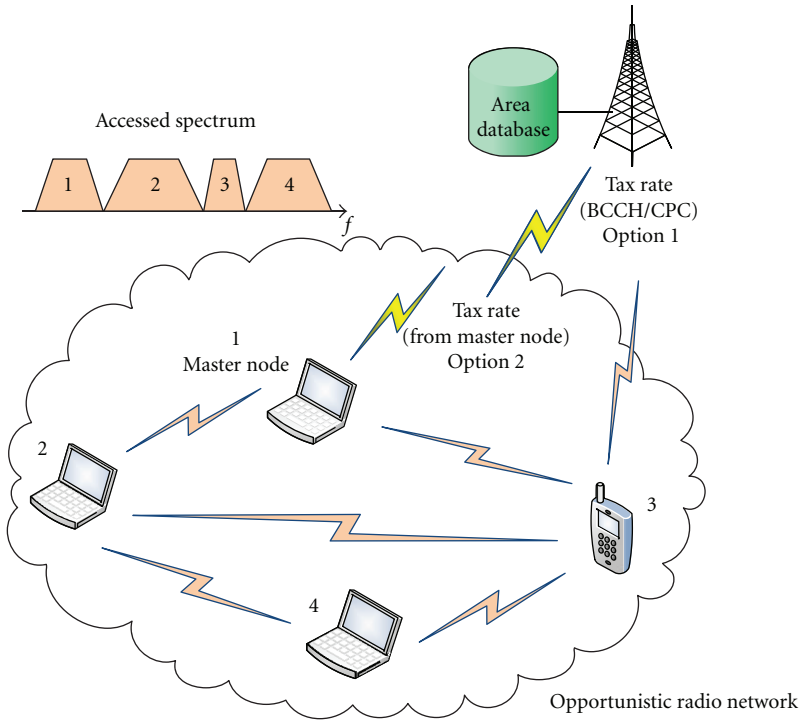

Figure 1: The scenery of the cognitive radio network with the taxation-based opportunistic spectrum access.

in any way. It is only viewed as such by a single player. Moreover, we let the players take decisions independently and subsequently one after another, as they appear in the network. It is a usual case in all wireless networks that some collision avoidance mechanism is implemented, or an access to decision-making entity (e.g., base-station) makes use of the random access channel to avoid taking decisions at the same time. We also limit the players in the maximum amount of bandwidth they can take at a time as a countermeasure for their greedy behavior, and let this maximum allowed bandwidth be B_I. The rationale behind such a limitation is proved in [21].

Let us first look at the utility defined for the kth player so, as to reflect the player's throughput:

$$\zeta_k(b_k) = \int_{f\in \mathbf{S}_k} \log_2[1+\delta_k P_k(f)\gamma_k(f)]df - r_0 b_k, \quad (3)$$

where $\mathbf{S}_k$ is the (noncountable) set of frequencies player k occupies. Let us note that before a decision is taken by player k, she senses the available spectrum resources and knows which frequency bands are already occupied (the amount of available bandwidth for the kth player is B_k, and there is no possibility that different players acquire the same frequencies: $\forall k \neq j : S_k \cap S_j = \emptyset$). Thus, the game model is dynamic. Moreover, the game for each player is two-dimensional only, what noticeably simplifies the problem.

The model defined above is not really a commonly understood game, since the decision of the NNC is not represented in the utility function (unless we call it a game against the radio environment, or a game against the nature as in [22]). This model reflects selfish behavior of the players, who care only for their own throughput. In the reminder of the paper we will call this model Selfish-Behavior Model.

In [17] we have proposed a noncooperative complete-information two-dimensional game, where the payoffs of both players (player k and the NCC at the kth game stage) reflect their decisions. In such a case, being the alternative to the framework discussed above, the strategy space of the considered kth player is the same (consists of possible number of the orthogonal channels the player acquires). The strategies of the NNC are the numbers of channels this community may occupy all together apart from the considered player. The utility function of the considered kth player is defined as follows:

$$\xi_k(b_k, c_k) = \left\{\frac{1}{B}\int_{f\in \mathbf{S}_k} \log_2[1+\delta_k P_k(f)\gamma_k(f)]df\right\} \cdot\{B_k - b_k - c_k\} - r_0 b_k, \quad (4)$$

where c_k is the amount of bandwidth that will be occupied by NNC, and B_k is the amount of bandwidth available at the kth game stage. One may interpret formula (4) as the total normalized throughput (throughput per frequency unit of the total available bandwidth B) which could be obtained by the new incoming players in case they occupied the remaining bandwidth and had the same average spectral efficiency as the considered player. This way, in the decision making on how much of the spectrum to occupy, the players factor the social aspect of the network (to serve multiple nodes) and not just their own benefit. In the reminder of the paper the game model with the kth player's utility function defined by (4) will be called the Social-Behavior Model.

Finally, the payoff for the NNC at the kth game stage can be defined as $\varepsilon_k = c_k$, where $c_k \in [0, \max(0, B_k - B_I)]$, that is, the number of resources that can be potentially occupied by NNC.

3. Optimal Choice of Spectrum Resources: The Players' Perspective

Let us now consider how the players choose their strategic options, and how to coerce their desired behavior to obtain specifically defined network benefit.

3.1. Selfish-Behavior Model. As the practical approach to the Selfish-Behavior Model (SelBM) described by the utility function (3), we propose to eliminate dominated (disadvantageous) strategies of the players. Taking the kth player's strongest frequencies (the ones that have the highest $\gamma_k(f)$ values) into account is in fact the elimination of dominated strategies of the considered player. Note, that from both the individual node and the whole network perspective, making use of the strongest channels results in higher spectral efficiency. Thus, the strategies of a single node are all possible channels of the strongest frequencies (from 0 to B_I). In order to find the optimum taxation, let us consider rewriting formula (3):

$$\dot{\zeta}_k(b_k) = \int_0^{b_k} \log_2[1 + \delta_k \dot{P}_k(f_k)\dot{\gamma}_k(f_k)]df_k - r_0 b_k, \tag{5}$$

where $\dot{\gamma}_k(f_k)$ is the function resulting from *ordering* (in the descending manner) of the continuous values of $\gamma_k(f)$: (*Ordering* operation described by (6) is a hypothetical bijective mapping, which cannot be generically defined for any continuous space of values and depends on $\gamma_k(f)$. This operation involves mapping of both the domain arguments and the codomain images of $\gamma_k(f)$ to new arguments and images of $\dot{\gamma}_k(f_k)$ belonging to the same domain and codomain, respectively. For a discrete set of values ordering can be done by a standard sorting algorithm.)

$$\dot{\gamma}_k(f_k) \longleftrightarrow \gamma_k(f) : \forall n, m f_{k_n} \le f_{k_m} \Longrightarrow \dot{\gamma}_k(f_{k_n}) \ge \dot{\gamma}_k(f_{k_m}), \tag{6}$$

and $\dot{P}_k(f_k)$ is the power spectral density resulting from the optimal power allocation for a total-power constraint, that is, from the water filling. Note that this ordering takes place at every stage, so in (5), the lower integration endpoint is always equal to zero. Moreover, as mentioned before

$$b_k \le \min\{B_I, B_k\}, \tag{7}$$

where B_I is the maximum allowable bandwidth one player can take at a time, and B_k is the bandwidth available at the kth game stage (for the kth player). We also limit our choices of b_k to only useful frequencies, that is,

$$b_k \le B_{\mathrm{WF}_k}, \tag{8}$$

where B_{WF_k} is the useful bandwidth after the water-filling, that is, the bandwidth, in which: $\dot{P}_k(f_k) > 0$ for all $f_k \in [0, B_{\mathrm{WF}_k}]$. In such a case:

$$\forall f_k \le b_k : \dot{P}_k(f_k) = \frac{1}{\gamma_{0k}(b_k)} - \frac{1}{\delta_k \dot{\gamma}_k(f_k)}, \tag{9}$$

where $1/\gamma_{0k}(b_k)$ is the water level obtained in the water-filling algorithm over the acquired bandwidth b_k of player k. The utility function $\dot{\zeta}_k(b_k)$ can be thus expressed as:

$$\dot{\zeta}_k(b_k) = \int_0^{b_k} \log_2[\delta_k \dot{\gamma}_k(f_k)/\gamma_{0k}(b_k)]df_k - r_0 b_k. \tag{10}$$

It can be easily shown that the above-defined function is concave, (For all b_k defined by (7) and (8), the first summand is concave and monotonically increasing because $\delta_k \dot{\gamma}_k(f_k)/\gamma_{0k}(b_k) > 1$ for all f_k, and the second summand is linearly decreasing with b_k) so we may find its maximum (as each rational player would do) by solving the following equation:

$$\frac{\partial}{\partial b_k}\dot{\zeta}_k(b_k) = 0. \tag{11}$$

As derived in Appendix A (formula (A.10)):

$$\frac{\partial}{\partial b_k}\dot{\zeta}_k(b_k) = \mathcal{F}_k(b_k) - r_0, \tag{12}$$

where $\mathcal{F}_k(b_k)$ can be defined in a number of ways depending on the player's CNR characteristic $\gamma_k(f)$, and its resulting sorted values at the kth game stage $\dot{\gamma}_k(f_k)$. As derived in Appendix A in (A.11) for the two-path propagation model it can be approximated as

$$\begin{aligned}\mathcal{F}(b_k) \simeq{}& \log_2\{A_k\delta_k[1 + \cos(2\pi b_k\tau_k - \varphi_k)]\} \\ &+ \log_2\left\{b_k^{-1}\left[\Gamma_k + \frac{1}{2\pi\tau_k A_k\delta_k}\left[\mathrm{tg}\left(\pi b_k\tau_k - \frac{\varphi_k}{2}\right)\right.\right.\right. \\ &\left.\left.\left. -\mathrm{tg}\left(\frac{\varphi_k}{2}\right)\right]\right]\right\} + \frac{b_k}{\ln 2} \\ &\times\left\{\Gamma_k + \frac{1}{2\pi\tau_k A_k\delta_k}\left[\mathrm{tg}\left(\pi b_k\tau_k - \frac{\varphi_k}{2}\right) - \mathrm{tg}\left(\frac{\varphi_k}{2}\right)\right]\right\}^{-1} \\ &\cdot\left\{2A_k\delta_k\cos^2\left(\pi b_k\tau_k - \frac{\varphi_k}{2}\right)\right\}^{-1},\end{aligned} \tag{13}$$

where the A_k, φ_k, and τ_k are the parameters of the considered multipath propagation model depending on the signal attenuation, average phase difference between the arriving multipath signal components, and the multipath delay spread (see Appendix A). Thus, by solving (11) we obtain the amount of bandwidth b_k^* the kth player is inclined to acquire

$$b_k = b_k^* : \mathcal{F}\left(b_k^*\right) = r_0. \tag{14}$$

Note, that for a given r_0, user k can find b_k^*, not knowing other players CSI, and this finding is independent from other players' choices.

3.2. Social-Behavior Model. Let us now consider formula (4) reflecting the Social Behavior Model (SocBM) in the form with ordered values of $\gamma_k(f)$ (similarly as in the previous section):

$$\dot{\xi}_k(b_k, c_k) = \frac{1}{B}\left\{\int_0^{b_k} \log_2[1 + \delta_k \dot{P}_k(f_k)\dot{\gamma}_k(f_k)]df_k\right\} \cdot\{B_k - b_k - c_k\} - r_0 b_k, \tag{15}$$

Based on (6)–(9), the above formula can be easily (again similarly as in the previous section) converted to

$$\dot{\xi}_k(b_k, c_k) = \frac{1}{B}\left\{\int_0^{b_k} \log_2[\delta_k \dot{\gamma}_k(f_k)/\gamma_{0k}(b_k)]df_k\right\} \cdot \{B_k - b_k - c_k\} - r_0 b_k. \tag{16}$$

It can be shown that function (16) is concave, (For all b_k defined by (7) and (8), the first factor in the first summand is concave and monotonically increasing, the second factor in the first summand is linearly decreasing with b_k, and so is the second summand.) so we may find its maximum (as each rational player would do) by solving the following equation:

$$\frac{\partial}{\partial b_k}\dot{\xi}_k(b_k, c_k) = 0. \tag{17}$$

The derivative $(\partial/\partial b_k)\dot{\xi}_k(b_k, c_k)$ is defined by formula (B.1) obtained in Appendix B, whose simplified form is the following:

$$\frac{\partial}{\partial b_k}\dot{\xi}_k(b_k, c_k) = \mathcal{G}_k(b_k, c_k) - r_0, \tag{18}$$

where $\mathcal{G}_k(b_k, c_k)$ can be defined as in (B.3) for rural areas. (We do not repeat its long formula here. See Appendix B for its definition.) Thus, by solving (16) we obtain the amount of bandwidth b_k^* which the kth player is inclined to acquire taking into account the considered amount of bandwidth to be occupied by the NNC at the kth game stage:

$$b_k(c_k) = b_k^*(c_k) : \mathcal{G}\left(b_k^*\right) = r_0. \tag{19}$$

In other words, $b_k^*(c_k)$ is the best-response function in the considered two-dimensional game.

Let us recall that the payoff of the NNC is defined as $\varepsilon_k = c_k$, where $c_k \in [0, \max(0, B_k - \mathrm{B}_I)]$ and is not dependent on the strategy of the kth player b_k. Thus, the NNC would always choose the strategy $c_k^* = \max(0, B_k - B_I)$ resulting in its highest possible payoff. For this NNC strategy (c_k^*) and for $b_k^*(c_k^*)$ we obtain the NE. Thus, for the calculated equilibrium strategies the players acquire a portion of bandwidth for their transmission.

4. Optimal Tax Rates

To obtain the desired behavior of the players and high overall network efficiency, the tax rate for the considered games (presenting either the SelBM or SocMB) should be properly chosen to obtain the maximum benefit for the whole network in the considered framework, for example, the maximum sum throughput reflecting the efficiency of the spectrum distribution. We can define our objective function as

$$\eta_{\mathrm{ST}} = \frac{1}{B}\sum_{k=0}^{K-1}\int_0^{b_k^*} \log_2\left[\delta_k \dot{\gamma}_k(f_k)/\gamma_{0k}\left(b_k^*\right)\right]df_k, \tag{20}$$

which is the sum throughput (ST) of all players averaged over the total available bandwidth B. Alternatively, we may look at maximizing the actual spectral efficiency (SE) of the transmission in the network (the sum throughput averaged over the actually used frequency bandwidth):

$$\eta_{\mathrm{SE}} = \frac{1}{\sum_{k=0}^{K-1} b_k^*}\sum_{k=0}^{K-1}\int_0^{b_k^*} \log_2\left[\delta_k \dot{\gamma}_k(f_k)/\gamma_{0k}\left(b_k^*\right)\right]df_k. \tag{21}$$

The next step would be to find the optimum value of r_0 to maximize either function (20) or (21). Note that many other definitions of the objective function are possible, that could reflect the fairness or proportional fairness in the distribution of resources, as well as other factors, for example, the percentage of used bandwidth or the percentage of served players. Below, we will examine the two objective functions defined above by (20) and (21) and show that some fairness in resource distribution is also achieved with a tax-rate optimal for (20).

The values of η_{ST} or η_{SE} depend on r_0, and on the values of $\dot{\gamma}_k(f_k)$. (This is because r_0 and $\dot{\gamma}_k(f_k)$ have the implication on b_k^* and on the throughput obtained by player k.) Moreover, the order of appearance of the players in the game matters, since $\dot{\gamma}_k(f_k)$ depends on $\dot{\gamma}_j(f_j)$ for all $j < k$ (frequencies allocated to players taking decisions before player k must be excluded from this player considerations). Unfortunately, both η_{ST} and η_{SE} are neither strictly concave or convex functions of r_0. In general, for low r_0 it pays off for all players to acquire the highest possible amount of bandwidth, irrespective to their channel qualities. As r_0 increases, it becomes affordable to acquire some bandwidth only for the players with good channel conditions (high $\gamma_k(f)$ and $\dot{\gamma}_k(f_k)$). Thus, in such a case, the spectral efficiency η_{SE} is increased, and the average sum-throughput η_{ST} may be decreased. However, when r_0 is too high, that is, close to the barrage tax rate, only very few players can afford some small portion of the frequency band, so a lot of available bandwidth is not used, and thus both the average sum-throughput η_{ST} and the spectral efficiency of the network η_{SE} are low. Thus, there exist some optimum values for r_0 to maximize either η_{ST} or η_{SE}:

$$r_0 = r_{\mathrm{ST}_0}^* : \eta_{\mathrm{ST}}\left(r_{\mathrm{ST}_0}^*\right) = \max \eta_{\mathrm{ST}}(r_0),$$
$$r_0 = r_{\mathrm{SE}_0}^* : \eta_{\mathrm{SE}}\left(r_{\mathrm{SE}_0}^*\right) = \max \eta_{\mathrm{SE}}(r_0). \tag{22}$$

However, it is not straightforward to determine these optimum values. (As mentioned before, η_{ST} and η_{ST} depend on $\dot{\gamma}_k(f_k)$ functions, which have different arguments f_k for different players, and on the order of players' appearance.)

To find this optimum, even numerically, is a complex NP-hard problem, and the optimization procedure has to be performed every time the users' channels change. Some simplifications can be obtained in finding this optimum in a proper time span (not necessarily shorter than the coherence time of the tracked processes: $\gamma_k(f)$), because the value of the optimum in the next time instant should be found close to the optimum value in the previous time instant. For this purpose we may apply a method that actually traces the variations of the objective function (η_{ST} or η_{SE}) rather than the variations of the players' channel conditions.

The considerations presented in this section for continuous orthogonal channels can be easily translated to discrete orthogonal channels, that is, to the case of having a set of N available channels (e.g., OFDM subcarriers) to be acquired by the players. In such a case, the integrations in (5), (10), (15), (16), (20), and (21) should be replaced by summations, and the value of b_k and b_k^* should be approximated by the discrete number of channels i_k of a particular bandwidth Δ_f (with a particular resolution). Moreover, as shown in [17], there exists the NE for the discrete orthogonal channels (like in OFDMA). Below, for such a case of the available bandwidth discretization, we present the optimal tax-rate-searching algorithm with reduced complexity tracing the instantaneous variations of the network-objective function η_{ST} around its maximal value.

Step 1. Initialize algorithm:
Determine N available channels of Δ_f bandwidth,
Determine the range of $r_0 \in [r_{\min}, r_{\max}]$,
Determine the increment of r_0: Δ_{r_0},
Determine acceptable value of η_{ST}: $\eta_{ST_{\min}}$,
Determine K, B_I, measure the players' $\gamma_k(f)$,
Determine the order of players' appearance.

Step 2. Find the b_k^* values for all considered tax-rates r_0.

Step 3. Calculate η_{ST} for all r_0.

Step 4. Find optimal tax-rate $r^*_{ST_0}$ that maximizes η_{ST}.

Loop 1:

Step L1.1. Monitor the network-objective function η_{ST}.
Step L1.2. If $\eta_{ST} < \eta_{ST_{\min}}$, go to Loop 2,
else go to Loop 1.

Step 5. Update (increase) $r^*_{ST_0}$: $r^*_{ST_+} := r^*_{ST_0} + \Delta_{r_0}$,

Step 6. Calculate the resulting $\eta_{ST_+} = \eta_{ST}(r^*_{ST_+})$,

Step 7. If $\eta_{ST_+} > \eta_{ST}$, go to Step 9
else go to Loop 3.

Loop 2: Repeat

Step L2.1. $r^*_{ST_0} := r^*_{ST_+}$,
Step L2.2. $\eta_{ST} := \eta_{ST_+}$,
Step L2.3. $r^*_{ST_+} := r^*_{ST_0} + \Delta_{r_0}$,
Step L2.4. Calculate $\eta_{ST_+} = \eta_{ST}(r^*_{ST_+})$,
Until $\eta_{ST_+} > \eta_{ST}$.

Step 8. Go to Step 12.

Step 9. Update (decrease) $r^*_{ST_0}$: $r^*_{ST_-} := r^*_{ST_0} - \Delta_{r_0}$,

Step 10. Calculate the resulting $\eta_{ST_-} = \eta_{ST}(r^*_{ST_-})$,

Step 11. If $\eta_{ST_-} > \eta_{ST}$, go to Loop 3
else go to Step 12.

Loop 3: Repeat

Step L3.1. $r^*_{ST_0} := r^*_{ST_-}$,
Step L3.2. $\eta_{ST} := \eta_{ST_-}$,
Step L3.3. $r^*_{ST_-} := r^*_{ST_0} - \Delta_{r_0}$,
Step L3.4. Calculate $\eta_{ST_-} = \eta_{ST}(r^*_{ST_-})$,
Until $\eta_{ST_-} > \eta_{ST}$.

Step 12. If $\eta_{ST} \geq \eta_{ST_{\min}}$
communicate new tax-rate and go to Loop 1,
else Warn: "No tax-rate meeting the objectives".

As it will be shown in the next section, η_{ST} is more appropriate as the network-objective function for the fairness of resource distribution among the players in the case of both SelBM and SocBM, and always has a maximum when B_I is properly chosen (not too small) for a given K and B. Analogous algorithm to the one presented below can be performed for searching the maximum of η_{SE}. The presented algorithm has reduced complexity due to the application of the following methods: optimum tax-rate searching around the previous optimum and optimization procedure running only when η_{ST} drops below the required value: $\eta_{ST_{\min}}$.

Alternatively, to reduce the rate of necessary calculations to solve the optimization problem, we may maximize the expected values of (20) or (21) over the set of random variables $\dot{\gamma}_k(f_k)$: $\overline{\eta}_{ST} = \mathbb{E}_{\dot{\gamma}_k}\{\eta_{ST}\}$, $\overline{\eta}_{SE} = \mathbb{E}_{\dot{\gamma}_k}\{\eta_{SE}\}$. Such definitions of the objective functions could be useful if we were able to approximate the expectation values with the average values and use them in a static (or slowly changing) environment. The resulting tax rate would approximate the optimum one (either $r^*_{ST_0}$ or $r^*_{SE_0}$) with unknown accuracy, while the optimization procedure can be performed off-line. This option is to be investigated in the future.

5. Numerical Results

Our simulation setup is the following. We have considered an available bandwidth B with the resolution $\Delta_f = B/256$, where Δ_f can be considered as the smallest spectrum unit, that can be occupied by orthogonal signals, for example, OFDM subcarriers. In our considered scenario, the total transmission power has been fixed. The power constraint for each link results from the distance between the transmitter

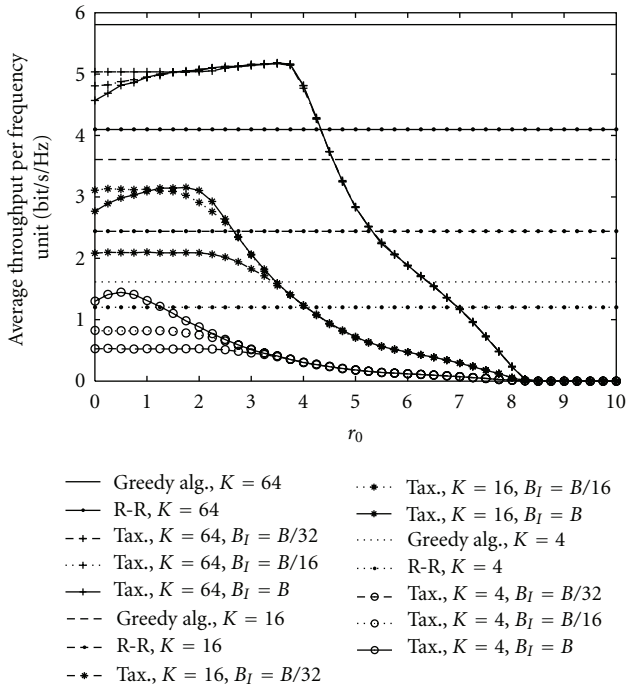

Figure 2: Average sum throughput η_{ST} versus the tax rate for SelBM; two-path channel model.

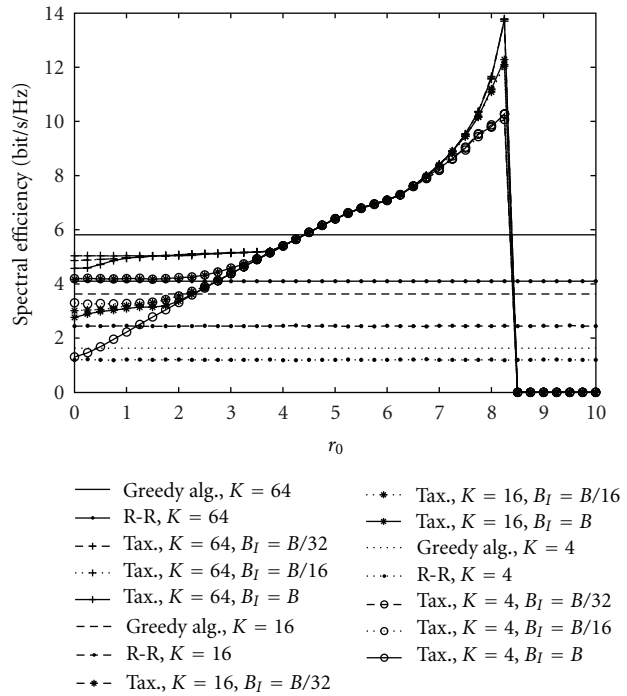

Figure 3: Spectral efficiency η_{SE} versus the tax rate for SelBM; two-path channel model.

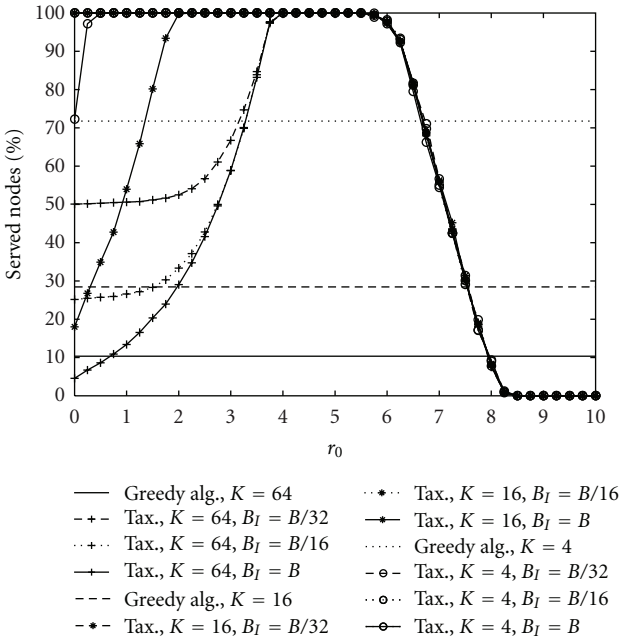

Figure 4: The percentage of served nodes versus the tax rate for SelBM; two-path channel model.

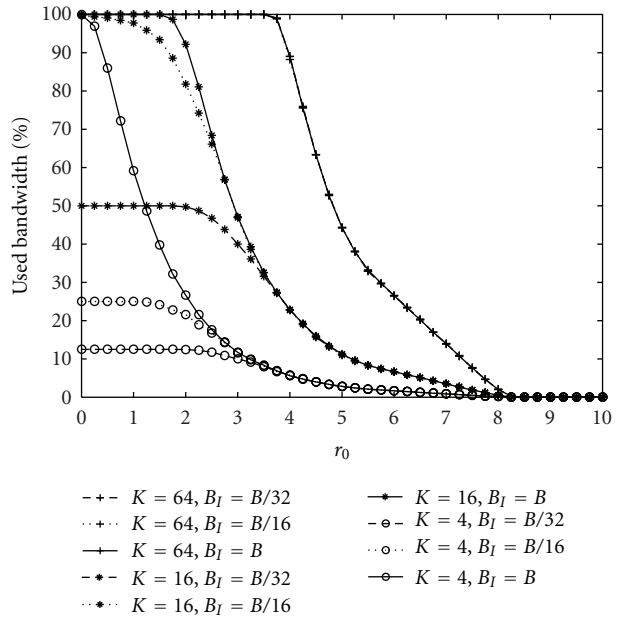

Figure 5: The percentage of used bandwidth versus the tax rate for SelBM; two-path channel model.

and the receiver and from the power-control mechanism. (Usually this mechanism is applied to combat the near-far effect and the interference between the users; however, here, we assume orthogonal frequency channels, so this mechanism is only used to assure the appropriate quality of the link, i.e., the required average SNR, which in our case has been set to 30 dB). For our simulation purposes, it has

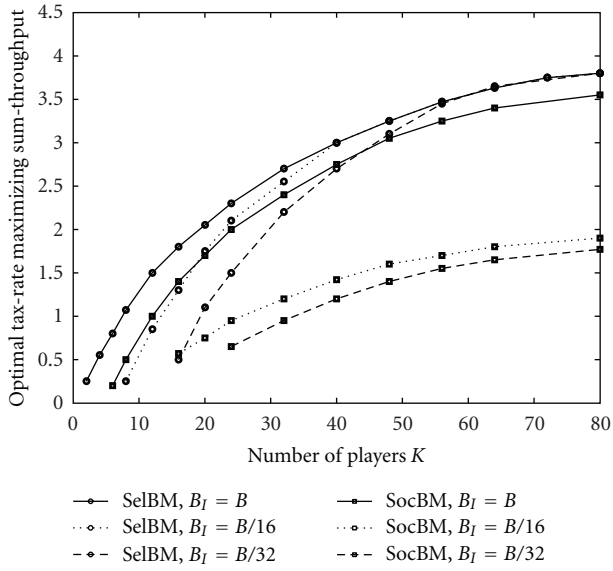

FIGURE 6: Optimal tax rate for sum throughput $r^*_{ST_0}$ versus the number of competing players for the SelBM and the SocBM; two-path channel model.

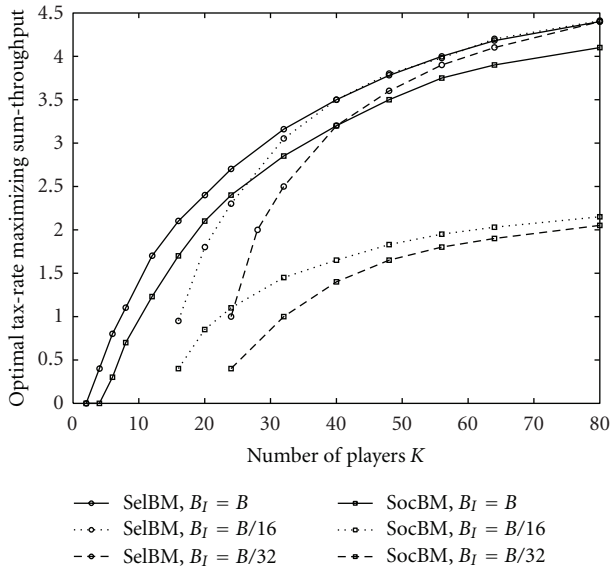

FIGURE 7: Optimal tax rate for sum throughput $r^*_{ST_0}$ versus the number of competing players for the SelBM and the SocBM; six-path channel model.

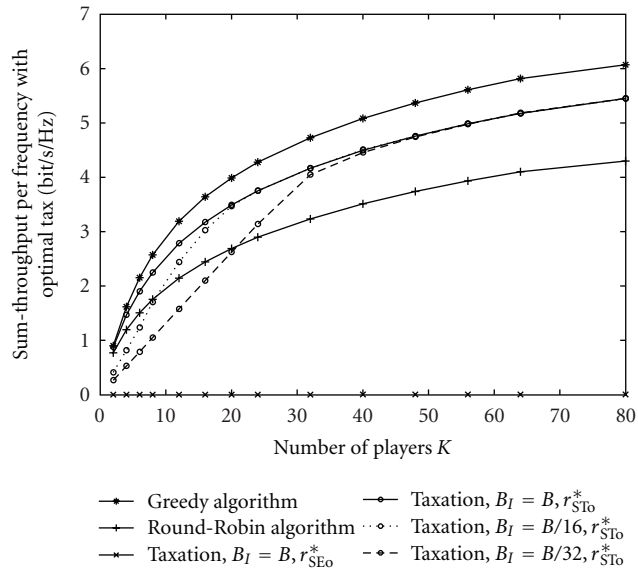

FIGURE 8: Average sum throughput for the optimal tax rate for both SelBM and SocBM; two-path channel model.

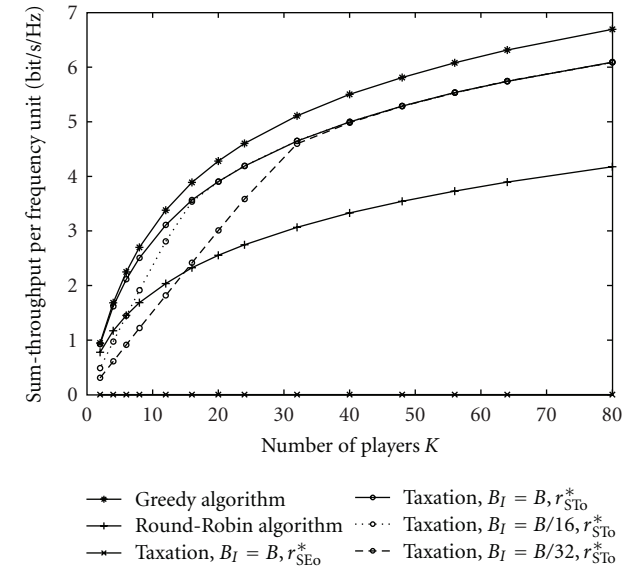

FIGURE 9: Average sum throughput for the optimal tax rate for both SelBM and SocBM; six-path channel model.

been assumed that the order of appearance of the players in a game is random. Furthermore, we assume that the power control mechanism has a tolerance of 3 dB, so that random deviation from the average SNR is possible for any node (average SNR $= (30 \pm 3)$ dB). This average SNR deviation (which also reflects the accuracy of power-control in modern radio systems) has been chosen to differentiate possible link qualities. Moreover, two example channel models have been compared. The first one is the two-path Rayleigh-fading channel with the delay spread ranging from 0 to $1/64$ of $1/B$, and the average power of the second path being -3 dB relative to the first path (such a model can be considered as suitable for rural environment). The second considered model is the six-path channel, with paths having the same power, and delays uniformly spread between 0 to $1/B$. (This is a test-channel model often used for the test of equalizers that reflects particularly hostile environment with very small coherence bandwidth and very deep fading.) We

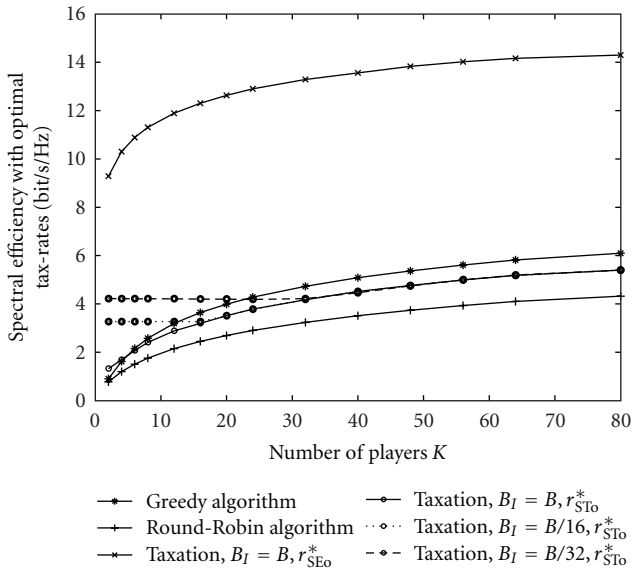

Figure 10: Spectral efficiency for the optimal tax rate for both SelBM and SocBM; two-path channel model.

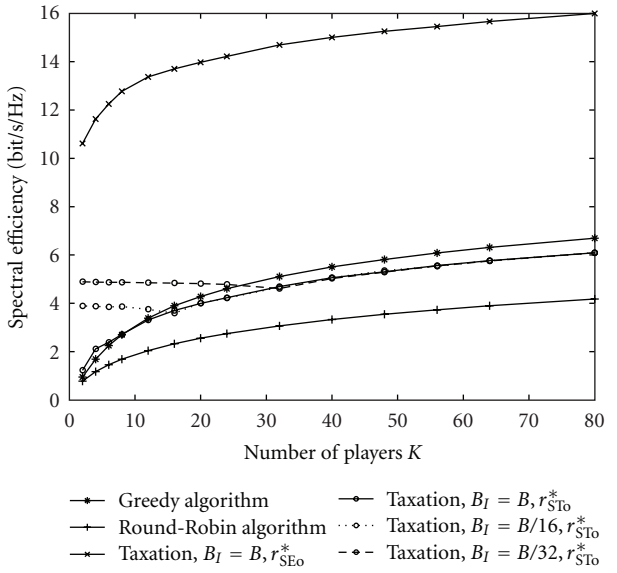

Figure 11: Spectral efficiency for the optimal tax rate for both SelBM and SocBM; six-path channel model.

have observed 1000 channel realizations and assumed the target BEP $P_{e_k} = 10^{-3}$ for all links (for all k).

For the comparison purposes, we present results of our proposed framework and the reduced-complexity algorithm of finding the optimal tax rate together with the results of the greedy algorithm (that assigns the frequencies to the players with the highest CNR values at these frequencies) and Round-Robin algorithm of resource distribution. Although both of these algorithms can be only implemented in a centralized manner, they give the two opposite extremes: either maximum spectral efficiency or maximum fairness for the case of the whole used bandwidth.

Let us first analyze the network performance in the case of the users' SelBM and the influence of the tax rate r_0, the restricted amount of bandwidth B_{I}, and the number of players K on the network behavior. In Figures 2 and 3 we observe the averaged sum throughput η_{ST} defined by (20) and the network spectral efficiency η_{SE} defined by (21), respectively, for the two-path channel model. As we can see, there is some optimum tax rate $r^*_{\mathrm{ST}_0}$ that maximizes η_{ST} when B_{I} is not too small for a given K. Otherwise, η_{ST} is constant for low tax rates, and then, for higher tax rates decreases to zero. The optimal tax rate $r^*_{\mathrm{SE}_0}$ that maximizes η_{SE} is close to the barrage tax.

To better understand the mechanism of increasing tax rates in the network, already discussed in the previous section, let us analyze Figures 4 and 5. There, the percentage of served nodes and the percentage of used bandwidth are shown versus the tax rate r_0. (We assume that the node is served if it is able to acquire a portion of bandwidth satisfying her target BEP.) As we can see, low taxes allow to utilize most of the bandwidth and serve most of the users, again when B_{I} is properly chosen. In general, restricting the players in the amount of bandwidth they can take at their turn has negative influence on η_{ST} (the maximum is always achieved for $B_I = B$) and on the percentage of used bandwidth, and positive influence on η_{SE} and the percentage of served nodes, but only for relatively low tax rates. For higher tax rates, for which η_{ST} and the percentage of used bandwidth dramatically drop, both η_{SE} and the percentage of served nodes are not dependent on B_I. Thus, our first conclusion is that for the fairness of the resource distribution, it is better to apply $B_I = B$, and calibrate just the tax rate to optimize η_{ST} rather than η_{SE}. Similar (analogous) conclusions can be derived for the SocBM and for the other channel model.

In Figures 6 and 7 we can observe the tax rates $r^*_{\mathrm{ST}_0}$ optimizing η_{ST} for both the SelBM and the SocBM and in the case of two-path and six-path channel models. These tax rates have been found using the algorithm defined in the previous section. As we can see, for the SelBM the optimum tax rates $r^*_{\mathrm{ST}_0}$ for different B_I, converge to the same value as K increases. It is not the case for the SocBM. Moreover, for the two-path channel model, the values of the optimum tax rate $r^*_{\mathrm{ST}_0}$ are higher than for the six-path channel model.

The tax-rate that optimizes η_{SE} does not depend on K. For the SelBM, it also does not depend on B_I, but only varies for different channel models. For the SocBM, $r^*_{\mathrm{SE}_0}$ depends on both, B_I and the channel model. This can be observed in Table 1.

In Figures 8 and 9 one can observe the average sum throughput η_{ST} resulting from the optimal taxation versus the number of competing players K, for both the SelBM and the SocBM and in the case of two-path (Figure 8) and six-path (Figure 9) channel models. In Figures 10 and 11 the network spectral efficiency η_{SE} is presented versus K for the same cases. Note, that for a given channel model the achievable average sum throughput η_{ST} is exactly the same for both behavior models: either SelBM or SocBM (although the respective optimal tax rates are different). The same

Table 1: Optimal tax rates $r^*_{\mathrm{SE}_0}$ maximizing the network spectral efficiency η_{SE} for all values of K.

Behavior	Two-path			Six-path		
Model	$B_I = B$	$B/16$	$B/32$	$B_I = B$	$B/16$	$B/32$
SelBM	8.3	8.3	8.3	9.65	9.65	9.65
SocBM	8.2	4.35	4.25	9.6	5.05	4.9

holds for the achievable spectral efficiency η_{SE}. The difference between the plots occurs for different channel models. The achievable η_{ST} as well as η_{SE} are higher for the six-path channel model than for the two-path channel model due to the fact that this six-path model presents higher diversity in the subbands qualities for each player, so the players can make better choices. Finally, we have observed that when the optimum tax rate $r^*_{\mathrm{ST}_0}$ is applied in either scenario, 99–100% of nodes are served.

Note, that our framework cannot result in the maximal achievable sum throughput, which can be only obtained when the problem described by (1) is solved, which assumes complete-information of all links CSI and K-dimensional game that can be solved in either cooperative or noncooperative manner.

6. Conclusions

Here above, we have presented a game-theory-related framework for distributed allocation of spectrum resources in the opportunistic radio access networks. Contrary to the methods presented in the literature so far, in our game models, we do not assume the complete knowledge of the players CSI. Each player has the information on her own CSI only. Additionally, the taxation-rate parameter available in a data base and mandatory in the considered area is made known to the players through the broadcast channel (BCCH or the CPC). This significantly reduces the amount of control traffic in the network when compared with the frequent exchange of the all links CSI in the dedicated channels. Above, we have proposed a reduced-complexity algorithm of finding and tracing the optimum tax-rate value maximizing the network objective function. Our presented framework and the algorithm of finding the optimal taxation-rate result in high network benefit reflected in the sum throughput, but also in fairness of resource distribution (understood as the number of served nodes). The simulation results show that it is more beneficial for the network and for the individual players to use taxation with the tax rate maximizing the network sum throughput rather than to additionally limit the users in the maximum bandwidth they can acquire at the time. It is also more beneficial than maximization of the network spectral efficiency due to better utilization of the spectrum resources and higher percentage of served nodes. Simulation results also show that in the considered scenarios, when the optimal tax rate is applied the achievable sum throughput per frequency unit is as high as 5.5–6 [bits/s/Hz] (depending on the considered propagation model) for sufficiently high number of players. Moreover, in such a case, 99-100% of nodes are served in the network, that is, are able to acquire some resources satisfying their target BEP.

Appendices

A.

Below, we calculate the derivative of $\dot{\zeta}_k(b_k)$:

$$\begin{aligned}\frac{\partial}{\partial b_k}\dot{\zeta}_k(b_k) &= \frac{\partial}{\partial b_k}\left\{\int_0^{b_k}\log_2[\delta_k\dot{\gamma}_k(f_k)/\gamma_{0k}(b_k)]df_k\right\}\\ &\quad-\frac{\partial}{\partial b_k}\{r_0 b_k\}\\ &= \frac{\partial}{\partial b_k}\left\{\int_0^{b_k}\log_2[\delta_k\dot{\gamma}_k(f_k)]df_k\right\}\\ &\quad-\frac{\partial}{\partial b_k}\left\{\int_0^{b_k}\log_2[\gamma_{0k}(b_k)]df_k\right\}-r_0.\end{aligned}\tag{A.1}$$

Because the one integrand in the first summand does not depend on b_k, and the one integrand in the second summand does not depend on f_k, further derivation of the above formula is the following:

$$\begin{aligned}\frac{\partial}{\partial b_k}\dot{\zeta}_k(b_k) &= \log_2[\delta_k\dot{\gamma}_k(b_k)]\\ &\quad-\frac{\partial}{\partial b_k}\left\{b_k\log_2[\gamma_{0k}(b_k)]\right\}-r_0\\ &= \log_2[\delta_k\dot{\gamma}_k(b_k)]-b_k\frac{\partial}{\partial b_k}\left\{\log_2[\gamma_{0k}(b_k)]\right\}\\ &\quad-\log_2[\gamma_{0k}(b_k)]-r_0\\ &= \log_2[\delta_k\dot{\gamma}_k(b_k)]-\frac{1}{\ln 2}\frac{b_k}{\gamma_{0k}(b_k)}\frac{\partial}{\partial b_k}\{\gamma_{0k}(b_k)\}\\ &\quad-\log_2[\gamma_{0k}(b_k)]-r_0.\end{aligned}\tag{A.2}$$

Now, this formula does not have a closed form, that is, $(\partial/\partial b_k)\dot{\zeta}_k(b_k)$ depends on the particular shapes of $\dot{\gamma}_k(b_k)$ and of $\gamma_{0k}(b_k)$ (where the later function in turn depends on the shape of the former). As an example, let us consider the rural area with the two-path propagation. In such a case, the channel power characteristic can be described as

$$\gamma_k(f) = |\alpha_k|^2\,|1-\beta_k\exp\{-j(2\pi f\tau_k-\varphi_k)\}|^2,\tag{A.3}$$

where α_k is the complex amplitude attenuation of the first path, β_k is the attenuation of the second path relative to the first path, τ_k is the multipath delay spread, and φ_k is average phase difference between the arriving multipath signal components. Let us denote $\phi_k = 2\pi f\tau_k - \varphi_k$. For the sufficient distance between the transmitting and receiving antennas $\beta_k \approx 1$. Consequently,

$$\begin{aligned}\gamma_k(f) &\simeq \alpha_k^2(1-\cos\phi_k+j\sin\phi_k)(1-\cos\phi_k-j\sin\phi_k)\\ &= 2\alpha_k^2(1-\cos\phi_k) = 2\alpha_k^2[1-\cos(2\pi f\tau_k-\varphi_k)].\end{aligned}\tag{A.4}$$

The above function is periodic and monotonically increasing for $\phi \in [0, \pi]$. Therefore, its sorted (in a descending order) version $\dot{\gamma}_k(f_k)$ can be approximated as

$$\dot{\gamma}_k(f_k) \simeq A_k[1 + \cos(2\pi f_k \tau_k - \varphi_k)], \tag{A.5}$$

where A_k is the proportionality constant.

Now, for our propagation model, let us find the formula for the water-level $\gamma_{0k}(b_k)$ dependent on the shape of function $\dot{\gamma}_k(f_k)$ and on the considered bandwidth b_k. To this end we will integrate both sides of (9) resulting in

$$\frac{b_k}{\gamma_{0k}(b_k)} = \Gamma_k + \int_0^{b_k} \frac{1}{\delta_k \dot{\gamma}_k(f_k)} df_k, \tag{A.6}$$

where Γ_k is the power limit for player k. Consequently

$$\gamma_{0k}(b_k) \simeq b_k \left\{ \Gamma_k + \int_0^{b_k} \frac{1}{A_k \delta_k [1 + \cos(2\pi f_k \tau_k - \varphi_k)]} df_k \right\}^{-1}, \tag{A.7}$$

and because $\int (1/\cos\phi_k) d\phi_k = \mathrm{tg}\phi_k/2$, we obtain

$$\gamma_{0k}(b_k) \simeq b_k \left\{ \Gamma_k + \frac{1}{2\pi\tau_k A_k \delta_k} \left[\mathrm{tg}\left(\pi b_k \tau_k - \frac{\varphi_k}{2}\right) - \mathrm{tg}\left(\frac{\varphi_k}{2}\right) \right] \right\}^{-1}. \tag{A.8}$$

Using the above expression we will derive the second term in (A.2):

$$\begin{aligned}
&\frac{b_k}{\gamma_{0k}(b_k)} \frac{\partial}{\partial b_k} \{\gamma_{0k}(b_k)\} \\
&\quad \simeq \left\{ \Gamma_k + \frac{1}{2\pi\tau_k A_k \delta_k} \left[\mathrm{tg}\left(\pi b_k \tau_k - \frac{\varphi_k}{2}\right) - \mathrm{tg}\left(\frac{\varphi_k}{2}\right) \right] \right\} \\
&\qquad \cdot (-b_k) \left\{ \Gamma_k + \frac{1}{2\pi\tau_k A_k \delta_k} \right. \\
&\qquad\qquad \left. \times \left[\mathrm{tg}\left(\pi b_k \tau_k - \frac{\varphi_k}{2}\right) - \mathrm{tg}\left(\frac{\varphi_k}{2}\right) \right] \right\}^{-2} \\
&\qquad \cdot \left\{ 2A_k \delta_k \cos^2\left(\pi b_k \tau_k - \frac{\varphi_k}{2}\right) \right\}^{-1} \\
&\quad = (-b_k) \\
&\qquad \times \left\{ \Gamma_k + \frac{1}{2\pi\tau_k A_k \delta_k} \left[\mathrm{tg}\left(\pi b_k \tau_k - \frac{\varphi_k}{2}\right) - \mathrm{tg}\left(\frac{\varphi_k}{2}\right) \right] \right\}^{-1} \\
&\qquad \cdot \left\{ 2A_k \delta_k \cos^2\left(\pi b_k \tau_k - \frac{\varphi_k}{2}\right) \right\}^{-1}.
\end{aligned} \tag{A.9}$$

We can now substitute (A.5)–(A.9) to (A.2), which results in

$$\frac{\partial}{\partial b_k} \dot{\zeta}_k(b_k) = \mathcal{F}_k(b_k) - r_0, \tag{A.10}$$

where the first term on the right-hand side of the above equation $\mathcal{F}_k(b_k)$ does not depend on r_0, and for the considered channel model can be approximated as

$$\begin{aligned}
\mathcal{F}_k(b_k) &\simeq \log_2\{A_k \delta_k [1 + \cos(2\pi b_k \tau_k - \varphi_k)]\} \\
&\quad + \log_2 \left\{ b_k^{-1} \left[\Gamma_k + \frac{1}{2\pi\tau_k A_k \delta_k} \left[\mathrm{tg}\left(\pi b_k \tau_k - \frac{\varphi_k}{2}\right) \right.\right.\right. \\
&\qquad \left.\left.\left. - \mathrm{tg}\left(\frac{\varphi_k}{2}\right) \right] \right] \right\} \\
&\quad + \frac{b_k}{\ln 2} \left\{ \Gamma_k + \frac{1}{2\pi\tau_k A_k \delta_k} \left[\mathrm{tg}\left(\pi b_k \tau_k - \frac{\varphi_k}{2}\right) \right.\right. \\
&\qquad \left.\left. - \mathrm{tg}\left(\frac{\varphi_k}{2}\right) \right] \right\}^{-1} \\
&\quad \times \left\{ 2A_k \delta_k \cos^2\left(\pi b_k \tau_k - \frac{\varphi_k}{2}\right) \right\}^{-1}.
\end{aligned} \tag{A.11}$$

The above formula can be further simplified, when we assume that the phase difference between the arriving two-path waveform components is negligible due to similar distance that both waves travel, that is, when $\varphi_k \approx 0$. Note, that formula (A.10) is very general, and function $\mathcal{F}(b_k)$ can be defined in a number of ways depending on the assumed propagation environment models.

B.

Below, we calculate the derivative of $\ddot{\xi}(b_k, c_k)$:

$$\begin{aligned}
\frac{\partial}{\partial b_k} \ddot{\xi}_k(b_k, c_k) &= \frac{\partial}{\partial b_k} \left\{ \left[\int_0^{b_k} \log_2(\delta_k \dot{\gamma}_k(f_k)/\gamma_{0k}(b_k)) df_k \right] \right. \\
&\qquad \left. \times (B_k - b_k - c_k) \right\} - \frac{\partial}{\partial b_k} \{r_0 b_k\} \\
&= \frac{\partial}{\partial b_k} \left\{ \int_0^{b_k} \log_2(\delta_k \dot{\gamma}_k(f_k)/\gamma_{0k}(b_k)) df_k \right\} \\
&\quad \times (B_k - b_k - c_k) \\
&\quad - \int_0^{b_k} \log_2(\delta_k \dot{\gamma}_k(f_k)/\gamma_{0k}(b_k)) df_k - r_0 \\
&= \frac{\partial}{\partial b_k} \left\{ \int_0^{b_k} \log_2[\delta_k \dot{\gamma}_k(f_k)] df_k \right\} (B_k - b_k - c_k) \\
&\quad - \frac{\partial}{\partial b_k} \left\{ \int_0^{b_k} \log_2[\gamma_{0k}(b_k)] df_k \right\} \\
&\quad \cdot (B_k - b_k - c_k) \\
&\quad - \int_0^{b_k} \log_2(\delta_k \dot{\gamma}_k(f_k)/\gamma_{0k}(b_k)) df_k - r_0 \\
&= \left\{ \log_2[\delta_k \dot{\gamma}_k(b_k)] - \frac{\partial}{\partial b_k} \left\{ b_k \log_2[\gamma_{0k}(b_k)] \right\} \right\}
\end{aligned}$$

$$
\begin{aligned}
&\times (B_k - b_k - c_k) \\
&- \int_0^{b_k} \log_2[\delta_k \dot{\gamma}_k(f_k)]\, df_k \\
&+ \int_0^{b_k} \log_2[\gamma_{0k}(b_k)]\, df_k - r_0 \\
&= \left\{\log_2[\delta_k \dot{\gamma}_k(b_k)] - \log_2[\gamma_{0k}(b_k)]\right\} \\
&\times (B_k - b_k - c_k) \\
&- \left\{\frac{1}{\ln 2}\frac{b_k}{\gamma_{0k}(b_k)}\frac{\partial}{\partial b_k}\{\gamma_{0k}(b_k)\}\right\} \\
&\times (B_k - b_k - c_k) - \int_0^{b_k} \log_2[\delta_k \dot{\gamma}_k(f_k)]\, df_k \\
&+ b_k \log_2[\gamma_{0k}(b_k)] - r_0.
\end{aligned} \tag{B.1}
$$

We can write the above expression in a simpler form:

$$
\frac{\partial}{\partial b_k}\dot{\xi}_k(b_k, c_k) = \mathcal{G}_k(b_k, c_k) - r_0, \tag{B.2}
$$

and we can substitute expressions (A.5)–(A.9) to formula (B.1) to obtain the derivative of function $\dot{\xi}_k(b_k, c_k)$ for the rural channel model and the expression for $\mathcal{G}_k(b_k)$:

$$
\begin{aligned}
\mathcal{G}_k(b_k) \simeq\ & \left\{\log_2\{A_k\delta_k[1 + \cos(2\pi b_k\tau_k - \varphi_k)]\}\right\} \\
&\cdot (B_k - b_k - c_k) \\
&+ \log_2\left\{b_k^{-1}\left[\Gamma_k + \frac{1}{2\pi\tau_k A_k\delta_k}\left[\operatorname{tg}\left(\pi b_k\tau_k - \frac{\varphi_k}{2}\right)\right.\right.\right. \\
&\qquad \left.\left.\left. - \operatorname{tg}\left(\frac{\varphi_k}{2}\right)\right]\right]\right\} \\
&\times (B_k - b_k - c_k) + \frac{b_k}{\ln 2} \\
&\times \left\{\Gamma_k + \frac{1}{2\pi\tau_k A_k\delta_k}\left[\operatorname{tg}\left(\pi b_k\tau_k - \frac{\varphi_k}{2}\right) - \operatorname{tg}\left(\frac{\varphi_k}{2}\right)\right]\right\}^{-1} \\
&\times \left\{2A_k\delta_k\cos^2\left(\pi b_k\tau_k - \frac{\varphi_k}{2}\right)\right\}^{-1}(B_k - b_k - c_k) \\
&- \int_0^{b_k} \log_2\{A_k\delta_k[1 + \cos(2\pi f_k\tau_k - \varphi_k)]\}\, df_k \\
&- b_k\log_2\left\{\frac{1}{b_k}\left[\Gamma_k + \frac{1}{2\pi\tau_k A_k\delta_k}\left[\operatorname{tg}\left(\pi b_k\tau_k - \frac{\varphi_k}{2}\right)\right.\right.\right. \\
&\qquad \left.\left.\left. - \operatorname{tg}\left(\frac{\varphi_k}{2}\right)\right]\right]\right\}.
\end{aligned} \tag{B.3}
$$

References

[1] Z. Zhang, Y. He, and E. K. P. Chong, "Opportunistic scheduling for OFDM systems with fairness constraints," *Eurasip Journal on Wireless Communications and Networking*, vol. 2008, Article ID 215939, 2008.

[2] Z. Han, Z. Ji, and K. J. R. Liu, "Fair multiuser channel allocation for OFDMA networks using Nash bargaining solutions and coalitions," *IEEE Transactions on Communications*, vol. 53, no. 8, pp. 1366–1376, 2005.

[3] C. Sacchi, F. Granelli, and C. Schlegel, "A QoE-oriented strategy for OFDMA radio resource allocation based on min-MOS maximization," *IEEE Communications Letters*, vol. 15, no. 5, pp. 494–496, 2011.

[4] J. Chen and A. L. Swindlehurst, "Applying bargaining solutions to resource allocation in multiuser MIMO-OFDMA broadcast systems," *IEEE Journal of Selected Topics in Signal Processing*, vol. 6, no. 2, pp. 127–139, 2012.

[5] Z. Han, Z. Ji, and K. J. R. Liu, "Non-cooperative resource competition game by virtual referee in multi-cell OFDMA networks," *IEEE Journal on Selected Areas in Communications*, vol. 25, no. 6, pp. 1079–1090, 2007.

[6] S. Buzzi, G. Colavolpe, D. Saturnino, and A. Zappone, "Potential games for energy-efficient power control and subcarrier allocation in uplink multicell OFDMA systems," *IEEE Journal of Selected Topics in Signal Processing*, vol. 6, no. 2, pp. 89–103, 2012.

[7] D. Wu, D. Yu, and Y. Cai, "Subcarrier and power allocation in uplink OFDMA systems based on game theory," in *Proceedings of the IEEE International Conference Neural Networks and Signal Processing (ICNNSP '08)*, pp. 522–526, June 2008.

[8] D. Yu, D. Wu, Y. Cai, and W. Zhong, "Power allocation based on power efficiency in uplink OFDMA systems: a game theoretic approach," in *Proceedings of the 11th IEEE Singapore International Conference on Communication Systems (ICCS '08)*, pp. 92–97, November 2008.

[9] F. Chen, L. Xu, S. Mei, T. Zhenhui, and L. Huan, "OFDM bit and power allocation based on game theory," in *Proceedings of the IEEE International Symposium on Microwave, Antenna, Propagation, and EMC Technologies for Wireless Communications (MAPE '07)*, pp. 1147–1150, August 2007.

[10] H. Yu, L. Gao, Z. Li, X. Wang, and E. Hossain, "Pricing for uplink power control in cognitive radio networks," *IEEE Transactions on Vehicular Technology*, vol. 59, no. 4, pp. 1769–1778, 2010.

[11] H. Kwon and B. G. Lee, "Distributed resource allocation through noncooperative game approach in multi-cell OFDMA systems," in *Proceedings of the IEEE International Conference on Communications (ICC '06)*, pp. 4345–4350, July 2006.

[12] L. Wang, Y. Xue, and E. Schulz, "Resource allocation in multicell OFDM systems based on noncooperative game," in *Proceedings of the IEEE 17th International Symposium on Personal, Indoor and Mobile Radio Communications (PIMRC '06)*, pp. 1–5, September 2006.

[13] Z. Liang, Y. H. Chew, and C. C. Ko, "Decentralized bit, subcarrier and power allocation with interference avoidance in multicell OFDMA systems using game theoretic approach," in *Proceedings of the IEEE Military Communications Conference (MILCOM '08)*, pp. 1–7, November 2008.

[14] F. Wang, M. Krunz, and S. Cui, "Price-based spectrum management in cognitive radio networks," *IEEE Journal on Selected Topics in Signal Processing*, vol. 2, no. 1, pp. 74–87, 2008.

[15] S. K. Jayaweera, G. Vazquez-Vilar, and C. Mosquera, "Dynamic spectrum leasing: a new paradigm for spectrum sharing in cognitive radio networks," *IEEE Transactions on Vehicular Technology*, vol. 59, no. 5, pp. 2328–2339, 2010.

[16] D. Niyato and E. Hossain, "Competitive pricing for spectrum sharing in cognitive radio networks: dynamic game, inefficiency of nash equilibrium, and collusion," *IEEE Journal on Selected Areas in Communications*, vol. 26, no. 1, pp. 192–202, 2008.

[17] H. Bogucka, "Efficient and rational spectrum utilization in opportunistic OFDMA networks with imperfect CSI: a utility-based top-down approach," *Wireless Communications and Mobile Computing*, vol. 12, no. 5, pp. 431–444, 2012.

[18] G. Hardin, "The tragedy of the commons," *Science*, vol. 162, no. 3859, pp. 1243–1248, 1968.

[19] J. Perez-Romero, O. Sallent, R. Agusti, and L. Giupponi, "A novel on-demand cognitive pilot channel enabling dynamic spectrum allocation," in *Proceedings of the 2nd IEEE International Symposium on New Frontiers in Dynamic Spectrum Access Networks (DySPAN '07)*, pp. 46–54, Dublin, Ireland, April 2007.

[20] G. J. Foschini and J. Salz, "Digital communications over fading radio channels," *The Bell System Technical Journal*, vol. 62, no. 2, pp. 429–456, 1983.

[21] S. M. Perlaza, M. Debbah, S. Lasaulce, and H. Bogucka, "On the benefits of bandwidth limiting in decentralized vector multiple access channels," in *Proceedings of the 4th International Conference on Cognitive Radio Oriented Wireless Networks and Communications (CROWNCOM '09)*, Hannover, Germany, June 2009.

[22] P. Straffin, *Game Theory and Strategy*, The Mathematical Association of America, 2002.

Hindawi Publishing Corporation
Journal of Computer Networks and Communications
Volume 2012, Article ID 160327, 11 pages
doi:10.1155/2012/160327

Research Article

Cognitive Scout Node for Communication in Disaster Scenarios

Rajesh K. Sharma,[1] Anastasia Lavrenko,[1] Dirk Kolb,[2] and Reiner S. Thomä[1]

[1] *International Graduate School on Mobile Communications, Ilmenau University of Technology, Helmholtzplatz 2, 98684 Ilmenau, Germany*
[2] *Reconnaissance Research & Development (RRD) Division, MEDAV GmbH, Gräfenberger Straβe 32-34, 91080 Uttenreuth, Germany*

Correspondence should be addressed to Rajesh K. Sharma, rajesh-kumar.sharma@tu-ilmenau.de

Received 13 January 2012; Revised 26 April 2012; Accepted 22 May 2012

Academic Editor: Enrico Del Re

The cognitive radio (CR) concept has appeared as a promising technology to cope with the spectrum scarcity caused by increased spectrum demand due to the emergence of new applications. CR can be an appropriate mean to establish self-organization and situation awareness at the radio interface, which is highly desired to manage unexpected situations that may happen in a disaster scenario. The scout node proposed in this paper is an extended concept based on a powerful CR node in a heterogeneous nodes environment which takes a leading role for highly flexible, fast, and robust establishment of cooperative wireless links in a disaster situation. This node should have two components: one is a passive sensor unit that collects and stores the technical knowledge about the electromagnetic environment in a data processing unit so-called "radio environment map" in the form of a dynamically updated database, and other is an active transceiver unit which can automatically be configured either as a secondary node for opportunistic communication or as a cooperative base station or access point for primary network in emergency communications. Scout solution can be viable by taking advantage of the technologies used by existing radio surveillance systems in the context of CR.

1. Introduction

Communication has been an indispensable part of everyday life in the present days. Apart from making the general life better, modern communications should also be applicable for relief and support to the victims of exceptional adverse situations which include disaster scenarios like earthquakes, floods, cyclones, forest fires and terrorist attacks. Such scenarios impose new requirements on the communication systems. Some of the tasks of a cognitive radio network for emergency situations may be (1) to support specific service requests (higher traffic, coverage, localization, emergency messages, etc.), (2) to re-establish communications in a short time, and (3) to assist rescue forces communications and provide interoperability among them and also among rescue forces and public network.

One of the first tasks in disaster is to organize rescue operations in a quick and efficient manner which as well requires rescue forces to be provided with reliable and stable communication facilities. One of the common problems here is providing interoperability among rescue responders originally using different communication standards [1, 2]. In terms of public communication systems, obvious problems in such scenarios are capacity overload with the resulting service denial and absence of coverage in some areas. Whereas the communication capabilities are in higher demand both for rescue responders and public users, the situation gets worse since the communication infrastructure may be fully or partially destroyed. Repairing the original network in a conventional way is time consuming and is not a correct measure in an exceptional situation. In such scenarios actual needs and requirements for communications can vary significantly depending on the scale of the disaster, place, and time elapsed since the beginning of the event. Therefore, a flexible and intelligent communication system which is aware of the situation and gets self-organized and adapted to the current operational demands is highly beneficial to deal with an unpredictable and time-varying situation. Naturally,

cognitive radio (CR) capabilities seem to be highly potential for these purposes.

Cognitive radio (CR) has been considered as a technology for increasing spectral efficiency in wireless communications systems, by having sophisticated radios that can sense and take advantage of spectral opportunities [3]. Unlicensed CR users adaptively adjust radio parameters to the network environment, resulting in improved spectral efficiency. Cognitive radios (referred to as secondary users) may temporarily use spectrum as long as they do not interfere with primary users (PUs) that own the license to that spectrum. Although CR is often considered solely in terms of the use of temporary "white spaces" in the given frequency range detected by a secondary system, its capabilities can be useful for many other applications. Recently, several additional applications of CR have been investigated. For example, in [1], the application of CR for public safety along with other emerging applications has been discussed. The authors have also raised the related standardization issues for a CR technology to support such emerging applications. In [2], CR has been considered as an appropriate solution to the problems of public safety and emergency case communications, especially those related to interoperability issues.

If we consider exploiting CR in the disaster situation we need to address, however, a much broader and more exceptional problem area where the postdisaster unpredictable situation and its solution is needed to be taken into account. This includes analysis of the situation and reaction according to the current needs and priorities. Different levels of possible support should be envisaged: from providing additional services for local groups of users to establishing cooperation between the secondary and the primary system [4, 5]. This results in a very broad range of requirements for the CR node. Therefore, the secondary node must be equipped with strong cognitive abilities to explore the situation, identify the available resources, and act according to the current need.

To utilize CR capabilities efficiently for an adequate and timely assistance in disaster situation, there is a need for obtaining relevant information on the service or system which requires support. For instance, to provide interoperability to the various emergency responders information on their modes of operation must be available which is not always a case especially in the presence of the forces subordinate to the different departments. In case of partial damage of the existing system infrastructure, there might be a need of support for its re-establishment which as well requires information on the system's operational parameters, capabilities, and current needs which demands increased cost and complexity. Here, the advantage can be taken from the current developments in the radio surveillance systems which basically solve similar problems but for different goals. Although the increased cost and complexity for advanced capabilities may not be justifiable for all of the secondary nodes, this can be justifiable for a single powerful node in the network which can assist other nodes for the improved performance.

In this paper, we propose a concept of a powerful cognitive node having extended capabilities which coexists in a network, where heterogeneous primary as well as secondary cognitive radios are in operation. This proposed node is different from other nodes in its features and missions. Firstly, it has more advanced sensing, signal processing capabilities, and additional flexibility in terms of mobility which are not available in normal cognitive nodes. Secondly, in the case of exceptional situation it gets self-organized in the system which needs support and provides some emergency services or reinforce affected services. Thirdly, during normal operation scenario it works as a secondary user (SU) in CR system making the cognitive communication more efficient and reliable avoiding interference to the primary system. The requirements of such node, its operating modes, its application scenarios, and research components for its design and development are discussed in this paper. The proposed system is found to have remarkable similarities with radio surveillance system; therefore, it can take the advantage of the later in several aspects. Note that the principal goal of such a node is an altruistic (cooperative) support in the disaster scenario rather than spectrum efficiency and throughput as it is considered in normal situations. Due to its foremost function of reconnaissance and observation in the radio environment, this node will be termed "scout" in this paper.

The remainder of the paper is organized as follows. Section 2 provides the general concept overview of the scout including its applications, operating scenarios and modes, and requirements. Section 3 discusses several issues and solutions for the most important task, the resource estimation and awareness, of the scout. Scout design and implementation issues are discussed in Section 4. Section 5 discusses briefly the current developments and operational issues in radio surveillance system from which scout can take advantage in terms of signal intelligence for its viability. Finally, the concluding remarks are given in Section 6.

2. Scout System Concept

Since one of the main aims of the cognitive radio node with extended capabilities is scouting-related radio resources, it is proposed here to call it "scout." The resources consist of radio spectrum resources that may be available in several dimensions like frequency, time, code, space, direction, polarization as well as the radio network infrastructure. The scout needs global information about radio resources for centralized decision to be taken by it and to act globally in the network. Some of the important global information related to radio resources include information about the primary systems and their modes of operation, unused frequency bands, the spatial and temporal statistics of its use, the distribution of the available nodes of the primary and secondary (CR) network, propagation characteristics in the primary and secondary network, and so forth. Although the need for knowing so many details about the primary system is unusual form the viewpoint of conventional (opportunistic) CR, it is important for scout since the "cooperative CR" vision is to be addressed by it. All the collected information must be stored in a database which in the literature is commonly referred to as a radio environment map (REM) [6].

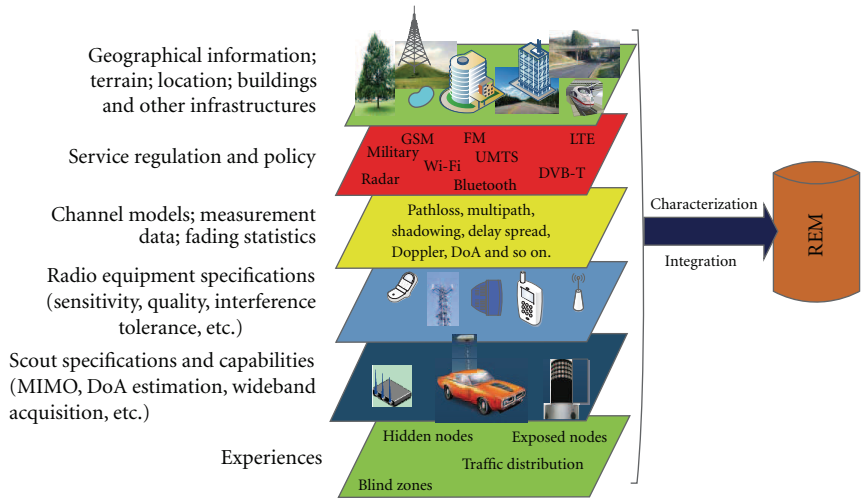

Figure 1: A REM obtained by integrating various databases (modified from [6]).

Radio environment map (REM) is an abstraction of real-world radio scenarios. It is an integrated spatiotemporal database which characterizes the radio environment of cognitive radios in multiple domains. It can be exploited to support cognitive functionality of the user equipment, even if the subscriber unit is relatively simple [6]. The illustration of how a REM is obtained from various information sources is shown in Figure 1. REM is assigned a central role in scout because different classes of collected sensor data (e.g., from the spectrum analysis and the physical layer analysis) and a priori knowledge are kept updated in it. It means that it consists of static and dynamic as well as temporally and spatially varying information in a well-managed form.

The cognitive engine is the brain of the CR system which executes a set of nested loops constituting a cognition cycle, drawing on experience and stored knowledge in REM to optimize a set of user-chosen quality-of-service measures [7]. Naturally, the scout must also be equipped with a more powerful cognitive engine than other CR nodes because it may need higher processing power for sensor signal data reduction or compression using relatively large database from the REM as well as real observation during its operation. Since it should be a more strategic database-supported planning tool having situation awareness, it is something more than a simple cognitive engine and we can better term it as "cognitive planning tool."

The scout needs to take cognitive decision for its "act" phase which may be either a cooperation to the primary system or secondary communication according to its mission plan. Based on the sensing data, the a priori knowledge to the environment, the situation based on REM analysis, and agreed requirements the cognitive planning tool of the mobile scout provides the local decision as well as the decision based on the global (network-based) data processing in the heterogeneous nodes environment. Cognitive planning tool, which employs artificial intelligent (AI) techniques for cognitive mission control [8], has well defined cognitive control and decision rules, with the prioritization, classification, and consideration of various application requirements (disaster or mass event scenarios, etc.). It implements the duties of a mission control for the scout and also interacts with sensing and detection unit for learning.

During the operation of the network, the tasks (mission) of the scout could change and adapt according to the network status. While its first mission will be dominated by the simple exploration of the environment for supporting network establishment, the scout in later stages can switch to either altruistic or opportunistic communication mode in the network operation. A simple functional architecture of scout is shown in Figure 2(a), which is also expressed in the form of a scout cycle as shown in Figure 2(b) derived from a classical cognitive radio cycle [3].

Since scouts are envisaged to be powerful and versatile nodes working in a partially destroyed infrastructure primary network as well as a centralized/distributed secondary network, they should be able to estimate the resource, support the primary communication as an altruistic node in the form of relay nodes as well as communicate as secondary cognitive nodes in an opportunistic manner. The operation of the scout consists of two parts: one is the "observation and awareness" which is the task of collecting information from radio environment and storing it in REM. This can be also termed the scout mode of operation. The another operation is the "planning, deciding, and acting" by the scout which further results in two different roles to be played by it, based on which this operation can be classified into two modes: (1) altruistic support for primary communication as a relay node and (2) secondary opportunistic communication. These two operating modes can be seen in Figures 3(a) and 3(b), respectively. It is apparent that the node requires to possess high level of reconfigurability in order to be able to operate in both of these modes.

In the altruistic communication mode, scout communicates to the primary network based on the collected information by it. It discovers the network status and

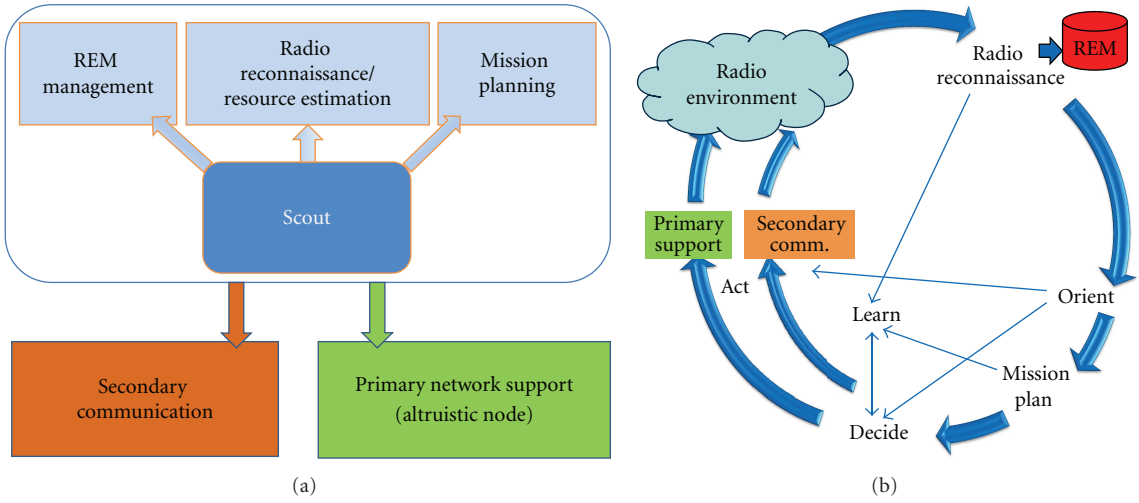

Figure 2: (a) A functional architecture of the scout and (b) a simple scout cycle of operation.

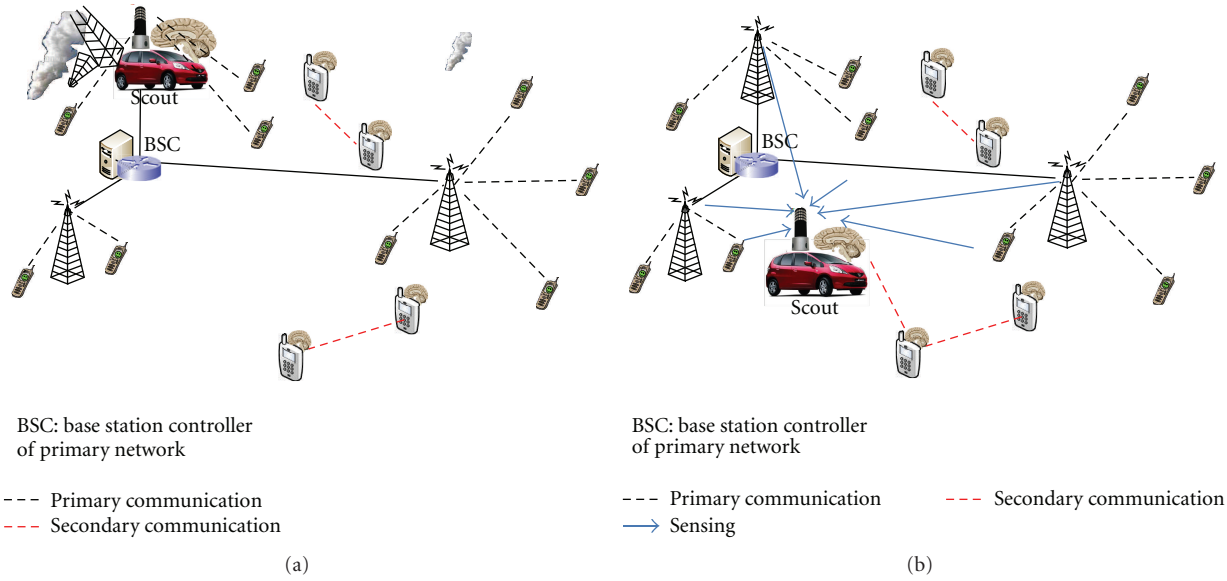

Figure 3: Scout in (a) altruistic primary communication support mode and (b) opportunistic secondary communication mode.

identifies the location of the failure. It gets self-organized itself in the primary network as a communication node and, even possibly, replaces the failed node and takes its role. This mode of operation requires signalling and synchronization issues to be resolved, and it poses highly sophisticated system requirements.

In the secondary opportunistic communication mode, the scout behaves simply as a CR node, but due to its extended capabilities it can contribute significantly more than other nodes for filling the REM whose information can be provided to other CR nodes in the network. Thus, it can support SU CR nodes which may have very limited sensing capabilities by giving valuable advice for radio resource access.

3. Resource Estimation Capabilities of Scout

Resource estimation is the first and the most important part of the scout task. Since the very exceptional operational conditions are considered, all the available equipment capabilities should be used in order to achieve the most robust and reliable estimation to ensure that resources would be fully and efficiently exploited in all the possible dimensions like spectrum, direction, location, and time. There may be different requirements for estimation depending upon the action to be taken by the scout. If the PU is observed for the purpose of secondary communication, the identification of white spaces may be sufficient. If the purpose of estimation is to help the victim users in primary system, the scout has

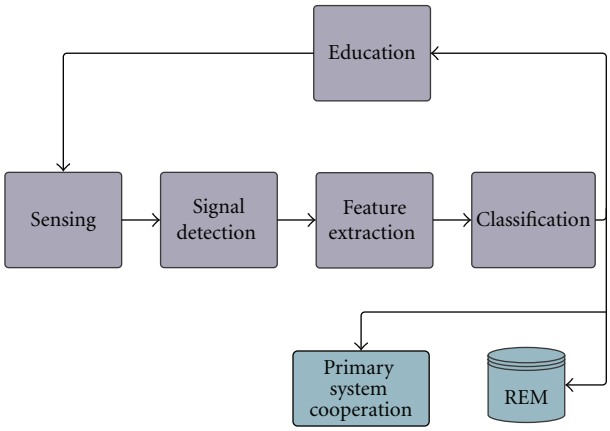

Figure 4: PHY mode identification and classification work-flow.

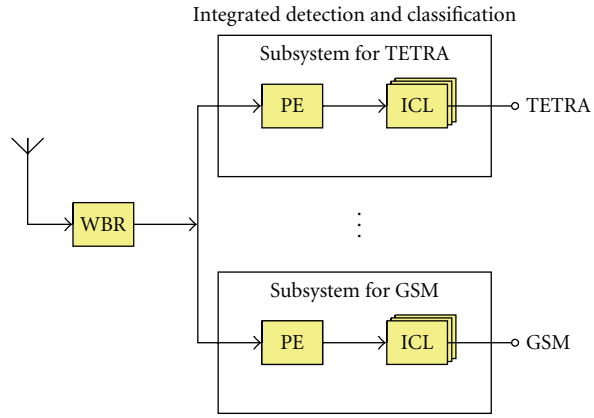

Figure 5: Processing chain with a common wideband receiver (WBR), transmission class-specific subsystems for pattern extraction (PE) and for integrated detection and classification (ICL).

to find out what the primary users need and what physical layer (PHY) signalling they can accept. PU PHY mode identification and classification (from finite sets) is, therefore, essentially required especially for the second purpose. This includes detection of primary and/or secondary users and identification of their operational parameters. Here, one of the core tasks to perform is signal classification which could be implemented on the basis of pattern recognition theory using specific signal features of the considered communication standard. Features could characterize frequency domain like central frequency, bandwidth of a signal, frequency hopping pattern and/or time domain like waveform, and signal duration. A simple block diagram showing the work-flow for PHY mode identification is shown in Figure 4.

Another possible estimation object is temporary statistics of primary and/or secondary users. To make the sensing and identification easy and reliable for the future events, the estimation of PU and SU statistics and storing the data in REM is important. It could involve time, frequency, and space domains as well as primary network state estimation, traffic estimation, and so forth. Some statistics is to be obtained from the measurements using the scout node itself. However, many background data including geographical information, terrain, buildings, service regulation, and so forth, provide additional valuable information for the estimation of primary user statistics. This information could be used as a base for prediction of the network status, choice of the secondary network PHY mode, and compiling higher level network protocols.

3.1. Advanced Spectrum Sensing. Some existing spectrum sensing techniques are matched filtering, waveform-based sensing [9], cyclostationary-based sensing [10–12], energy detection (ED) [13–16], autocorrelation-based sensing [17, 18], sample covariance-based detection [19], and cepstral-based detection [20, 21].

For scout, it is mandatory to select the most reliable combination of features to handle the current radio scenarios successfully and to decrease the probability of errors. Talking about the combination of spectrum sensing together with REM, the question whether it is a good idea to use the information of the current radio environment to ease the processing always appears. If this information is used to support spectrum sensing, one should keep in mind that the radio scenario changes over time and location. Thus, it is mandatory that the spectrum sensing is updated automatically to fit to the current REM. Due to the fact that in some cases a priori information can be accessed and applied easily, however, in other cases the opposite happens as the current a priori information becomes irrelevant due to the new requirements. Nevertheless, for the operator of the scout, it is not obvious which kind of sensing technique is the best for a given radio scenario. So, the goal is to make the decision to choose the sensing features as automatically as possible.

If the scout starts in a new environment with noneducated sensing and PHY identification, it can later switch to educated sensing which not only makes the sensing easier but also enhance the sensing performance. This is actually the simple and straightforward application of cognitive principle which involves learning, cognition, and then educating other nodes.

In [21], a new sensing approach has been introduced where the main idea is to combine modern object detection techniques with new upcoming ideas from CR. By doing, this it was possible to combine different sensing approaches in such a way that a highly robust and real-time capable system for radio signal detection and classification emerged. The decision which sensing approach fits to the defined requirements was done automatically based on the current radio scenario or rather the current REM. Figure 5 shows the structure of the new system. It contains several subsystems for classification which are adapted to the radio standards of interest. This allows the operator of the scout to focus on updating the REM and not to spend too many efforts in trying to set up a spectrum sensing manually. In such case the sensing can be robust, fast, and reliable compared to the uneducated (blind) sensing. The neighbouring nodes with reduced sensing capabilities also can take advantage from the sensing decision of the scout.

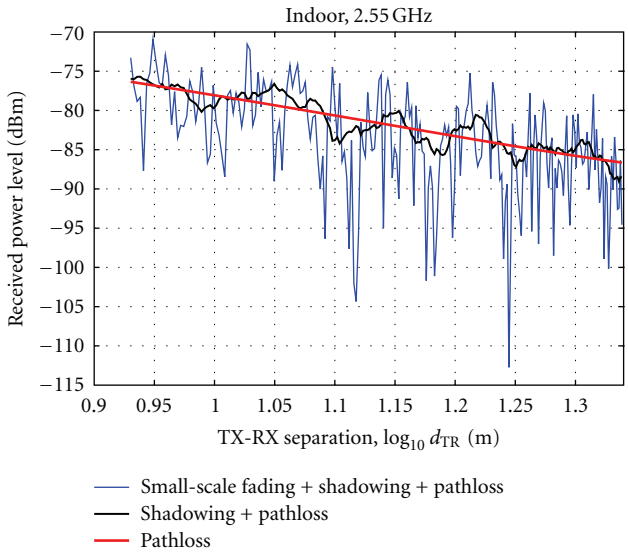

Figure 6: The received power in an indoor environment showing the effect of small-scale fading, shadowing, and pathloss.

3.2. Estimation of Channel Statistics. Since the sensing and estimation procedures all rely on the signals obtained from the sources in the environment, the reliability of the estimation from the received signal parameter depends upon the accuracy in the predicted channel parameters at the given location. The channel parameters of high importance are pathloss, small-scale fading parameters, and large-scale fading (shadowing) statistics. These parameters are illustrated in Figure 6 which is based on the real measurement in an indoor environment. Apart from these parameters delay spread based on power delay profile, Doppler spread, angle of arrival, and so forth in the given environment are the parameters to be estimated and stored in REM. Since exceptional disaster scenario is to be considered, the channel statistics and models used in the normal situation may not be applicable in this situation. Therefore, a realistic assumption of the channel statistics in disaster scenario is needed especially for initial attempts of estimation. Later, estimation of channel statistics based on current measurement results and the resource estimation and identification based on those new statistics will make the system highly reliable.

A main challenge in spectrum sensing and estimation arises due to hidden node problem. The hidden node problem can be caused by many factors including severe multipath fading or shadowing that secondary users observe while scanning PU transmissions. Here, the CR device causes unwanted interference to the PU (receiver) as the primary transmitter's signal could not be detected because of the positioning of devices in space. Since the hidden node problem arises due to the channel fading, the correct statistics of the fading in the radio environment helps to identify the hidden nodes. Channel statistics should be estimated by using PU and SU nodes as excitation signal sources.

It is important to note that fading goes along with other channel statistics, for example, angular spread and effective channel rank. So although knowledge about fading may be enough to explain the hidden node problem and to decide about channel availability for secondary communication, it will be not enough to assess the antennas influence and decide the optimum transmission mode including MIMO multiplexing versus diversity, beamforming, coding, and so forth. The small-as well as large-scale statistics are essential for cognitive link adaptation. In distributed and heterogeneous network, a cooperative link statistics are needed for the effective link and relay node implementation. For fulfilling these requirements, we should know more parameters and statistics related to the channel for the scout operation.

3.3. Tracking and Data Fusion. To use the information potential of the scout system in various decision tasks, the continuously collected data must not overwhelm the system. Instead, the data are to be condensed (fused) in such a way that high-quality information results serving as a basis for decision support in particular applications and on all levels of hierarchy [22].

Data fusion can also help to combine heterogeneous information having different types, sources, qualities, and so forth. It can help weight the quality and importance of information and help to handle incomplete and unreliable information. Data fusion is a very well-known method for the improvement of sensing performance. There might be different levels or layers of data fusion: from decision level that combines measured values(sensor decisions) [23] up to level where mostly data are retrieved, categorized, combined, and so forth [24].

Knowledge-based systems (KBS) can interpret the fusion results by considering and analysing issues such as the context in which the data are observed, the relationship among observed entitles, hierarchical groupings of targets or objects, and predictions of future actions of targets or entities [24]. Key issues for developing such a system include the creation of the knowledge base. Since the scout is a cognitive node equipped with a dynamically updated database (REM) and cognitive mission control unit, it can perform the knowledge-based data fusion for the better performance.

Fusion of sensor data may be utilized in different cases: data produced at different instants of time (i.e., target tracking), data being collected from different sensor sources, data with background information on the sensor performance as well as data with nonsensor context information [22]. Since scout is a single node, it can perform data fusion based on the information it collects at different instants of its movement (different locations) with a proper source tracking. If distributed nodes provide their local sensing results to the scout, it can also perform decision fusion based on the sensing results of the distributed nodes and its own sequential observations. And, as a consequence, the scout can plan its mission, which includes not only the choice of the track, to maximize its performance.

3.4. Information Compression (Compressive Sensing). It is a known fact from the success of lossy compression that most of the data we acquire are not important and do not cause the

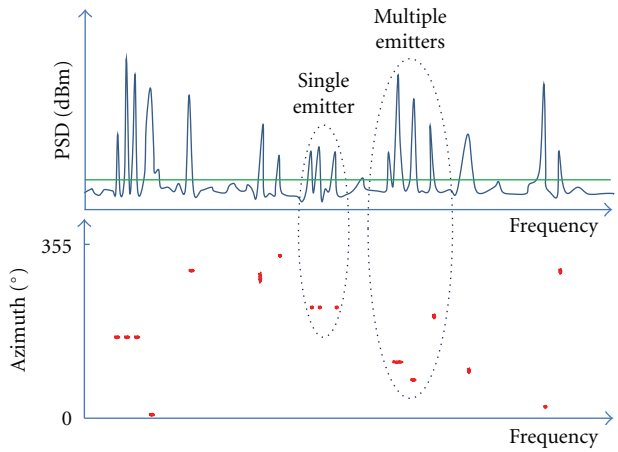

Figure 7: An example of data fusion between spectral and DoA information.

loss in information when they are discarded. If the sensing is performed just to acquire the important information, it makes the system efficient in the management of data. Practically, that might be the only possibility to handle the sensing process and to handle the huge amount of data.

There has been a significant research in the field of compressed sensing in the last few years. Compressed data acquisition protocols directly acquiring just the important information about the compressible signals have been proposed [25]. This sensing principle might enhance the sensing performance dramatically with reduced measurement time, reduced sampling rates, or reduced analog-to-digital (ADC) converter resources requirements [25].

A compressive sensing method capturing and representing compressible signals at a rate significantly below the Nyquist rate has been proposed in [26]. This method employs nonadaptive linear projections that preserve the structure of the signal. The signal is reconstructed from these projections using an optimization process. In [27], a Bayesian formalism has been employed for estimating the underlying signal based on compressive-sensing measurements. This framework has been utilized for CR primary user detection in [28], achieving the sampling reduction advantage with significantly less computational complexity.

Information compression using compressed sensing can play a significant role in scout performance by making the sensing more efficient and effective, whereas the REM remains efficient by storing compressed sensing data. Compression seems to be a solution to better exploit the limited hardware capabilities in terms of spectral coverage and speed, and also in terms of the required capacity of the data link to the fusion center.

4. Scout Design and Implementation Issues

The first task of the scout is to explore the spectral environment. The node should be compact enough for field operations on a mobile platform, for instance, a car. Accordingly, the requirements include the selection of appropriate algorithms for signal analysis and signal estimation, appropriate platforms and approaches for implementation procedures. The appropriate methods of information fusion and database programming are to be used to establish the REM.

The important requirements in the implementation of scout include coherent multichannel receivers with wideband fast sensing capabilities. The antenna and bandwidth requirements are some of the key issues to be considered. Quality of service (QoS) and security issues are also important. Some of these issues are discussed here.

4.1. Antenna Requirements. From implementation point of view one of the important system parts required to perform estimation tasks discussed in Section 3 is wideband and/or tunable directional antennas which can gather information about spectrum resource in different directions for the given geographic location. Antenna arrays having direction-of-arrival (DoA) estimation capability makes the scout much more powerful than having a single antenna for both altruistic and opportunistic modes of operation. Direction finding is important for scout because it provides a bearing for a detected signal allowing to focus on a target area rather than random detection under the unknown resource distribution. It may be considered as a prerequisite for localization of a node. It makes possibility of tracking the target and allows intelligence fusion with other sensor data. By jointly exploiting spectrum and azimuth information, a more reliable automated emitter detection in dense scenarios becomes possible. For example, the spectral information combined with DoA information can distinguish between single emitter and multiple emitters along with their directions over a given frequency band as illustrated in Figure 7. It also provides SNR gain for the detection of weak signals. Separation of multiple stations for certain signal types is possible by direction finding. Additionally, high-resolution direction finding algorithms allow separation of multiple cochannel signals in the radio environment. Location and direction finding methods have been studied for long time [29, 30]; however robust, fast, simple, and highly accurate algorithms are still interesting topics for today's research [31].

Although both beamforming and high-resolution DoA estimation are important for scout, they are different from each other. The beamforming gain in the former is strictly coupled to the size of the array. The latter can achieve high resolution performance in case of high SNR and precise antenna calibration. The requirements (and pitfalls) are described in [32].

The DoA estimation is possible with wideband array capability which makes scout more expensive and heavy. DoA estimation makes possibility of exploiting spatial dimension (direction) as an additional radio resource. Larger bandwidth, big antenna arrays, and multichannel receivers are needed for this purpose, which is a considerable effort in terms of cost and complexity. Adaptive beamforming [33], which requires also antenna arrays can be used by the node to

control and avoid interference so that coexistence of primary and secondary network can be possible. Opportunistic antenna selection using orthogonal radiation patterns and/or polarization can be possible with small antenna arrays, but they have limited direction finding capability. Although such wideband array equipment may cost more than a base station today, there have already been many efforts to get cheaper equipment in radio surveillance community with a fast technological progress. Since the scout concept is for tomorrow's technology, its use in exceptional situations will be certainly feasible both technically and economically.

4.2. Frequency and Bandwidth Related Issues. Bandwidth requirement of antennas depends upon the specific task to be performed by the scout. During the sensing and reconnaissance phase, very wideband antenna or multiband antennas which consist of several antennas for the different frequency bands to scan the whole available bands may be highly desirable. However, for the communication phase, narrower band antenna to filter unwanted signals may be required. Reconfigurable antenna seems to be highly useful whose radiation pattern (direction; beamwidth) and bandwidth versus gain characteristics play an important role in the performance of the device.

The size of the antenna needed for scout operation depends upon the frequency band it is used for. Sometimes the antennas look large physically, but are small electrically. For example, if we talk about a wideband antenna in 60 GHz band, the size will be small making the scout simple to implement. However, when lower VHF/UHF bands are considered, physically large antennas will be required, and obtaining same bandwidth will be also more difficult. Designing wideband antennas in these bands need more weight and space for scout device.

In general, the lowest frequency of operation determines the antenna size. Sometimes we can use antennas that are electrically small, for example, for DoA resolution, which might work reasonably, but price that we have to pay is the reduced gain. This is a typical option for lower frequency. Fortunately, in this case the gain disadvantage can be partly compensated by lower free space attenuation. But there is always a compromise between gain, DoA resolution, and antenna array size which is influenced by platform size. Since the application of scout is broad, the use of narrowband and wideband as well as small and large antennas should be considered while designing the system.

4.3. Quality-of-Service Issues. For the application scenarios discussed in Section 2, different quality-of-service (QoS) requirements are to be satisfied by the scout node. In opportunistic communication mode, the scout working as a conventional CR must satisfy the interference constraint to the primary users. It must be able to serve for both real-time and best-effort traffic with the desired data rate and delay. Since there are different applications demanding large variation of capacity and delay requirements, cognitive engine should be able to make optimal transmission decision for the opportunistic communication.

The QoS requirements for altruistic communication mode are even more wider. For example, in one case, the scout acting as an altruistic node may need to establish a backbone connection to a local network of some users to get them connected to the public network. In the other extreme case, there may be a situation where it is necessary to reach a single user in a large distance. So, depending upon the user distribution and the radio environment there will be a much wider scope of QoS requirements to be fulfilled as compared to the regular networks. This requires high flexibility in the capability of scout node in terms of coverage, throughput, latency, reliability, and so forth. Since the QoS requirements may be interdependent, the choice of optimal parameters for the communication is important, which is to be performed by the cognitive planning tool. For example, choice of a frequency band will have influence on coverage (e.g., lower frequency can be used to reach distant users or to broadcast short messages, whereas higher frequencies are to be used to satisfy the high data rate demand in shorter distances). Beamforming versus multiplexing MIMO can be used to trade-off between coverage and capacity.

4.4. Security Issues. It is a well-known fact that there are malicious organizations that can attempt interception of the signals to and from the scout and make it to take incorrect decision in its mission. Any information flaw may result with harmful effect in the scene instead of fulfilling the desired goals. Therefore, it is crucial that the over the air information should be secure, which adds more challenge in the implementation. Although a detailed study on addressing the security issues on scout is important, it is not discussed here since it is beyond the scope of this paper.

5. Current Developments in Signal Intelligence and Scout Viability

Although the scout node discussed in this paper is a new concept, there are already technological achievements to serve a base for the scout development, especially in the radio surveillance applications. Also, the capabilities mentioned in Section 3 are expected to be achieved in the near future as many researches are focussed on these areas in cognitive radio perspectives.

Since to know what is on air has always been of strong interest, this noncivil market of radio surveillance can look back on a long development of several decades. A typical radio surveillance system consists of one or several wideband receivers, digital signal processing units, and some postprocessing systems. Dependent on the task of such a system, different capabilities, for example, radio signal detection and classification; direction or location finding, can be enabled. Ongoing developments show that especially the tactical systems for direction or location finding get smaller and consume less power which is ideal for vehicle-based missions. To fulfil a radio surveillance task, high flexibility of the applied system is necessary. It can happen that the mission details, for example, a priori information regarding occupied frequencies, radio services and networks,

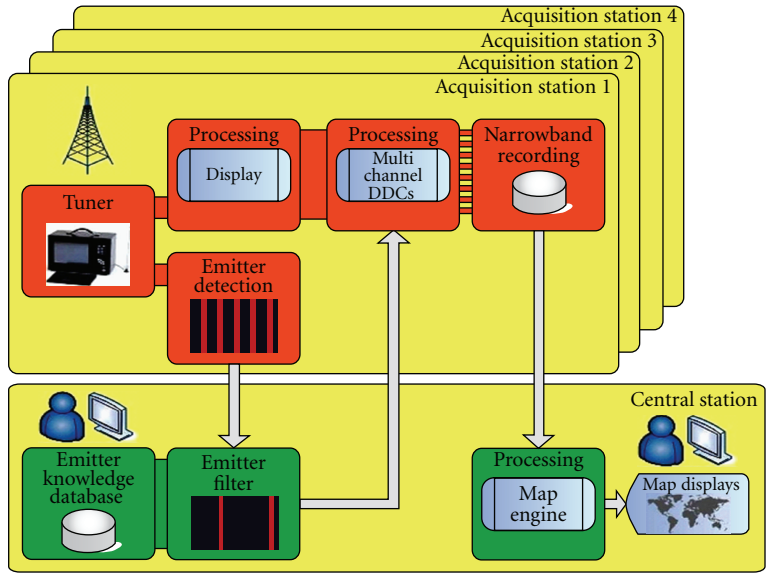

Figure 8: Multisensor setup of the new radio surveillance system developed by MEDAV.

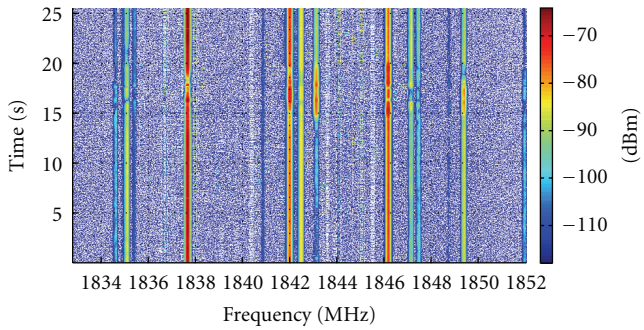

Figure 9: Spectrogram obtained by the wideband receiver IZT R3200 in GSM-1800 downlink.

and their assumed locations change over time, frequency, and especially over location. In case of a dislocation of a radio surveillance system, there is a high probability that new radio standards of interest appear. Thus, every stage of the processing chain, for example, the signal detection and classification, should be adaptable to new radio scenarios. It is obvious that the systems for radio surveillance are technically similar to the scout, which is proposed. In addition to the technical conformities, there are a lot of common aspects regarding the mission process itself. In sum, it would be a good idea to combine the knowledge gained from radio surveillance and the ideas of the research areas like cognitive radio in order to create smarter solutions.

As an example, a new system of MEDAV [34] for monitoring of fast changing radio scenarios contains tools for mission planning, sensor controlling, and real-time situation pictures. With this software it is possible to control and task not only the proposed direction finding (DF) system but also other sensor types. The modular concept allows to do most of the signal processing, for example, radio signal detection and classification, within the scout and to gather the resulting information in the fusion center to combine it with information coming from other sensors. The focus of the system is on mobile sensors with robust data links and low data rates between the sensor and the fusion center. Thus, it is a perfect basis for the proposed scout concept. Figure 8 shows the structure of a multisensor setup.

Keeping most of the signal processing and analysis in the software, antenna and radio front-end characteristics, however, still play a key role imposing the strongest restrictions on the overall sensing capabilities of scout. Since the main objective of scout is the assessment of the radio environment, one of the important aspects for its viability is existence of appropriate receivers. Currently, there are already some solutions available on the market which could be suitable for the scout design. For instance, digital wideband receiver R3200 developed by IZT GmbH [35] can cover frequency range from 9 kHz to 18 GHz with the maximum real-time instantaneous bandwidth of 19.2 MHz for I/Q baseband data. As an example, a spectrogram which is obtained by this receiver in an indoor location is shown in Figure 9, which gives a clear picture of the instantaneous user activity in GSM-1800 downlink.

Since the radio surveillance systems for small-sized vehicular platform are already available in the market [34, 36, 37], scout can take advantage from the technology used by these systems with the addition or enhancement of the capabilities in resource estimation as discussed in Section 3, including a full-fledged REM, and also addressing the issues mentioned in Section 4.

6. Conclusion

In this paper, we have discussed an extended concept based on cognitive radio which can be used as a secondary communication as well as a cooperative (altruistic) node

for partially destroyed primary network infrastructure. The different requirements and implementation issues for such a node (scout) have been discussed. Since the required functionalities are advanced but still achievable in the present day of very high speed processors as well as the storage devices, a special cognitive node with such advanced features can be a highly useful and feasible system for the communication support to the victims in the exceptional situations including disasters and terrorist attacks.

Acknowledgments

This work has been carried out within the International Graduate School on Mobile Communications supported by the German Research Foundation (DFG) under the project "GRK 1487," and the Carl-Zeiss Foundation.

References

[1] J. Wang, M. Ghosh, and K. Challapali, "Emerging cognitive radio applications: a survey," *IEEE Communications Magazine*, vol. 49, no. 3, pp. 74–81, 2011.

[2] A. Gorcin and H. Arslan, "Public safety and emergency case communications: opportunities from the aspect of cognitive radio," in *Proceedings of the 3rd IEEE Symposium on New Frontiers in Dynamic Spectrum Access Networks (DySPAN '08)*, pp. 1–10, October 2008.

[3] J. Mitola and G. Q. Maguire Jr., "Cognitive radio: making software radios more personal," *IEEE Personal Communications*, vol. 6, no. 4, pp. 13–18, 1999.

[4] Use Cases for Cognitive Applications in Public Safety Communications Systems—Volume 1: Review of the 7 July Bombing of the London Underground, Wireless Innovation Forum, 2007, http://groups.winnforum.org/d/do/1565.

[5] Use Cases for Cognitive Applications in Public Safety Communications Systems Volume 2, Chemical Plant Explosion Scenario, Wireless Innovation Forum, 2010, http://groups.winnforum.org/d/do/2325.

[6] Y. Zhao, J. H. Reed, S. Mao, and K. K. Bae, "Overhead analysis for radio environment mapenabled cognitive radio networks," in *Proceedings of the 1st IEEE Workshop on Networking Technologies for Software Defined Radio Networks (SDR '06)*, pp. 18–25, September 2006.

[7] B. Le, T. W. Rondeau, and C. W. Bostian, "Cognitive radio realities," *Wireless Communications and Mobile Computing*, vol. 7, no. 9, Article ID 129497, pp. 1037–1048, 2007.

[8] A. He, K. K. Bae, T. R. Newman et al., "A survey of artificial intelligence for cognitive radios," *IEEE Transactions on Vehicular Technology*, vol. 59, no. 4, pp. 1578–1592, 2010.

[9] A. Sahai, R. Tandra, S. M. Mishra, and N. Hoven, "Fundamental design tradeoffs in cognitive radio systems," in *Proceedings of the 1st International Workshop on Technology and Policy for Accessing Spectrum (TAPAS '06)*, August 2006.

[10] M. Öner and F. Jondral, "Cyclostationarity based air interface recognition for software radio systems," in *Proceedings of the IEEE Radio and Wireless Conference (RAWCON '04)*, pp. 263–266, September 2004.

[11] R. S. Roberts, W. A. Brown, and H. H. Loomis Jr., "Computationally efficient algorithms for cyclic spectral analysis," *IEEE SP Magazine*, vol. 8, no. 2, pp. 38–49, 1991.

[12] D. Cabric, "Addressing the feasibility of cognitive radios: using testbed implementation and experiments for exploration and demonstration," *IEEE Signal Processing Magazine*, vol. 25, no. 6, pp. 85–93, 2008.

[13] H. Urkowitz, "Energy detection of unknown deterministic signals," *Proceedings of the IEEE*, vol. 55, no. 4, pp. 523–531, 1967.

[14] V. I. Kostylev, "Energy detection of a signal with random amplitude," in *Proceedings of the International Conference on Communications (ICC '02)*, pp. 1606–1610, May 2002.

[15] F. F. Digham, M. S. Alouini, and M. K. Simon, "On the energy detection of unknown signals over fading channels," in *Proceedings of the International Conference on Communications (ICC '03)*, pp. 3575–3579, May 2003.

[16] A. Ghasemi and E. S. Sousa, "Asymptotic performance of collaborative spectrum sensing under correlated log-normal shadowing," *IEEE Communications Letters*, vol. 11, no. 1, pp. 34–36, 2007.

[17] R. K. Sharma and J. W. Wallace, "Improved spectrum sensing by utilizing signal autocorrelation," in *Proceedings of the IEEE 69th Vehicular Technology Conference*, pp. 1–5, Barcelona, Spain, April 2009.

[18] R. K. Sharma and J. W. Wallace, "Correlation-based sensing for cognitive radio networks: bounds and experimental assessment," *IEEE Sensors Journal*, vol. 11, no. 3, pp. 657–666, 2011.

[19] Y. Zeng and Y. C. Liang, "Spectrum-sensing algorithms for cognitive radio based on statistical covariances," *IEEE Transactions on Vehicular Technology*, vol. 58, no. 4, pp. 1804–1815, 2009.

[20] M. Li, V. Rozgić, G. Thatte et al., "Multimodal physical activity recognition by fusing temporal and cepstral information," *IEEE Transactions on Neural Systems and Rehabilitation Engineering*, vol. 18, no. 4, pp. 369–380, 2010.

[21] D. Kolb, U. Uebler, and E. N. Nöth, "A novel transmission scanner framework for real-time applications," in *Proceedings of the RTO-MPIST-092- Military Communications and Networks. NATO Research and Technology Organisations*, 2010.

[22] W. Koch, "On Bayesian tracking and data fusion: a tutorial introduction with examples," *IEEE Aerospace and Electronic Systems Magazine*, vol. 25, no. 7, pp. 29–51, 2010.

[23] Z. Chair and P. K. Varshney, "Optimal data fusion in multiple sensor detection systems," *IEEE Transactions on Aerospace and Electronic Systems*, vol. 22, no. 1, pp. 98–101, 1986.

[24] D. L. Hall and J. Llinas, "An introduction to multisensor data fusion," *Proceedings of the IEEE*, vol. 85, no. 1, pp. 6–23, 1997.

[25] D. L. Donoho, "Compressed sensing," *IEEE Transactions on Information Theory*, vol. 52, no. 4, pp. 1289–1306, 2006.

[26] R. G. Baraniuk, "Compressive sensing," *IEEE Signal Processing Magazine*, vol. 24, no. 4, pp. 118–121, 2007.

[27] S. Ji, Y. Xue, and L. Carin, "Bayesian compressive sensing," *IEEE Transactions on Signal Processing*, vol. 56, no. 6, pp. 2346–2356, 2008.

[28] S. Hong, "Multi-resolution bayesian compressive sensing for cognitive radio primary user detection," in *Proceedings of the 53rd IEEE Global Communications Conference (GLOBECOM '10)*, pp. 1–6, December 2010.

[29] A. J. Berni, "Angle-of-arrival estimation using an adaptive antenna array," *IEEE Transactions on Aerospace and Electronic Systems*, vol. 11, no. 2, pp. 278–284, 1975.

[30] S. S. Reddi, "Multiple source location-a digital approach," *IEEE Transactions on Aerospace and Electronic Systems*, vol. 15, no. 1, pp. 95–105, 1979.

[31] S. D. Blunt, T. Chan, and K. Gerlach, "Robust DOA estimation: the reiterative superresolution (RISR) algorithm," *IEEE Transactions on Aerospace and Electronic Systems*, vol. 47, no. 1, pp. 332–346, 2011.

[32] M. Landmann, M. K. Käske, and R. S. Thomä, "Impact of incomplete and inaccurate data models on high resolution parameter estimation in multidimensional channel sounding," *IEEE Transactions on Antennas and Propagation*, vol. 60, no. 2, pp. 557–573, 2012.

[33] R. M. Radaydeh and M.-S. Alouini, "Impact of co-channel interference on the performance of adaptive generalized transmit beamforming," *IEEE Transactions on Wireless Communications*, vol. 10, no. 8, pp. 2616–2629, 2011.

[34] Radio Monitoring and Surveillance Solutions, MEDAV, 2011, http://www.medav.de/.

[35] IZT R3200 Digital Wideband Receiver, IZT GmbH, 2012, http://www.izt-labs.de/en/products/kategorie/receivers/produkt/izt-r3200-1/.

[36] Radio Surveillance Overview, Synectics, 2011, http://www.synx.com/index.php/Products/radio-surveillance.html.

[37] Radio Surveillance and Intelligence, Morcom, 2011, http://www.morcom.com/.

Hindawi Publishing Corporation
Journal of Computer Networks and Communications
Volume 2012, Article ID 837495, 8 pages
doi:10.1155/2012/837495

Research Article

On Spectrum Sensing for TV White Space in China

Christian Kocks,[1] Alexander Viessmann,[1] Peter Jung,[1] Lei Chen,[2] Qiu Jing,[2] and Rose Qingyang Hu[3]

[1] *Department of Communication Technologies, University of Duisburg-Essen, 47057 Duisburg, Germany*
[2] *Communication Technology Research Department, Huawei Tech. Co., Ltd, Chengdu, Sichuan Province 610041, China*
[3] *Department of Electrical and Computer Engineering, Utah State University, Logan, UT 84322, USA*

Correspondence should be addressed to Christian Kocks, christian.kocks@kt.uni-due.de

Received 13 February 2012; Accepted 7 May 2012

Academic Editor: Luca Ronga

In the field of wireless communications the idea of cognitive radio is of utmost interest. Due to its advantageous propagation properties, the TV white space can be considered to become the first commercial application of cognitive radio. It allows the usage of secondary communication systems at non-occupied frequency bands. Within this paper, spectrum sensing algorithms are introduced for the three predominant Chinese TV standards DTMB, CMMB, and PAL-D/K. A prototype platform is presented and its underlying architecture based on a combination of DSP and FPGA is illustrated including the setup of the cognitive radio application. Furthermore, the performance of the sensing algorithms implemented on the prototype platform is shown in comparison to simulation results.

1. Introduction

The recent decade revealed increasing interests in the field of cognitive radio (CR) for wireless communication systems. It is considered as a key technology for significantly alleviating spectrum scarcity.

The TV white space (TVWS), which refers to non-occupied frequency bands in the TV spectrum, that is below 900 MHz, is a desirable target for CR-based spectrum sharing due to its advantageous propagation properties compared to other frequency ranges on the one hand and due to its low utilization ratio on the other hand [1]. Hence, deploying CR mechanisms in TVWS will probably become the first commercial application that brings CR from concept to reality. In the United States, the FCC has already made an official request to allow unlicensed users reusing TV bands without causing interference to incumbent users [2]. In other countries, the corresponding regulatory authorities such as the CEPT in Europe are developing regulations on the unlicensed usage in TVWS as well. Besides the regulatory authorities, working groups such as IEEE 802.22 [3] have started the standardization for cognitive radio applications.

Spectrum sensing is a key element of CR and its application to TVWS has been widely studied. However, a variety of different TV standards exists which may differ from country to country, especially for digital TV standards. While in North America ATSC (Advanced Television Systems Committee) is deployed, in Europe, South Asia, and Africa, DVB-T/H (Digital Video Broadcasting-Terrestrial/Handheld) plays the predominant role. Further standards such as ISDB (Integrated Services Digital Broadcasting) developed in Japan or DMB (Digital Multimedia Broadcasting) developed in Korea are also used in various countries [4]. As a result, it is hardly feasible to design a universal sensing algorithm for all TV standards. This paper focuses on spectrum sensing for Chinese TV standards using an autocorrelation approach. Although the autocorrelation approach has been widely studied for the purpose of spectrum sensing, the application to Chinese TV standards has not been considered thoroughly yet.

In China, mainly three terrestrial and handheld TV standards are deployed: DTMB (Digital Terrestrial Multimedia Broadcast) [5] for terrestrial reception, CMMB (China Mobile Multimedia Broadcasting) [6] for handheld reception

and PAL-D/K (Phase Alternating Line) [7] for analog TV. While other countries such as the USA have already stopped the provision of analog TV, the nationwide switchover from analog to digital TV will not occur until the year 2015. Therefore, the analog TV will still coexist with the digital TV for many years to come. However, measurements on the channel occupancy rate revealed many unused channels although the analog TV is still provided. As a result, the detection of both analog and digital signals is necessary for CR implementations.

The spectrum sensing requirements in China are based on the IEEE 802.22 specifications. That is, the sensing threshold is −114 dBm for 6 MHz channel bandwidth yielding −112.8 dBm for 8 MHz wide channels. For analog TV, the threshold is −114 dBm in 100 kHz bandwidth yielding −95.0 dBm in 8 MHz bandwidth.

The United Kingdom and the United States are the most active countries in exploiting the unlicensed usage of TVWS. The spectrum sensing technology for ATSC signals has been intensively studied. Several detection algorithms for ATSC and its analog predecessor NTSC (National Television System Committee) can be found in the IEEE standard 802.22 [8]. In 2008, a sensing prototype test campaign was organized by the FCC [9]. As an example, Motorola, Philips, and I2R have submitted their prototype designs which have been tested both in the laboratory as well as in the field. The results showed that the ATSC and NTSC signals can be detected correctly with a certain probability. As another widely used TV standard, DVB-T has also been intensively studied with respect to spectrum sensing. In [10], a robust sensing approach is discussed using a prototype sensor developed by Philips. Several detection algorithms for a Chinese standard, that is DTMB, have also been studied and published [11, 12]. In this paper, an experimental spectrum sensing prototype platform for Chinese TV standards is presented and results are discussed.

This paper is structured as follows. Section 2 gives an introduction to the Chinese TV standards DTMB, CMMB, and PAL-D/K. The corresponding sensing algorithms are presented in Section 3. In Section 4, the prototype platform is illustrated including the signal flow for the spectrum sensing operation. Section 5 shows selected results in a comparison between the simulated algorithms' performance and the performance measured with the prototype platform. Finally, a conclusion is given.

2. Chinese TV Standards

The intention of this section is to give a brief overview of the various Chinese TV standards. The focus is on the main aspects which are relevant for feature-based signal detection. For a full description of the TV systems, please refer to [5–7].

2.1. DTMB. DTMB, also referred to as DMB-T (Digital Multimedia Broadcast-Terrestrial), is a mandatory TV standard in China. DTMB can be used in either single-carrier or in multi-carrier mode. Three FEC (Forward Error Correction) code rates, five modulation orders, and two interleaving depths are specified for DTMB [5]. A block diagram of a DTMB transmitter is shown in Figure 1.

DTMB defines three different header types with different lengths. The frame body itself has a fixed length of 500 μs. The frame structure of DTMB including the different header types is illustrated in Figure 2. The frames are hierarchically structured in a calendar day frame, a minute frame, and a super frame. One calendar day frame lasts for 24 hours and contains 1440 minute frames with a duration of one minute each. Each minute frame, in turn, consists of 480 super frames. One super frame consists of either 225 frames with frame header mode 1 or of 216 frames with frame header mode 2 or of 200 frames with frame header mode 3.

The three frame headers are generated by different generator polynomials which are [5]

$$G_1(x) = 1 + x + x^5 + x^6 + x^8 \quad (1)$$

for mode 1,

$$G_2(x) = 1 + x^3 + x^{10} \quad (2)$$

for mode 2, and

$$G_3(x) = 1 + x^2 + x^7 + x^8 + x^9 \quad (3)$$

for mode 3. The generation of the sequence can be realized by a linear feedback shift register. The selection on the frame header mode depends on the desired coverage and is fixed once the transmission has begun.

2.2. CMMB. CMMB is a system fully based on the well-known OFDM (Orthogonal Frequency Division Multiplexing). The transmitter structure is depicted in Figure 3. A combination of Reed-Solomon (RS) and Low-Density Parity-Check (LDPC) codes is used for FEC. Unlike many other OFDM systems such as DVB-T [13], the OFDM symbol of length T_0 in time-domain is not only extended by inserting a cyclic prefix (length T_1), but it is also extended by a pre-guard interval and a post-guard interval of length T_{GI} each. As illustrated in Figure 4, the post-guard interval of a certain OFDM symbol in CMMB overlaps with the pre-guard interval of the subsequent symbol [6].

In CMMB, one frame has a duration of 1 s and consists of 40 time slots. Each time slot contains one beacon and 53 OFDM symbols. The beacon contains a transmitter identification field and two synchronization signals. The OFDM symbols consist of data-bearing subcarriers as well as of pilot subcarriers. These pilot subcarriers are subdivided into continual pilots and scattered pilots [6].

2.3. PAL-D/K. A variety of different PAL-based standards exist which mainly differ in the channel bandwidth or in the underlying modulation scheme. The PAL standard used in China is called PAL-D/K with 8 MHz channel bandwidth, 50 Hz field frequency, and 625 lines per frame [7]. A PAL signal consists of separate video and audio parts. Within this paper, only the bandwidth occupied by the video part is subject to spectrum sensing. The video signal used in PAL

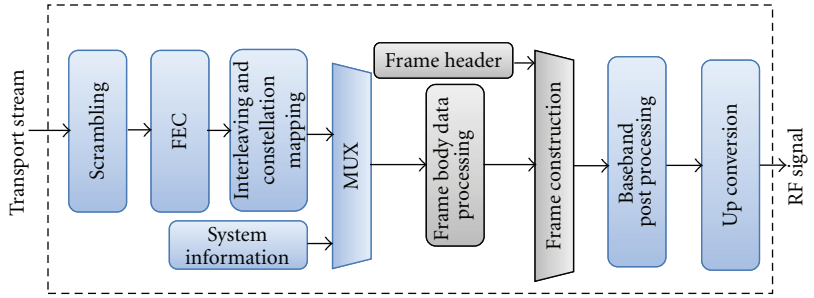

Figure 1: DTMB transmitter [5].

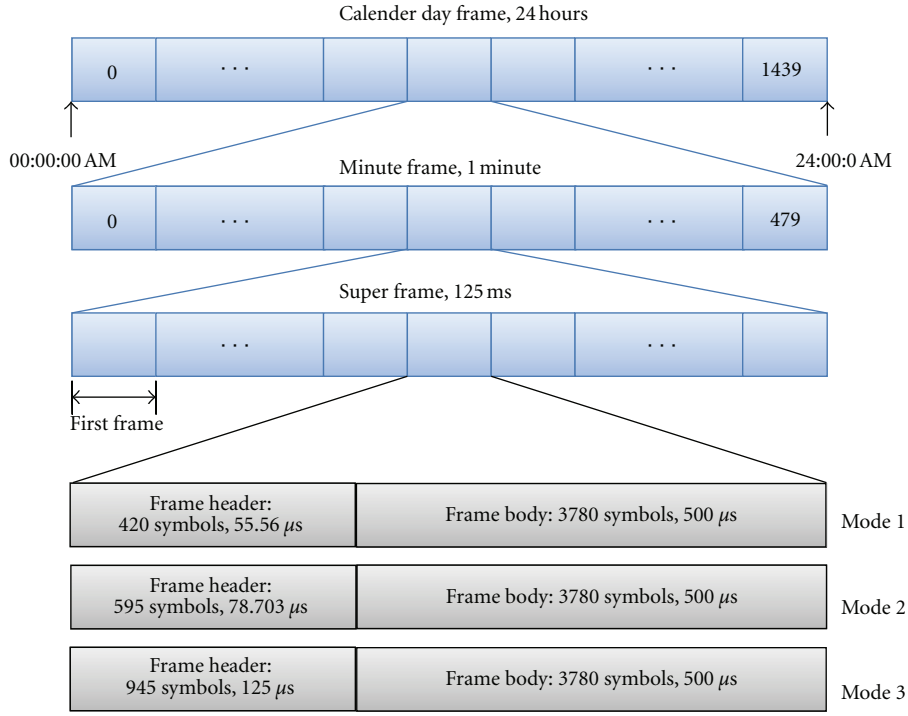

Figure 2: DTMB frame structure [5].

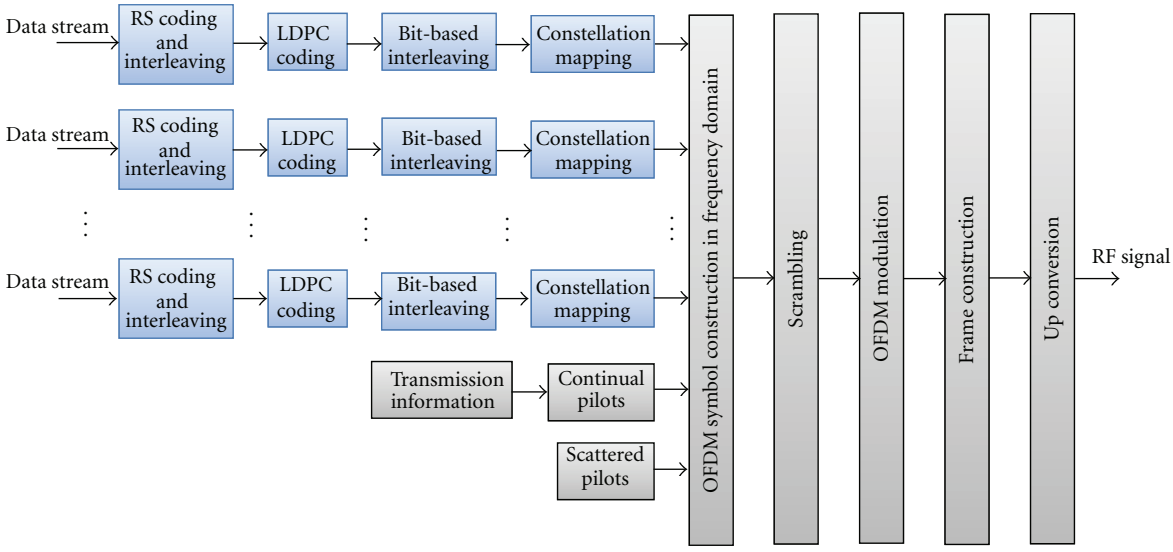

Figure 3: CMMB transmitter [6].

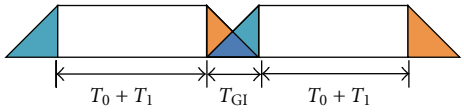

Figure 4: CMMB symbol overlapping.

is a CVBS (Color Video, Blanking and Sync) signal which is an extension to the monochrome VBS (Video, Blanking and Sync) signal. A snapshot of a VBS signal is depicted in Figure 5. In addition to the video signal itself, the VBS signal has some additional components which are required for example for synchronization at the receiver. The black-level signal components after and before the video signal are referred to as front porch and back porch, respectively. The time values shown in Figure 5 are compliant to the PAL-D/K standard. The total duration of one line is 64 μs resulting in a line frequency of 15625 Hz [7].

3. Spectrum Sensing Algorithms

After the brief introduction to the various Chinese TV standards, this section describes the spectrum sensing algorithms. All algorithms have in common that they are based on autocorrelation of the digital baseband signal. In general, the autocorrelation function $\varphi_{ss}(t)$ of a complex signal $s(t)$ is defined as

$$\varphi_{ss}(\tau) = \int_{-\infty}^{\infty} s^*(t)s(t+\tau)dt, \tag{4}$$

where $(\cdot)^*$ denotes the complex conjugation.

3.1. DTMB. In DTMB, the frame header appears periodically at the beginning of each frame which can be exploited for the sensing operation. The presented autocorrelation-based sensing algorithm for DTMB can be divided into three stages:

(i) autocorrelation stage,

(ii) comb-correlation stage,

(iii) decision stage.

A flow diagram of the algorithm is shown in Figure 6. For the autocorrelation the digitized baseband signal is multiplied with a delayed and complex conjugated version of the signal where the delay itself depends on the frame header mode. In case the frame header mode is unknown, the algorithm needs to be carried out for each frame header mode separately. The running average filter cumulates a certain number of the multiplication output samples. Resulting from the periodical appearance of the frame header, the first stage's output is applied to a comb correlator which is a correlation with a Dirac comb $g(t)$ with a distance Δt corresponding to the frame header period, that is,

$$g(t) = \sum_{k=-\infty}^{\infty} \delta(t - k \cdot \Delta t). \tag{5}$$

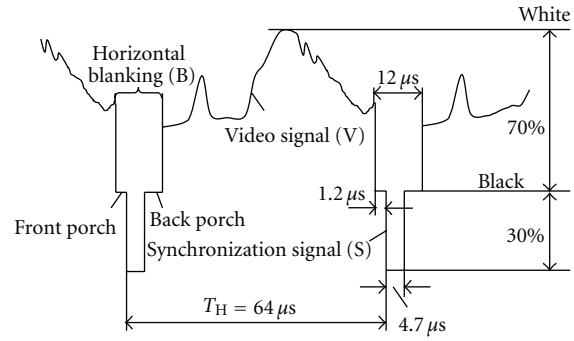

Figure 5: VBS signal.

This stage allows collecting the energy of all frames within the sensing period. The squared magnitude of the cumulated comb-correlation output φ_{cc} is given to the decision stage. In this stage, the ratio λ of the maximum and the average of the previous stage's output is calculated:

$$\lambda = \frac{\max(\varphi_{cc}(t))}{\overline{\varphi_{cc}(t)}}. \tag{6}$$

By applying a soft-decision metric to λ, a measure for the probability of the presence of a DTMB signal is generated. Furthermore, comparing the ratio with a threshold Γ gives a hard-decision on the presence of a DTMB signal. This threshold is generated by using a threshold metric based on the available sensing interval t_{sense} and the desired false-alarm probability P_{fa}.

By using the ratio λ for making the decision about the presence of a DTMB signal, the presented algorithm is robust against dynamic range variations as well as varying signal-to-noise ratios and, thus, independent of the underlying AGC (Automatic Gain Control) implementation.

3.2. CMMB. The sensing algorithm for CMMB is very similar to the sensing algorithm for DTMB. As shown in Section 2, CMMB uses a cyclic repetition of certain parts of the OFDM symbol, denoted as cyclic prefix. Since this cyclic prefix equals the last part of the corresponding OFDM symbol, it is well suited for the sensing operation. The general data flow of the algorithm is identical to the DTMB algorithm depicted in Figure 6. However, the timings must be adapted according to the CMMB parameters.

3.3. PAL-D/K. The sensing algorithm for PAL-D/K relies on the periodicity of certain parts of the CVBS signal as depicted in Figure 5. The CVBS signal exhibits a periodic pattern of the synchronization pulses in every transmitted line of the resulting TV picture. In addition to the synchronization pulses itself with a length of $t_{hsync} = 4.7\,\mu$s, the front as well as the back porch with lengths of $t_{fp} = 1.2\,\mu$s and $t_{bp} = 6.1\,\mu$s, respectively, can be used for sensing purposes. The time between two consecutive synchronization pulses is

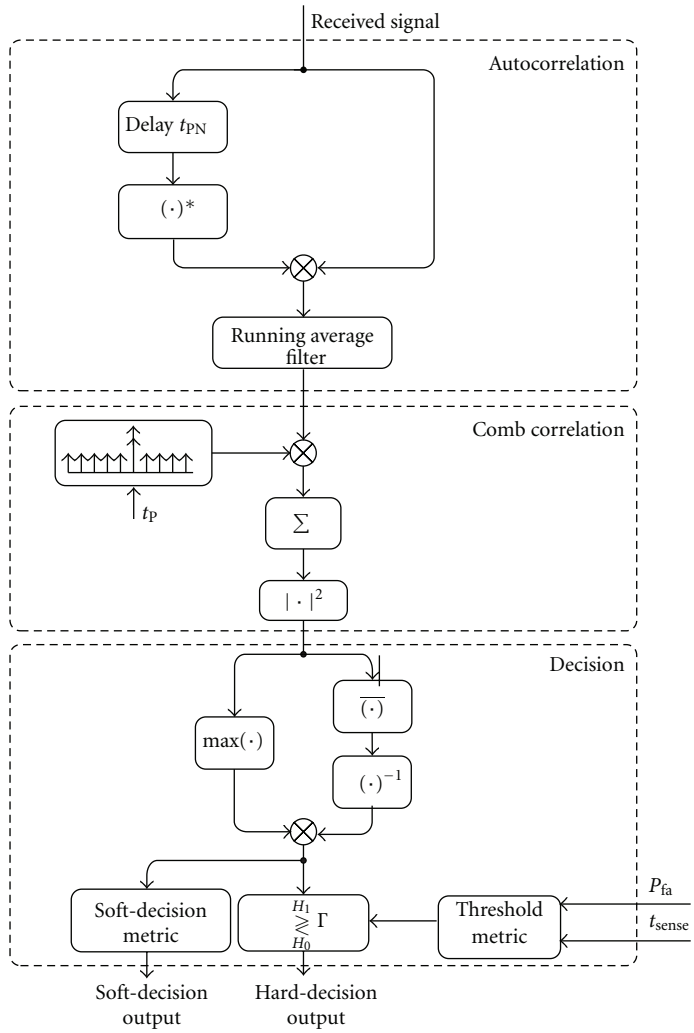

Figure 6: Flow diagram of the DTMB sensing algorithm.

$t_H = 64\,\mu$s. A flow diagram of the PAL-D/K sensing algorithm is depicted in Figure 7 and consists of two stages:

(i) autocorrelation stage,

(ii) decision stage.

While the delay in the autocorrelation corresponds to the periodicity of the CVBS signal, the length of the running average filter is set to t_H as well. This improves the sensing performance by exploiting similarities in the video signal for consecutive lines. In the decision stage, the average of the output of the autocorrelation stage is calculated. The residual parts of the decision stage are identical to the corresponding parts in the decision stages for DTMB and CMMB signals.

4. Spectrum Sensing Prototype Platform

This section presents the underlying prototype platform for the spectrum sensing application. The spectrum sensing prototype presented here is a functional module as part of a TVWS device exploiting the non-occupied frequency for a secondary communication system. The TVWS device can be a base station or user equipment. The sensing prototype must be able to interact with the TVWS device. A synchronization is necessary to match the quiet periods used for the sensing operation. Therefore, two interfaces are defined for the sensing prototype:

(i) Interface to the external clock source by which the prototype can get the synchronization signal for the TVWS device.

(ii) Interface with the spectrum management entity by which the sensing requests and sensing results can be transmitted.

A block diagram of the spectrum sensing entity is shown in Figure 8. It consists of an RF front end, a mixed-signal daughter card, and a C6455 DSP (Digital Signal Processor) Starter Kit (DSK). Core part of the RF front end is a commercially available tuner module. It receives the RF signal by an antenna and down-converts it to an intermediate frequency (IF). This analog IF signal is given to the mixed-signal daughter card and digitized using

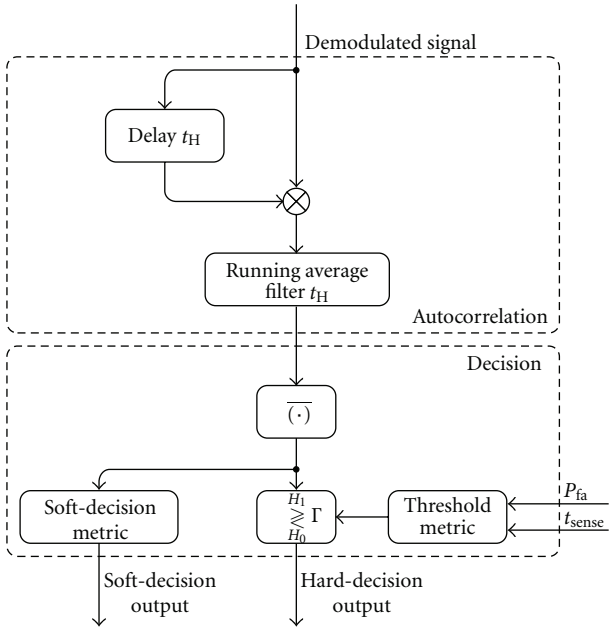

Figure 7: Flow diagram of the PAL-D/K sensing algorithm.

an AD6655 analog-to-digital converter (ADC) by Analog Devices. Further filtering and decimation is carried out on the FPGA (Field-Programmable Gate Array) residing on the daughter card as well. The digital baseband signal is transferred to the DSP located on the DSK. The transfer is carried out via DMA (Direct Memory Access) using the Texas Instruments proprietary EMIF (External Memory Interface). The DSP itself is a powerful Texas Instruments TMS320C6455 running at 1.2 GHz system clock. The sensing algorithms for the various TV standards are carried out on the DSP and the results are transferred to the spectrum management entity which is implemented as a program running on a PC. The connection is realized using an Ethernet interface.

The signal flow within the DSP is illustrated in Figure 9. The digital baseband data coming from the FPGA is stored in a local buffer on the DSP. A control unit, which itself is directly controlled by the spectrum management entity, defines to which detectors the signal is passed. There are different operation modes depending on the a priori knowledge about the underlying TV usage. In case the frequency band of interest may only be used by one TV standard, this information is communicated to the control unit so that only the corresponding detection algorithm is carried out. Otherwise, in case this frequency band may be used by any of the available TV standards, the control unit passes the captured data first to the DTMB detector followed by the CMMB detector and, finally, the PAL-D/K detector. The soft-decision outputs of all detectors are then processed by a combination metric to give an overall information about the presence of any of these signals.

A graphical user interface (GUI) has been developed which allows a simple configuration of the sensing parameters and an immediate demonstration of the sensing results. The synchronization signals are generated by a commercially available Huawei LTE eNodeB. Its signals are received and decoded by the spectrum sensing entity for synchronization with the LTE (Long-Term Evolution) data transmission.

A photography of the spectrum sensing prototype is given in Figure 10. It shows the three aforementioned modules with the RF front end at the top and the DSK at the bottom. In between, the PCB of the daughter card is located. Additionally, a separate PCB is located on the right-hand side for debugging purposes and for interfacing with the synchronization entity.

5. Results

This section presents both simulation results and laboratory measurement results for the previously presented sensing algorithms. The TV signals are generated by a Rohde & Schwarz signal generator. The signals are sent to the prototype module for detection. Additionally, the actual signal power is measured using a Rohde & Schwarz power meter. The parameters used for the simulations as well as for the measurements are as follows: the bandwidth used for all TV standards is 8 MHz and the sensing interval t_{sense} is set to 20 ms. The target false-alarm probabilities are chosen to be 10% and 0.1%, while the target detection probability is 90%. For the simulations, a noise figure of 8 dB is considered. Figure 11 shows the detection probability P_d versus the received signal power p_{rx}. The considered DTMB signal uses frame header mode 1. The blue curves show the simulation results for a false-alarm probability of 10% and 0.1%, respectively. The red curves show the corresponding measurement results. For the target detection probability of 90%, the measurement results are 3 dB to 4 dB worse than the simulation results. Thus, with the given algorithms, a sensitivity of approximately −110 dBm and −108.5 dBm can be reached in the presented hardware setup. There are several reasons that could result in such degradations. The simulations assume a perfect AGC while in the real system the maximum gain is limited by the tuner module leading to an increased quantization noise in case of very low signal powers at the input of the tuner. The TV tuner shows highly unstable behavior in terms of amplitude and phase when the input signal is very weak. Such a property results from the fact that the tuner is designed for receiving TV signals at significantly higher power levels. The required sensing sensitivity is much higher than the TV receiver sensitivity. This causes unexpected distortion when the signal level is below the target receiver sensitivity. This aspect is also the reason why autocorrelation algorithms are favorable compared to cross-correlation algorithms. Cross-correlation algorithms suffer more seriously from such distortions of the tuner, leading maximally to the same overall performance as the autocorrelation algorithms although in simulations such cross-correlation algorithms perform better than their autocorrelation counterparts. However, the computational complexity of cross-correlation implementations is much higher and, hence, autocorrelation algorithms are preferred. Further reasons for the difference between the

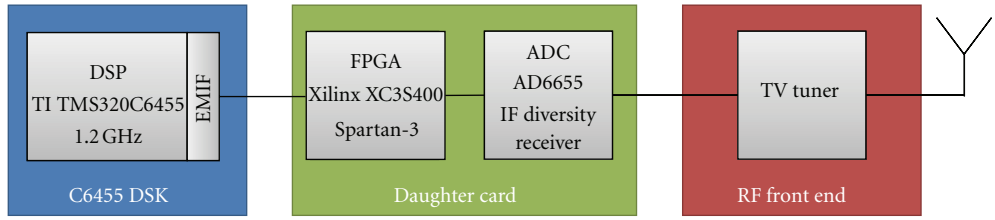

Figure 8: Spectrum sensing entity.

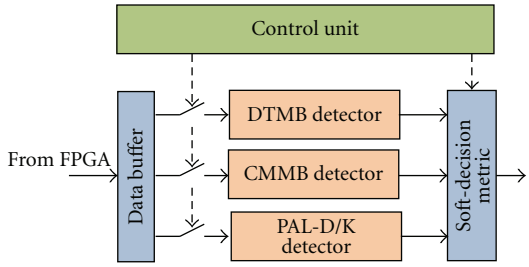

Figure 9: DSP signal flow.

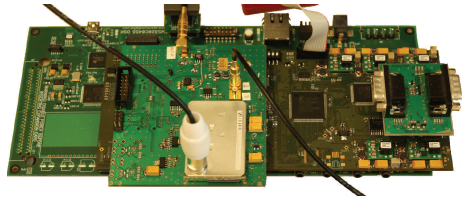

Figure 10: Spectrum sensing entity.

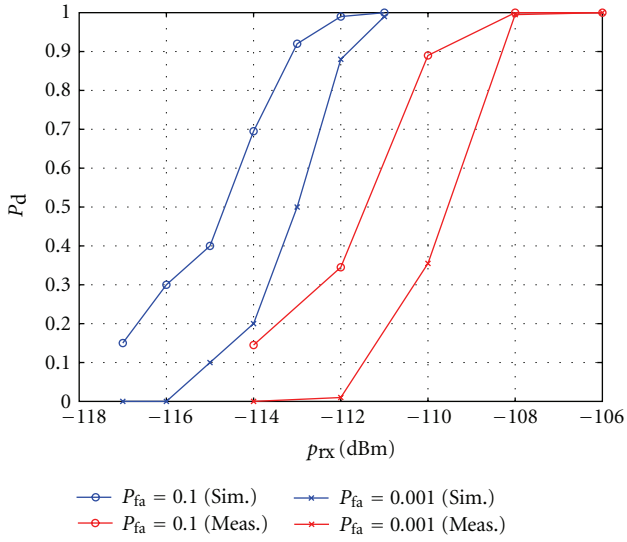

Figure 11: Simulation and measurement results for DTMB (t_{sense} = 20 ms).

simulated and measured sensing results are effects such as frequency offsets and amplifier non-linearities in the RF stage which cannot be avoided in hardware implementations and may lead to significant performance degradations.

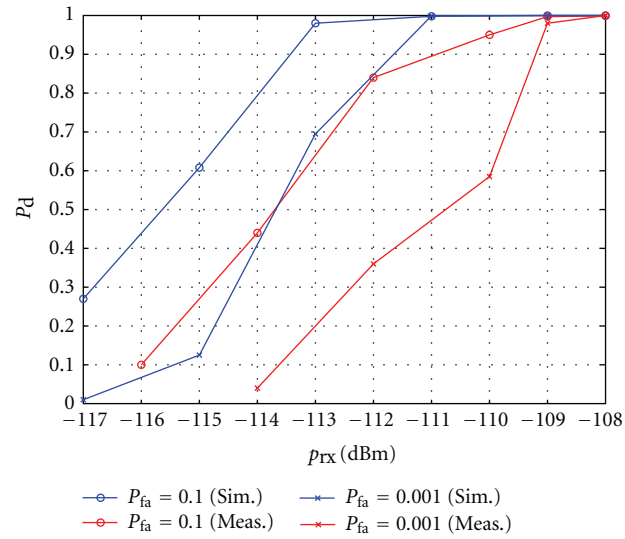

Figure 12: Simulation and measurement results for CMMB (t_{sense} = 20 ms).

However, these effects have not been considered in the simulations.

Figure 12 shows the results for CMMB. Again, a degradation of the measurement performance of almost 3 dB compared to the simulation performance can be identified. With the implemented algorithms, a sensitivity of −111 dBm (P_{fa} = 10%) and −109.5 dBm (P_{fa} = 0.1%), respectively, can be reached for the given target detection probability of 90%.

For PAL-D/K, the measured performance is much worse than the simulated performance as shown in Figure 13. One contribution to the performance loss stems from the additional signal processing steps, which are necessary to extract the CVBS signal from the received PAL-D/K signal. These signal processing steps need to be carried out before the sensing operation. However, they are implemented in a way to minimize the processing latency rather than for utilizing the dynamic range most efficiently. This leads to a significant performance degradation in comparison to the simulation results which are based on floating-point calculations without any constraints regarding the dynamic range. The sensing threshold for PAL-D/K is about −102 dBm.

The simulation results reveal that the sensing algorithms are suitable to fulfill the Chinese spectrum sensing requirements. However, in case of the digital TV standards DTMB

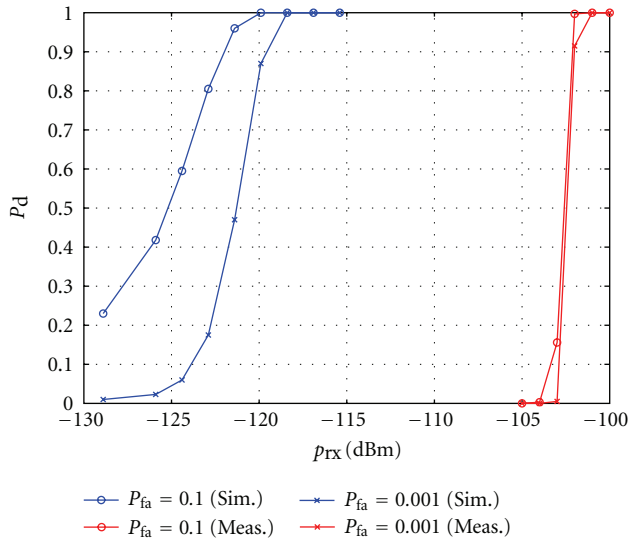

FIGURE 13: Simulation and measurement results for PAL-D/K (t_{sense} = 20 ms).

and CMMB, the measurements slightly fail the requirements using a sensing interval of 20 ms. In case of the analog TV standard PAL-D/K, the requirements are more relaxed so that even for the significant difference between the simulation results and the measurements, the obtained results are sufficient for the Chinese spectrum sensing requirements.

6. Conclusion

Within this paper, an application of cognitive radio for TV white space in China was addressed. Therefore, spectrum sensing algorithms for the three predominant TV standards in China were presented. A prototype platform was introduced and the signal flow was illustrated allowing to sense for the TV standards DTMB, CMMB and PAL-D/K. The performance results revealed that the developed platform allows signal detection even at very low levels of the receive power. Considering a false-alarm probability of 10% and a target detection probability of 90%, the prototype platform achieves a sensitivity of −110 dBm for DTMB while for CMMB and PAL-D/K the sensitivity is −111 dBm and −102 dBm, respectively.

References

[1] J. Van De Beek, J. Riihijärvi, A. Achtzehn, and P. Mähönen, "UHF white space in Europe—a quantitative study into the potential of the 470–790 MHz band," in *Proceedings of the IEEE International Symposium on Dynamic Spectrum Access Networks (DySPAN '11)*, pp. 1–9, May 2011.

[2] FCC, "Report 10-174: in the matter of unlicensed operation in the TV broadcast bands, additional spectrum for unlicensed devices below 900 MHz and in the 3 GHz band—second memorandum opinion and order," Tech. Rep. 10-174, September 2010.

[3] IEEE, "IEEE 802.22 Working Group on Wireless Regional Area Networks," http://www.ieee802.org/22.

[4] W. Fischer, *Digital Video and Audio Broadcasting Technology: A Practical Engineering Guide*, Springer, Berlin, Germany, 3rd edition, 2010.

[5] Std. GB 20 600-2006, "Framing structure, channel coding and modulation for digital television terrestrial broadcasting system," Std. GB 20 600-2006, August 2006.

[6] Std. GY/T 220.1-2006, "Mobile multimedia broadcasting part 1—frame structure, channel coding and modulation for broadcasting channel, SARFT—the state administration of radio, film and television," Std. GY/T 220.1-2006, 2006.

[7] Std. GB 3174-1995, "Characteristics of PAL-D television broadcasting system," Std. GB 3174-1995, December 1995.

[8] IEEE Std. 802.22, "Standard for cognitive wireless regional area networks (RAN) for operation in TV band," IEEE Std. 802.22, July 2011.

[9] FCC, *Evaluation of the Performance of Prototype TV-Band White Space Devices Phase II*, October 2008.

[10] V. Gaddam and M. Ghosh, "Robust sensing of DVB-T signals," in *Proceedings of the IEEE Symposium on New Frontiers in Dynamic Spectrum (DySPAN '10)*, pp. 1–8, April 2010.

[11] A. Xu, Q. Shi, Z. Yang, K. Peng, and J. Song, "Spectrum sensing for DTMB system based on PN cross-correlation," in *Proceedings of the IEEE International Conference on Communications (ICC '10)*, pp. 1–5, May 2010.

[12] L. Wenqi, X. Ning, G. Lijun, Z. Yingxin, and W. Hong, "Spectrum sensing methods for DTMB based cognitive radio systems," in *Proceedings of the 1st International Conference on Information Science and Engineering (ICISE '09)*, pp. 2730–2733, December 2009.

[13] ETSI Std. EN 300 744 V1.6.1, "Digital Video Broadcasting (DVB): framing structure, channel coding and modulation for digital terrestrial television (DVB-T)," ETSI Std. EN 300 744 V1.6.1, January 2009.

Hindawi Publishing Corporation
Journal of Computer Networks and Communications
Volume 2012, Article ID 294581, 9 pages
doi:10.1155/2012/294581

Research Article

Optimizing Cooperative Cognitive Radio Networks with Opportunistic Access

Ammar Zafar,[1] Mohamed-Slim Alouini,[1] Yunfei Chen,[2] and Redha M. Radaydeh[3,4]

[1] *Electrical Engineering Program, KAUST, Al Khawarizmi Applied Mathematics Building 1, Mail Box 2675, Makkah Province, Thuwal 23955-6900, Saudi Arabia*
[2] *School of Engineering, University of Warwick, Coventry, CV4 7AL, UK*
[3] *Electrical Engineering Department, KAUST, Thuwal 23955-6900, Saudi Arabia*
[4] *Department of Electrical and Computer Engineering, Texas A&M University, Texas A&M Engineering Building, Education City, Doha, Qatar*

Correspondence should be addressed to Ammar Zafar, ammar.zafar@kaust.edu.sa

Received 9 January 2012; Revised 19 March 2012; Accepted 20 March 2012

Academic Editor: Enrico Del Re

Optimal resource allocation for cooperative cognitive radio networks with opportunistic access to the licensed spectrum is studied. Resource allocation is based on minimizing the symbol error rate at the receiver. Both the cases of all-participate relaying and selective relaying are considered. The objective function is derived and the constraints are detailed for both scenarios. It is then shown that the objective functions and the constraints are nonlinear and nonconvex functions of the parameters of interest, that is, source and relay powers, symbol time, and sensing time. Therefore, it is difficult to obtain closed-form solutions for the optimal resource allocation. The optimization problem is then solved using numerical techniques. Numerical results show that the all-participate system provides better performance than its selection counterpart, at the cost of greater resources.

1. Introduction

The ever increasing wireless communication networks have put great stress on the already limited spectrum. Due to the fixed spectrum allocation policy, only the licensed users, otherwise known as primary users, are able to access the licensed spectrum. Additionally, the Federal Communications Commission (FCC) task force highlighted in their report the fact that at any given time only 2% of the spectrum is being used [1]. Therefore, ensuring better spectrum usage is of paramount importance.

Cognitive radios have been proposed to resolve this issue [2]. In cognitive radio, the unlicensed users, otherwise known as secondary users, first sense the licensed bands for spectrum holes (parts of the licensed spectrum which are not being employed by the primary users at some time in certain geographical location) [3]. Then, if a spectrum hole is found, the secondary users transmit data to the intended destination. However, the secondary user has to be careful so as not to cause interference to the primary user. The two stages of spectrum sensing and data transmission are related and for optimal performance must be optimized jointly. This is due to the probability of detection, P_d, and probability of false alarm, P_f, associated with spectrum sensing. If the secondary user with probability P_f misses a spectrum hole, then it will keep silent and miss an opportunity to transmit, reducing throughput. However, if a transmission from the primary is missed, with probability $1 - P_d$, then the secondary user transmits and causes interference to the primary user. Moreover, due to interference, the signal-to-noise-ratio (SNR) of the secondary user also decreases, decreasing the throughput and the symbol error rate (SER). Resource allocation that optimizes this sensing-throughput tradeoff has been discussed in [4]. Other optimal resource allocation algorithms for cognitive radio networks have been discussed in [5]. More specifically, in [5], the authors considered a multiband system and considered the two cases of sensing-based spectrum sharing and opportunistic

spectrum access. However, both the above-mentioned works maximize the throughput.

In this paper, optimal resource allocation is discussed to minimize the SER. In order to achieve minimum SER, cooperation is introduced into the system as it decreases the SER due to diversity [6]. Hence, the transmitting secondary user now, upon sensing a spectrum hole, transmits to the relays as well as the destination. Power allocation for relay-assisted cognitive radio networks has been discussed in [7–15]. These works proposed strategies to maximize the throughput for a cognitive relay network that is allowed to share the frequency band with the primary user. Thus, they did not consider spectrum sensing for opportunistic access. Here, we consider an opportunistic system with amplify-and-forward (AF) relays. Full channel state information is assumed at the central controller which performs the resource allocation. Firstly, an all-participate (AP) system is discussed and it is shown that the optimization problem is nonconvex and hence cannot be solved using analytical means. It is then noted that the AP system is limited due to the systems resources being orthogonally distributed. To rectify this, a selection scheme is proposed and the optimal resource allocation, in this case, is discussed.

The rest of the paper is organized as follows. Section 2 gives the system model. The AP system is considered in Section 3. Section 4 details selective relaying. Numerical results are discussed in Section 5. Finally, Section 6 concludes the paper.

2. System Model

Consider a cognitive radio network in which the secondary source utilizes m relays to send data to the secondary destination as shown in Figure 1. The secondary network only has opportunistic access to the licensed spectrum. Therefore, it needs to perform spectrum sensing. The source performs the spectrum sensing and then transmits information to the relays and destination if it finds a "spectral hole" in the first time slot. The relays then forward the received signal to the destination after amplification. In this paper narrowband channel is assumed. The source and the relays can use frequency orthogonal channels to avoid causing interference to each other in wideband channels. For ease of analysis, we consider time orthogonal channels here. Hence, a total of $m+1$ time slots are used.

2.1. Received Signal Model. Based on the spectrum sensing result, there are two possible received signal models.

2.1.1. Without Interference from the Primary User. In this scenario, with probability $1-P_f$, where P_f is the probability of false alarm, the source correctly detects the presence of a "spectral hole" and transmits. The signals received at the destination and the relays are

$$\begin{aligned} y_{r_t} &= \sqrt{E_{\mathrm{ST}}} h_{r_t} s + n_{r_t}, \\ y_{i_t} &= \sqrt{E_{\mathrm{ST}}} h_{i_t} s + n_{i_t}, \end{aligned} \tag{1}$$

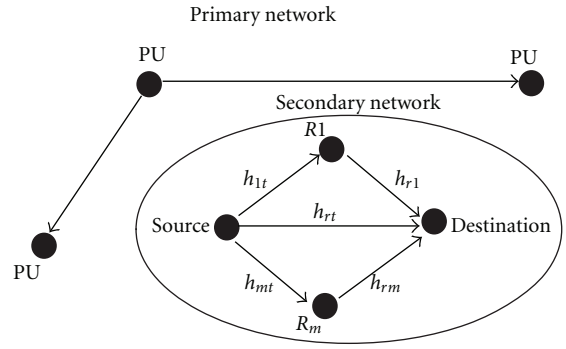

Figure 1: Primary and secondary networks.

where s is the zero-mean and unit-energy transmitted symbol, E_{ST} is the source energy, h_{r_t} is the channel response between the source and the destination, h_{i_t} is the channel response between the ith relay and the source, and $n_{r_t} \sim \mathrm{CN}(0, \sigma^2_{n_{r_t}})$ and $n_{i_t} \sim \mathrm{CN}(0, \sigma^2_{n_{i_t}})$ are the complex Gaussian noise samples. The relay, after normalization and amplification, forwards the received signal to the destination. The signal after normalization becomes

$$s_i = \sqrt{\frac{E_{\mathrm{ST}}}{E_{\mathrm{ST}} |h_{i_t}|^2 + \sigma^2_{n_{i_t}}}} h_{i_t} s + \sqrt{\frac{1}{E_{\mathrm{ST}} |h_{i_t}|^2 + \sigma^2_{n_{i_t}}}} n_{i_t}. \tag{2}$$

Therefore, the received signal at the destination from the ith relay is

$$y_{r_i} = \sqrt{E_i} h_{r_i} s_i + n_{r_i}, \tag{3}$$

where h_{r_i} is the known channel response between the receiver and the ith relay, E_i is the ith relay's energy, and $n_{r_i} \sim \mathrm{CN}(0, \sigma^2_{n_{r_i}})$ is the complex Gaussian noise. Substituting s_i in (3) gives

$$y_{r_i} = \sqrt{\frac{E_{\mathrm{ST}} E_i}{E_{\mathrm{ST}} |h_{i_t}|^2 + \sigma^2_{n_{i_t}}}} h_{r_i} h_{i_t} s + \widetilde{n}_{r_i}, \tag{4}$$

where $\widetilde{n}_{r_i} \sim \mathrm{CN}(0, \widetilde{\sigma}^2_{n_{r_i}})$ and

$$\widetilde{\sigma}^2_{n_{r_i}} = \frac{E_i |h_{r_i}|^2 \sigma^2_{n_{i_t}}}{E_{\mathrm{ST}} |h_{i_t}|^2 + \sigma^2_{n_{i_t}}} + \sigma^2_{n_{r_i}}. \tag{5}$$

Writing the $m+1$ received signals in matrix form, one has

$$\mathbf{y} = \mathbf{h} s + \mathbf{n}, \tag{6}$$

where

$$\mathbf{y}=\left[\frac{1}{\sigma_{n_{r_t}}}y_{r_t}\frac{1}{\widetilde{\sigma}_{n_{r_1}}}y_{r_1}\cdots\frac{1}{\widetilde{\sigma}_{n_{r_m}}}y_{r_m}\right]^T,$$

$$\mathbf{h}=\left[\sqrt{\frac{E_{\mathrm{ST}}}{\sigma^2_{n_{r_t}}}}h_{r_t}\sqrt{\frac{E_{\mathrm{ST}}E_1}{\widetilde{\sigma}^2_{n_{r_1}}\left(E_{\mathrm{ST}}\left|h_{1_t}\right|^2+\sigma^2_{n_{1_t}}\right)}}\times h_{r_1}h_{1_t}\cdots\sqrt{\frac{E_{ST}E_m}{\widetilde{\sigma}^2_{n_{r_m}}\left(E_{\mathrm{ST}}\left|h_{m_t}\right|^2+\sigma^2_{n_{m_t}}\right)}}\times h_{r_m}h_{m_t}\right]^T, \tag{7}$$

and $\mathbf{n}$ is a $(m+1)$ dimensional vector whose components are zero mean and unit variance complex Gaussian random variables. Therefore $\mathbf{n}$ is also complex Gaussian with mean vector of all zeros and covariance matrix being the identity matrix, $\mathbf{I}_{(m+1)\times(m+1)}$, that is $\mathbf{n}\sim\mathrm{CN}(\mathbf{0},\mathbf{I})$.

2.1.2. With Interference from the Primary User. In this case, with probability $1-P_d$ where P_d is the probability of detection, the source misses the transmission from the primary user and transmits, which causes interference. The signals at the destination from both the source and the relays now also include an interfering signal due to primary user activity is

$$\begin{aligned} y_{r_t}&=\sqrt{E_{\mathrm{ST}}}h_{r_t}s+n_{r_t}+y_{I_{r_t}},\\ y_{i_t}&=\sqrt{E_{\mathrm{ST}}}h_{i_t}s+n_{i_t}+y_{I_{i_t}},\end{aligned} \tag{8}$$

where $y_{I_{r_t}}$ and $y_{I_{i_t}}$ are the interference signals.

Taking into account the fact that the source and relays have no knowledge of the interfering signal and adopting the same approach as previously, one can write

$$y_{r_i}=\sqrt{\frac{E_{\mathrm{ST}}E_i}{E_{\mathrm{ST}}\left|h_{i_t}\right|^2+\sigma^2_{n_{i_t}}}}h_{r_i}h_{i_t}s+\hat{n}_{r_i}+\hat{y}_{I_{r_i}}, \tag{9}$$

where $\hat{n}_{r_i}\sim\mathrm{CN}(0,\hat{\sigma}^2_{n_{r_i}})$ and

$$\begin{aligned}\hat{\sigma}^2_{n_{r_i}}&=\frac{E_i\left|h_{r_i}\right|^2\sigma^2_{n_{i_t}}}{E_{\mathrm{ST}}\left|h_{i_t}\right|^2+\sigma^2_{n_{i_t}}}+\sigma^2_{n_{r_i}},\\ \hat{y}_{I_i}&=y_{I_{r_i}}+\sqrt{\frac{E_i}{E_{\mathrm{ST}|h_{i_t}|^2+\sigma^2_{n_{i_t}}}}}h_{r_i}y_{I_{i_t}}.\end{aligned} \tag{10}$$

Again in matrix form one has

$$\mathbf{y}_I=\mathbf{h}_I s+\mathbf{n}_I+\mathbf{Y}_I, \tag{11}$$

where

$$\mathbf{y}_I=\left[\frac{1}{\sigma_{n_{r_t}}}y_{r_t}\frac{1}{\hat{\sigma}_{n_{r_1}}}y_{r_1}\cdots\frac{1}{\hat{\sigma}_{n_{r_m}}}y_{r_m}\right]^T,$$

$$\mathbf{h}_I=\left[\sqrt{\frac{E_{\mathrm{ST}}}{\sigma^2_{n_{r_t}}}}h_{r_t}\sqrt{\frac{E_{\mathrm{ST}}E_1}{\hat{\sigma}^2_{n_{r_1}}\left(E_{\mathrm{ST}}\left|h_{1_t}\right|^2+\sigma^2_{n_{1_t}}\right)}}\times h_{r_1}h_{1_t}\cdots\sqrt{\frac{E_{\mathrm{ST}}E_m}{\hat{\sigma}^2_{n_{r_m}}\left(E_{\mathrm{ST}}\left|h_{m_t}\right|^2+\sigma^2_{n_{m_t}}\right)}}\times h_{r_m}h_{m_t}\right]^T, \tag{12}$$

$$\mathbf{Y}_I=\left[\frac{1}{\sigma_{n_{r_t}}}y_{I_{r_t}}\frac{1}{\hat{\sigma}_{n_{r_1}}}\hat{y}_{I_1}\cdots\frac{1}{\hat{\sigma}_{n_{r_m}}}\hat{y}_{I_m}\right]^T,$$

and $\mathbf{n}_I\sim\mathrm{CN}(\mathbf{0},\mathbf{I})$.

2.2. Spectrum Sensing. Spectrum sensing is performed, by means of an energy detector, for the first t_s seconds out of total time slot duration of T seconds at the source node only. The remaining $T-t_s$ is used for transmission, after detecting a "spectral hole". The probabilities of detection and false alarm, according to [16], are given by

$$\begin{aligned}P_d&=Q\left(\frac{\lambda-N-\gamma_d}{\sqrt{2(N+2\gamma_d)}}\right),\\ P_f&=Q\left(\frac{\lambda-N}{\sqrt{2N}}\right),\end{aligned} \tag{13}$$

respectively, where λ is the threshold of the energy detector, $N=t_s f_s$ is the number of samples, f_s is the sampling frequency, γ_d equals N times the SNR at the output of the detector and $Q(\cdots)$ is the Gaussian Q-function.

3. All Participate System

In this section, an all-participate (AP) system is discussed. In such a system, all the relays forward the signal to the destination. Firstly, the optimization problem is formulated. Then the constraints on the objective function are derived. The SER at the destination is given by

$$\begin{aligned}\mathrm{SER}=&P(H_0)\left(Q\left(\sqrt{k\gamma_0}\right)\right)\left(1-P_f\right)\\&+P(H_1)\left(Q\left(\sqrt{k\gamma_I}\right)\right)(1-P_d),\end{aligned} \tag{14}$$

where γ_0 is the SNR after combining, γ_I is the signal-to-interference-plus-noise-ratio (SINR) after combining, k is a constant which depends on the modulation scheme used, $P(H_0)$ is the probability of no primary user transmission, and $P(H_1)=1-P(H_0)$ is the probability of a primary user

transmission. The SNR γ_0 can be found, assuming maximal ratio combining (MRC), as

$$\gamma_0 = \alpha + \sum_{i=1}^{m} \frac{\beta_i}{\widetilde{\sigma}^2_{n_{r_i}}}, \tag{15}$$

where

$$\alpha = \frac{p_{\mathrm{ST}} T_s |h_{r_t}|^2}{\sigma^2_{n_{r_t}}}, \qquad \beta_i = \frac{p_{\mathrm{ST}} p_i T_s^2 |h_{r_i}|^2 |h_{i_t}|^2}{p_{\mathrm{ST}} T_s |h_{i_t}|^2 + \sigma^2_{n_{i_t}}}, \tag{16}$$

where the source and relay energies have been replaced by

$$E_{\mathrm{ST}} = p_{\mathrm{ST}} T_s, \qquad E_i = p_i T_S, \tag{17}$$

where p_{ST} and p_is are the source and relay powers, respectively, and T_s is the symbol time. Similarly, γ_I can be expressed as

$$\gamma_I = \frac{\left(\alpha + \sum_{i=1}^{m} \left(\beta_i / \widehat{\sigma}^2_{n_{r_i}}\right)\right)^2}{\alpha + \sum_{i=1}^{m} \left(\beta_i / \widehat{\sigma}^2_{n_{r_i}}\right) + \left(\alpha c / \sigma^2_{n_{r_t}}\right) + \sum_{i=1}^{m} \left(d_i / \widehat{\sigma}^2_{n_{r_i}}\right)\left(\beta_i / \widehat{\sigma}^2_{n_{r_i}}\right)}, \tag{18}$$

where

$$c = E\left[\left| y_{I_{r_t}} \right|^2\right], \tag{19}$$

$$d_i = E\left[\left| \widehat{y}_{I_i} \right|^2\right], \tag{20}$$

$$E\left[\left| \widehat{y}_{I_i} \right|^2\right] = E\left[\left| y_{I_{r_i}} \right|^2\right] + E\left[\left| y_{I_{i_t}} \right|^2\right] \left(\frac{E_i}{E_{ST|h_{i_t}|^2 + \sigma^2_{n_{i_t}}}} |h_{r_i}|^2\right). \tag{21}$$

After substituting (15) and (18) in (14), the SER can be obtained as

$$\begin{aligned} \mathrm{SER} = {} & P(H_0) Q\left(\sqrt{k\left(\alpha + \sum_{i=1}^{m} \frac{\beta_i}{\widetilde{\sigma}^2_{n_{r_i}}}\right)}\right) \\ & \times \left(1 - Q\left(\frac{\lambda - N}{\sqrt{2N}}\right)\right) \\ & + P(H_1)\left(1 - Q\left(\frac{\lambda - N - \gamma_d}{\sqrt{2(N + 2\gamma_d)}}\right)\right) Q \\ & \times \left(\sqrt{\frac{k\left(\alpha + \sum_{i=1}^{m} \left(\beta_i / \widehat{\sigma}^2_{n_{r_i}}\right)\right)^2}{\alpha + \sum_{i=1}^{m} \left(\beta_i / \widehat{\sigma}^2_{n_{r_i}}\right) + \left(\alpha c / \sigma^2_{n_{r_t}}\right) + \sum_{i=1}^{m} \left(d_i / \widehat{\sigma}^2_{n_{r_i}}\right)\left(\beta_i / \widehat{\sigma}^2_{n_{r_i}}\right)}}\right). \end{aligned} \tag{22}$$

Now we form the different constraints on the problem. First, we consider both individual power constraints at the source and the relay and a global power constraint on the whole system. Therefore, the constraints are given by

$$\begin{gathered} 0 \le p_{\mathrm{ST}} \le p_T, \quad 0 \le p_i \le p_i^{\max}, \quad P_f \le P_f^{\mathrm{th}}, \\ p_{\mathrm{ST}} + \sum_{i=1}^{m} p_i \le p_{\mathrm{total}}, \quad RT_s + t_s \le T, \end{gathered} \tag{23}$$

where p_{ST} is the power available at the source, $p_i^{\max}$ is the power available at each relay, p_{total} is the power available to the whole system, and P_f^{th} specifies the constraint on the probability of false alarm. The constraints on P_f, T_s, and t_s are introduced to maintain an acceptable throughput. Next the two cases of global power constraint only and individual power constraints only are considered. For the case of global power constraint only, the constraints will be

$$P_f \le P_f^{\mathrm{th}}, \quad p_{\mathrm{ST}} + \sum_{i=1}^{m} p_i \le p_{\mathrm{total}}, \quad RT_s + t_s \le T. \tag{24}$$

In the other scenario, the constraints are given by

$$\begin{gathered} 0 \le p_{\mathrm{ST}} \le p_T, \quad 0 \le p_i \le p_i^{\max}, \quad P_f \le P_f^{\mathrm{th}}, \\ RT_s + t_s \le T. \end{gathered} \tag{25}$$

The individual power constraints are set to limit the interference suffered by the primary user in the case of missed detection. As there is no individual power constraint, the interference caused to the user in the global power constraint only case, where the primary user is only protected by spectrum sensing, is greater.

The problem with optimizing (22) is that it is a nonlinear and nonconvex function due to the Gaussian Q-function being nonlinear and, in general, nonconvex. Thus, the Lagrangian multiplier method [17] cannot be applied here to obtain closed form expressions of the optimal resource allocation. One has to resort to numerical techniques to obtain the optimal solution.

A special case of importance is the absence of the direct link between source and destination, because the relays take on a more prominent role in the presence of no direct link. In this case, the SER is can be obtained by setting $\alpha = 0$ in (22).

4. Selective Relaying

The drawback of the all-participate (AP) scheme discussed in the previous section is that to avoid causing interference, the source and the relay transmit on orthogonal channels. Hence, consuming a considerable amount of resources. In our discussion of a time orthogonal systems, $m + 1$ time slots are utilized for the transmission of one data frame. Additionally, as no sensing is performed at the relays, the primary may become active over any one of the m time slots and cause interference.

To overcome these problems, a selection scheme is proposed in this section in which only one relay is selected to take part in forwarding the signal from the source. Now only 2 time slots are used in transmitting one frame of data and thus decreasing the likelihood of primary becoming active again during relay transmission. In the selection case, the SER is

$$\begin{aligned} \mathrm{SER} = {} & P(H_0) Q\left(\sqrt{k\left(\alpha + \frac{\beta_j}{\widetilde{\sigma}^2_{n_{r_j}}}\right)}\right)\left(1 - Q\left(\frac{\lambda - N}{\sqrt{2N}}\right)\right) \\ & + P(H_1) Q \end{aligned}$$

$$\times \left(\sqrt{\frac{k\left(\alpha + \left(\beta_j/\widehat{\sigma}^2_{n_{r_j}}\right)\right)^2}{\alpha + \left(\beta_j/\widehat{\sigma}^2_{n_{r_j}}\right) + \left(\alpha c/\sigma^2_{n_{r_t}}\right) + \left(d_j/\widehat{\sigma}^2_{n_{r_j}}\right)\left(\beta_j/\widehat{\sigma}^2_{n_{r_j}}\right)}} \right) \times \left(1 - Q\left(\frac{\lambda - N - \gamma}{\sqrt{2(N+2\gamma)}}\right)\right), \tag{26}$$

where b_j, d_j, and $\sigma^2_{n_{r_j}}$ correspond to the jth relay that is selected. The SER in (26) is first optimized for all the relays and the relay which gives the minimum optimum SER is selected. Again, all three cases given in (23), (24) and (25) of both global and individual constraints, global constraint only and individual constraint only are considered. The selection criteria of minimizing SER adds complexity. However, such a criteria provides results which can serve as a benchmark as minimizing SER is the optimal selection criteria.

It is again evident that, even in the selection case, the SER is still a nonlinear and nonconvex function. Therefore, one has to resort to numerical techniques to find the optimal solution. The special case of no direct link is again of particular interest and considered separately.

5. Numerical Results

In this section, numerical results are provided for the optimization problems discussed. First, the proposed AP system with optimal resource allocation is discussed and it is shown that the proposed AP schemes give better performance than the uniform power allocation (UPA) scheme. In UPA, the power is uniformly distributed among the source and the relays and the sensing time and the symbol time are set so that the inequality $RT_s + t_s \leq T$ is satisfied. The selection scheme is discussed next and its performance is compared with selection with UPA. To make it easy for the reader to follow the discussion, a glossary is included in Table 1.

An interior-point algorithm was used to perform the optimization. The MATLAB function *fmincon*, which performs constrained optimization, is used to run the interior-point algorithm. To ensure that the algorithm converged to the optimal solution, the algorithm was run for a large number of initial values. All the variances are set as equal, $\sigma^2_{n_{r_t}} = \sigma^2_{n_{i_t}} = \sigma^2_{n_{r_i}} = \sigma^2$. The constraint of P_f is set at $P_f^{\text{th}} = 0.1$. The total time duration is taken to be 100 ms. Binary phase shift keying (BPSK) is the modulation scheme employed. Due to the the number of samples and the sensing time being linearly related, the results are plotted against the number of samples.

The relationship between the number of samples (N) and SER is shown in Figure 2. As one can clearly observe from Figure 2, there is an optimal value of the number of samples, hence for the sensing time, which minimizes the SER. This is because of the tradeoff between symbol time, T_s and sensing time, t_s. Increasing sensing time means higher probability of detection which leads to a lower SER. However, an increase in sensing time comes at the cost of a decrease in symbol time which leads to lower γ_0 and γ_I. Therefore, the SER increases. Similarly, decreasing sensing time implies a lower probability of detection and, in turn, higher SER. However, it also means high values of γ_0 and γ_I due to increase in symbol time, which in turn leads to lower SER. Hence, there exists an optimal value. This optimal value is affected by the primary user's SNR. The higher the primary user's SNR, the lower the optimal value of the sensing time will be as it takes shorter time to reach the same value of P_d as it would take for a lower SNR of the primary user.

Figure 3 shows the relationship between the symbol time, T_s, and the SER. The relationship follows the opposite pattern as the sensing time. This is due to the constraint relating sensing time and the symbol time. Therefore, when

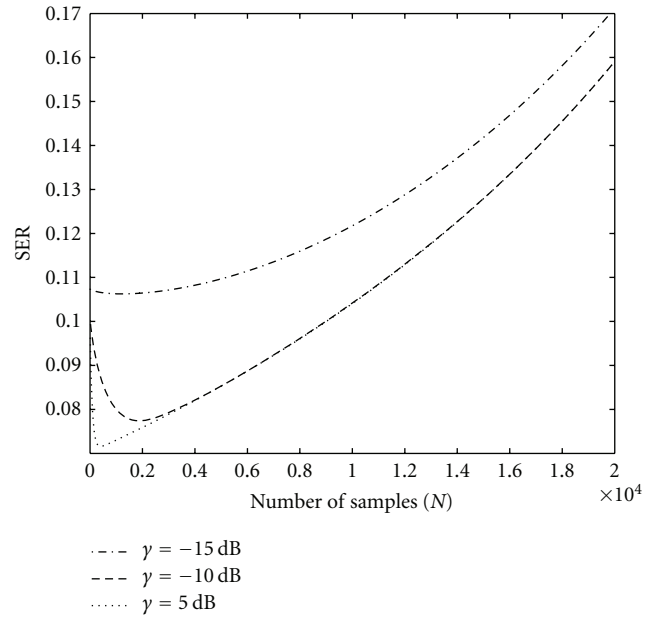

Figure 2: SER as a function of the number of samples (N).

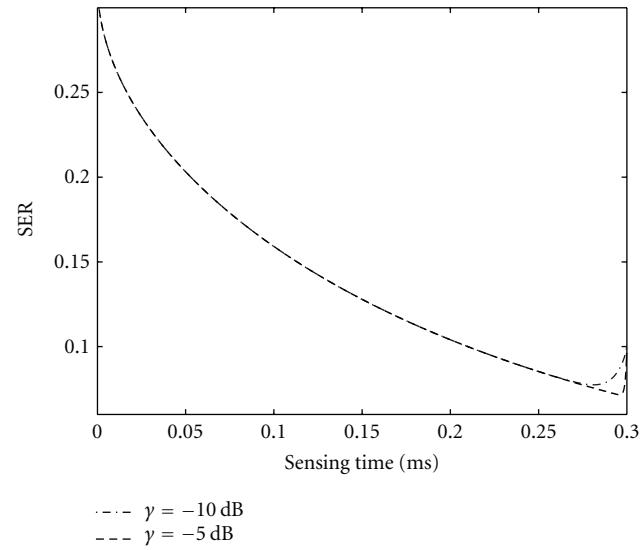

Figure 3: SER as a function of the symbol time (T_s).

Table 1: Glossary.

Acronym	Full name
AP-ORA	All-participate with optimal resource allocation
AP-ORA-GL	All-participate optimal resource allocation with global constraint only
AP-ORA-Ind	All-participate optimal resource allocation with individual constraints only
UPA	uniform power allocation
AP-ORA-NDL	All-participate optimal resource allocation with no direct link
AP-ORA-GL-NDL	All-participate optimal resource allocation with global constraint only and no direct link
AP-ORA-Ind-NDL	All-participate optimal resource allocation with individual constraints only and no direct link
UPA-NDL	uniform power allocation with no direct link
Sel-ORA	selection with optimal resource allocation
Sel-ORA-GL	selection optimal resource allocation with global constraint only
Sel-ORA-Ind	selection optimal resource allocation with individual constraints only
Sel-UPA	selection with uniform power allocation
Sel-ORA-NDL	selection optimal resource allocation with no direct link
Sel-ORA-GL-NDL	selection optimal resource allocation with global constraint only and no direct link
Sel-ORA-Ind-NDL	selection optimal resource allocation with individual constraints only and no direct link
Sel-UPA-NDL	selection uniform power allocation with no direct link

the optimal value of the sensing time is low, the optimal value of the symbol time is high.

Figure 4 shows the SER performance of the different AP schemes plotted against γ_s, where $\gamma_s = 1/\sigma^2$. As expected, for the case with a direct link, the three optimal resource allocation (ORA) scenarios, global constraint only (GL), individual constraints only (Ind), and both global and individual constraints, outperform the uniform power allocation (UPA) and the direct link only for all values of γ_s and the gap in performance becomes wider with increasing γ_s.

In Figure 4, in the case where there is no direct link (NDL) between source and destination, the performance is a little different. In this case, all three ORA schemes, AP-ORA-NDL, AP-ORA-GL-NDL, and AP-ORA-Ind-NDL, outperform the uniform power allocation scheme (UPA-NDL). However, for γ_s less than 0 dB, the direct link only case provides better SER performance than the three ORA cases with no direct link. The three ORA schemes with no direct link start to catch up to the direct link only scenario after 0 dB and completely outperform it after 5 dB. This phenomena coupled with the fact that AP-ORA-NDL, AP-ORA-GL-NDL, and AP-ORA-Ind-NDL, are handily outperformed by AP-ORA, AP-ORA-GL, and AP-ORA-Ind, respectively, demonstrate the significance of the presence of a link between the source and destination.

Comparing the different constraints, AP-ORA gives the worst performance in both scenarios of direct and no direct link. This is due to the fact that AP-ORA is constrained both globally and individually. Thus, even if one relay has more favourable conditions, the power allocated to it cannot exceed $p_i^{\max}$ which is not the case in global constraint only case. In global constraint only case more power can be allocated to the source and relay which has more favourable conditions. The comparison between global constraint only and individual constraints only requires further elaboration.

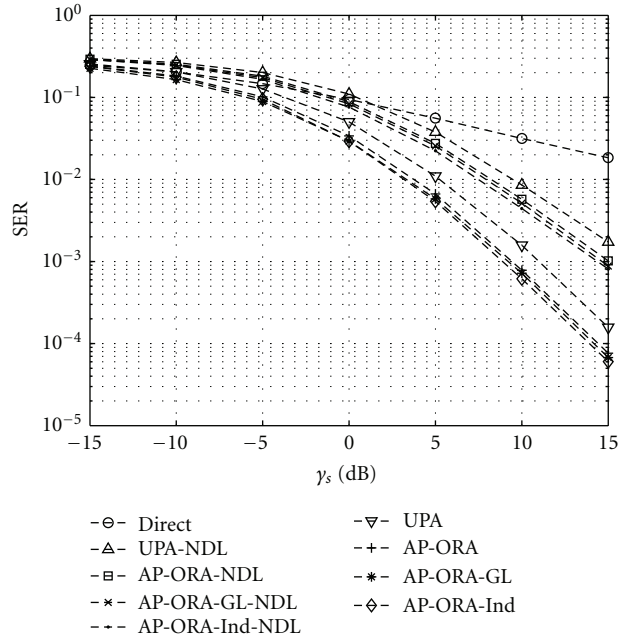

Figure 4: Comparison of SER performance of an all-participate under different schemes and constraints with $m = 3$.

First, the global constraints only and individual only scenarios are compared in the no direct link case. Here, AP-ORA-Ind-NDL provides lower SER than AP-ORA-GL-Ind for all values of γ_s. AP-ORA-GL-NDL has the advantage of allocating more power to relays with better channel conditions. However, AP-ORA-Ind-NDL makes up for this advantage by having more total power in the system as it is not constrained by a total power constraint.

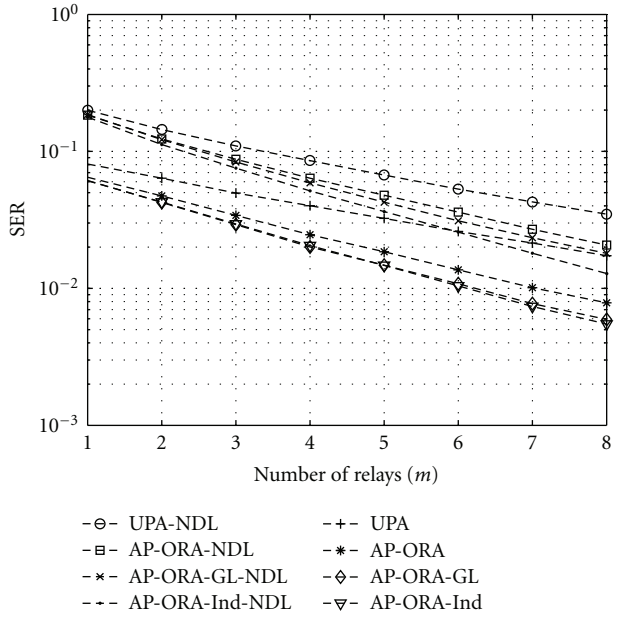

Figure 5: SER as a function of number of layers (m) for the AP system.

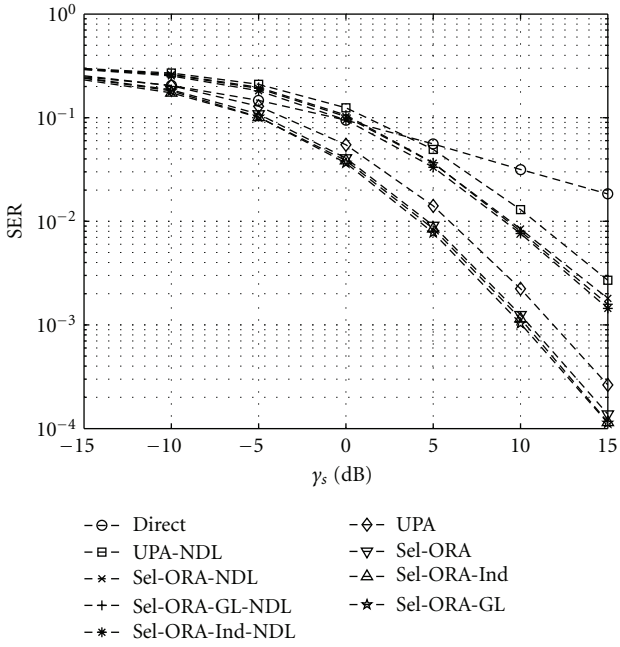

Figure 6: Comparison of SER performance of a selection system under different schemes and constraints with $m = 3$.

Now consider the direct link case. Here, AP-ORA-GL outperforms AP-ORA-Ind at low values of γ_s due to the presence of the direct link. As discussed before, the direct link is quite important, hence, as AP-ORA-GL is not limited by individual constraints, more power can be allocated to the direct link. This is not the case for AP-ORA-Ind. Therefore, AP-ORA-GL gives lower SER. However, with an increase in γ_s, the noise decreases and the greater total power in the case of AP-ORA-Ind comes more into play. Thus, AP-ORA-Ind starts to outperform AP-ORA-GL at higher values of γ_s. However, we must keep in mind that in the global power constraint only case, the interference to the primary is greater than those in the other two cases. Hence, the advantage in performance at low γ_s comes at the cost of greater interference to the primary.

Figure 5 shows the SER performance of the AP system as a function of the number of relays, m. A similar pattern to Figure 4 is observed. The ORA schemes outperform the UPA schemes in both cases of direct and no direct link. Among the proposed ORA schemes, AP-ORA-Ind-NDL provides lower SER than AP-ORA-NDL and AP-ORA-GL-NDL in the no direct link scenario while in the direct link scenario AP-ORA is outperformed by both AP-ORA-Ind and AP-ORA-GL. In addition, AP-ORA-GL has better performance than AP-ORA-Ind for a small number of relays. However, as the number of relays increases AP-ORA-Ind surpasses AP-ORA-GL in terms of performance due to greater total power. Moreover, AP-ORA-NDL, AP-ORA-GL-NDL, and AP-ORA-Ind-NDL even start to outperform UPA for a large number of relays which shows the gain in performance due to ORA.

Figure 6 shows the performance of the various selection schemes as a function of γ_s. The comparison in performance follows a similar pattern as in the AP case with the proposed

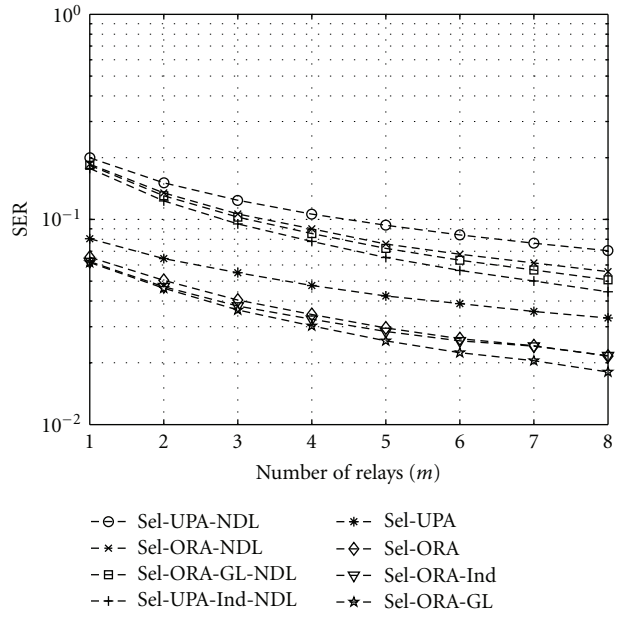

Figure 7: SER as a function of number of relays (m) for selective relaying.

selection ORA schemes outperforming their UPA counterparts and direct link only scenario. However, there is one major difference. In the presence of a direct link, Sel-ORA-Ind gives poorer performance than Sel-ORA-GL even for high values of γ_s. Only at around 15 dB does Sel-ORA-Ind starts to catch up to Sel-ORA-GL. This is due to the fact that as pointed out in the AP system, in the case of global constraints only more power can be allocated to the

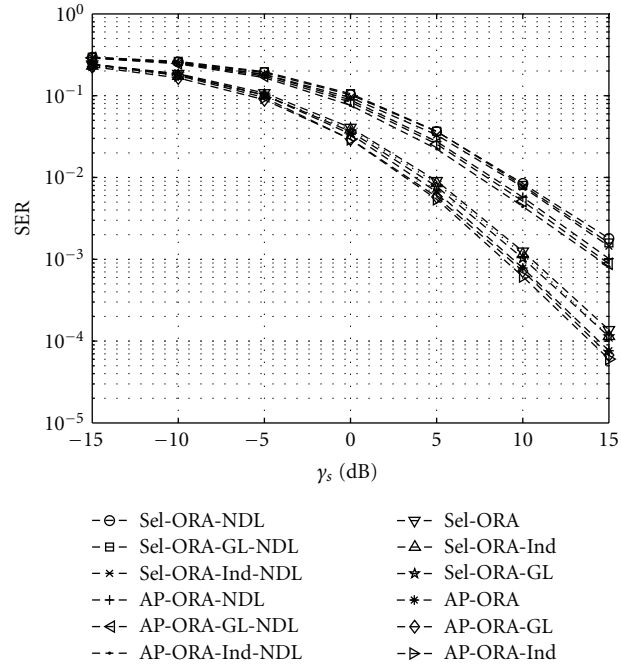

Figure 8: Comparison of AP vs Sel with $m = 3$.

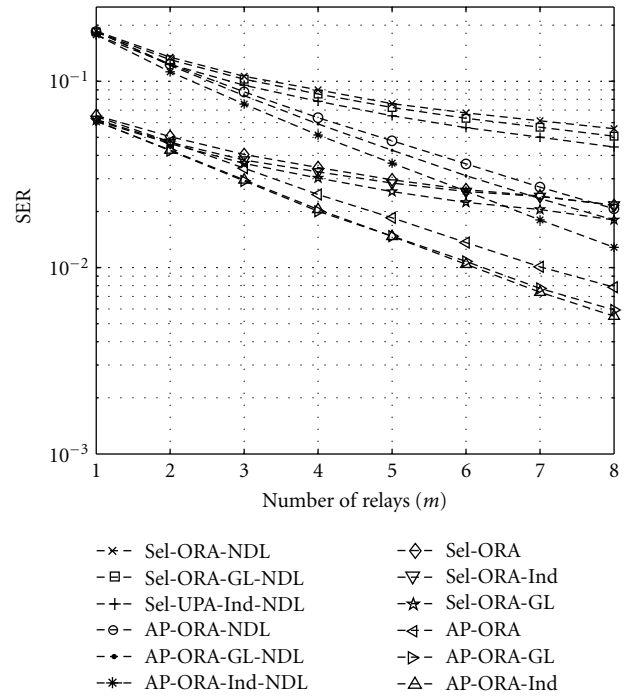

Figure 9: Comparison of AP versus Sel as a function of m.

source. However, unlike AP, in Sel there is only one additional relay which implies less total power for Sel-ORA-Ind and, therefore, requires a high value of γ_s to make the difference in total power count.

SER performance for selective relaying as a function of the number of relays is shown in Figure 7. Again, the main difference from the AP case is that Sel-ORA-GL outperforms Sel-ORA-Ind even for a large number of relays. This is due to the fact that even though the number of relays increase, the total power for Sel-ORA-Ind remains constant as only one relay in addition to the source takes part in data transmission. An interesting point to note here is that the there seems to be a minimum threshold for the SER for the selective system.

Figures 8 and 9 show the performance comparison between the AP and Sel system as a function of γ_s and m, respectively. The comparison is presented separately for clarity, as if it was included in the previous figures, they would have become cluttered. From Figure 8, one can see that AP scheme outperforms the selection scheme in all scenarios, however, the gap in performance is not too big. This is due to the fact that the total number of relays is 3. If m is increased, the performance gap will also increase. Still, one has to keep in mind the extra cost and spectral inefficiency associated with the AP scheme. This becomes more clear when the Figure 9 is examined.

As one can see, the difference in performance between the respective AP schemes and Sel schemes increases with increase in number of relays. As discussed earlier, the Sel schemes look to be bounded by a minimum threshold. Due to this, Sel with direct link scenarios even fall below the AP with no direct link scenarios for a large number of relays.

6. Conclusions

In this paper, ORA for a cognitive relay network has been discussed. It has been shown that for an AP system that ORA improves SER performance and the discussed schemes outperform the UPA schemes. The importance of the direct link between the source and the destination has also been demonstrated. Among the different constraints on the system, the case of both individual and global constraints gives the worst performance while global constraints only is the best for low γ_s. However, this comes at the cost of greater interference to the primary user. The individual constraints only case takes over as the best scheme as γ_s increases.

It was then noted that the AP scheme consumes considerable resources and is spectrally inefficient. Therefore, a simple relay selection scheme has been proposed. Optimal resource allocation was then discussed for the selection scheme. The performance comparison of the AP and Sel shows that while AP provides better SER performance, it comes at the cost of considerable resources.

Acknowledgment

This work was supported by King Abdullah University of Science and technology (KAUST).

References

[1] "Federal communications comission (fcc), et docket no 03-322 notice of proposed rule making and order," 2003.

[2] J. Mitola and G. Maguire Jr., "Cognitive radio: making software radios more personal," *IEEE Personal Communications*, vol. 6, no. 4, pp. 13–18, 1999.

[3] S. Haykin, "Cognitive radio: brain-empowered wireless communications," *IEEE Journal on Selected Areas in Communications*, vol. 23, no. 2, pp. 201–220, 2005.

[4] Y. Liang, Y. Zeng, E. C. Y. Peh, and A. T. Hoang, "Sensing-throughput tradeoff for cognitive radio networks," *IEEE Transactions on Wireless Communications*, vol. 7, no. 4, pp. 1326–1337, 2008.

[5] S. Stotas and A. Nallanathan, "Optimal sensing time and power allocation in multiband cognitive radio networks," *IEEE Transactions on Communications*, vol. 59, no. 1, pp. 226–235, 2011.

[6] J. Laneman, D. Tse, and G. Wornell, "Cooperative diversity in wireless networks: efficient protocols and outage behavior," *IEEE Transactions on Information Theory*, vol. 50, no. 12, pp. 3062–3080, 2004.

[7] W. Yue, B. Zheng, and Q. Meng, "Optimal power allocation for cognitive relay networks," in *Proceedings of the International Conference on Wireless Communications and Signal Processing (WCSP '09)*, pp. 1–5, Nanjing, China, November 2009.

[8] L. Li, X. Zhou, H. Xu, G. Y. Li, D. Wang, and A. Soong, "Simplified relay selection and power allocation in cooperative cognitive radio systems," *IEEE Transactions on Wireless Communications*, vol. 10, no. 1, pp. 33–36, 2011.

[9] J. Mietzner, L. Lampe, and R. Schober, "Distributed transmit power allocation for multihop cognitive-radio systems," *IEEE Transactions on Wireless Communications*, vol. 8, no. 10, pp. 5187–5201, 2009.

[10] Z. Liu, Y. Xu, D. Zhang, and S. Guan, "An efficient power allocation algorithm for relay assisted cognitive radio network," in *Proceedings of the International Conference on Wireless Communications and Signal Processing (WCSP '10)*, pp. 1–5, Suzhou, China, October 2010.

[11] X. Liu, B. Zheng, J. Cui, and W. Ji, "A new scheme for power allocation in cognitive radio networks based on cooperative relay," in *Proceedings of the 12th IEEE International Conference on Communication Technology (ICCT '10)*, pp. 861–864, Tsukuba Science City, Novmber 2010.

[12] X. Qiao, Z. Tan, S. Xu, and J. Li, "Combined power allocation in cognitive radio-based relay-assisted networks," in *Proceedings of the IEEE International Conference on Communications Workshops (ICC '10)*, pp. 1–5, Cape Town, South Africa, May 2010.

[13] X. Liu, B. Zheng, and W. Ji, "Cooperative relay with power control in cognitive radio networks," in *Proceedings of the 6th International Conference on Wireless Communications, Networking and Mobile Computing (WiCOM '10)*, pp. 1–5, Chengdu, China, September 2010.

[14] L. Jayasinghe and N. Rajatheva, "Optimal power allocation for relay assisted cognitive radio networks," in *Proceedings of the IEEE 72nd Vehicular Technology Conference Fall (VTC2010-Fall '10)*, pp. 1–5, Ottawa, Canada, September 2010.

[15] Z. Shu and W. Chen, "Optimal power allocation in cognitive relay networks under different power constraints," in *Proceedings of the IEEE International Conference on Wireless Communications, Networking and Information Security (WCNIS '10)*, pp. 647–652, Beijing, China, June 2010.

[16] H. Urkowitz, "Energy detection of unknown deterministic signals," *Proceedings of the IEEE*, vol. 55, no. 4, pp. 523–531, 1967.

[17] S. Boyd and L. Vandenberghe, *Convex Optimization*, Cambridge University Press, 2004.

Hindawi Publishing Corporation
Journal of Computer Networks and Communications
Volume 2012, Article ID 549106, 15 pages
doi:10.1155/2012/549106

Research Article

Hybrid Experiential-Heuristic Cognitive Radio Engine Architecture and Implementation

Ashwin Amanna, Daniel Ali, David Gonzalez Fitch, and Jeffrey H. Reed

Bradley Department of Electrical and Computer Engineering, Virginia Tech, Blacksburg, VA 24061, USA

Correspondence should be addressed to Ashwin Amanna, aamanna@vt.edu

Received 20 November 2011; Accepted 23 January 2012

Academic Editor: Luca Ronga

The concept of cognitive radio (CR) focuses on devices that can sense their environment, adapt configuration parameters, and learn from past behaviors. Architectures tend towards simplified decision-making algorithms inspired by human cognition. Initial works defined cognitive engines (CEs) founded on heuristics, such as genetic algorithms (GAs), and case-based reasoning (CBR) experiential learning algorithms. This hybrid architecture enables both long-term learning, faster decisions based on past experience, and capability to still adapt to new environments. This paper details an autonomous implementation of a hybrid CBR-GA CE architecture on a universal serial radio peripheral (USRP) software-defined radio focused on link adaptation. Details include overall process flow, case base structure/retrieval method, estimation approach within the GA, and hardware-software lessons learned. Unique solutions to realizing the concept include mechanisms for combining vector distance and past fitness into an aggregate quantification of similarity. Over-the-air performance under several interference conditions is measured using signal-to-noise ratio, packet error rate, spectral efficiency, and throughput as observable metrics. Results indicate that the CE is successfully able to autonomously change transmit power, modulation/coding, and packet size to maintain the link while a non-cognitive approach loses connectivity. Solutions to existing shortcomings are proposed for improving case-base searching and performance estimation methods.

1. Introduction

Wireless communication devices and networks face outside influences that degrade performance and have potential to render links useless. New advances in the area of cognitive radio (CR), inspired by artificial intelligence integration with reconfigurable platforms, enable devices and networks to observe, make a decision and learn from past experience. Key problems faced by CR are how to effectively integrate both learning and decision onto software-defined radio (SDR) over-the-air platforms such that they can react to situations quickly and effectively.

Specifically this paper address the realization and implementation of a cognitive engine (CE) on an SDR platform for the purpose of link adaptation. The problems addressed include incorporating mechanisms for system observation, triggering the engagement of a CE, architecting the CE such that it can both make decision when faced with new situations, and learn from past experience.

Prior art has defined CE architectures based on heuristic decision making, such as GA, as well as experiential CBR. Earlier works have also proposed hybrid architectures that combine both. This paper builds upon previous work to fully implement a hybrid CBR-GA engine such that the CBR feeds into a GA. The CBR makes decisions if past experiences are available, otherwise the GA is entrusted to identify radio parameter settings if the situation is not similar enough to past experiences. The top cases of the CBR feed into the GA as initial parents to improve the starting search points of the GA. Other contributions include overall process flow, case base structure/retrieval method, performance estimation approach within the GA, and hardware/software lessons learned.

Unique solutions to realizing the concept include mechanisms for combining vector distance and past fitness into an aggregate quantification of similarity. Current limitations within the architecture and implementation are discussed.

Solutions are proposed for case base searching based on a unique indexing scheme. Additional shortcomings in estimation methods are discussed with proposed solutions utilizing blind channel estimator feedback to the transmitter.

The remainder of this paper is structured as follows. Section 2 introduces the foundations of GA and CBR cognitive radio architectures. Note that our use of the term *cognitive* is trivial at best given the transformational work in the fields of psychology, education, and computer science studying true cognitive science. This section focuses on cognitively-inspired simple heuristic and experiential decision-making algorithms for integration with an SDR platform. We will not discuss rule, policy, or bayesian reasoners. Section 3 details our CE architecture and process flow. This includes the CBR case structure, retrieval mechanisms, and GA integration and process flow. Section 5 discusses the specific hardware platform and detailed integration issues related with coordinating a software-based CE with a stand-alone SDR. Section 6 presents performance metrics as the system places a load of an over-the-air file transfer across a transmitter/receiver link in the presence of a third party interference source. Three specific environmental cases were considered. Section 7 identifies specific limitations and assumptions in our current architecture related to CBR search and retrieval and current estimation algorithms within the GA. Unique and compelling solutions are proposed for each to attack the limitations. Finally, Section 8 summarizes and discusses areas for future research.

2. Background

This section focuses on background related to CR architectures with focus on GA and CBR-based architectures. CR's origin stem from the growth of reconfigurable SDR platforms. This transition from purely hardware-based platforms was the enabling factor for enabling the integration of artificial intelligence to wireless communications. Mitola is widely credited for jump starting the field with the original thesis of a system that can intelligently respond to the needs of a user [2]. Today's CE architectures maintain this vision with designs oriented around observing system performance metrics, also known as meters, in order to make decisions about how to set configuration parameters of the SDR to support a defined goal.

The foundation of the process loop that our CE follows lies in the observe, orient, decide, act (OODA) loop [3]. The meters provide the trigger for engaging a CE and define improvements. Radio goals, such as minimizing energy, minimizing error, or maximizing throughput provide an orientation that the CE uses to drive decision making. Simplified decision algorithms identify new radio configuration parameters that ideally will improve performance such that the observable meters fall within a defined threshold. Finally, these new radio parameters are passed to the SDR for implementation and return to the start of the loop. Note that this process flow is reactionary in nature and sometimes considered flawed due to its inability to be proactive.

Early CE architectures focused on rule-based decisions providing fast reaction time yet would operate the same way regardless of the situation. Biologically inspired heuristic methods were seen as an alternative approach that enabled multiobjective performance definitions and capability to react to new situations [4]. GAs take an initial radio configuration and evolve it through an iterative combination of random mutations and crossover of features of strong candidate solutions. Disadvantages of the method include time required to reach convergence, strong dependency on the definitions of fitness, and requirement for estimation algorithms to rank viability of candidate solutions. The engine described here, limits the number of generations the GA is allowed in order identify a potential solution before conditions have changed too much. It is acknowledged that the solution from the GA, especially one from generation-limited operations, will not be optimal.

Implementation of a GA requires conversion of metrics and radio configurations onto a unified scale in order to combine them into a fitness function for assessing a solution's potential for success. This requires the use of utility functions that normalize metrics onto similar scale [5].

While GAs enabled a CE to adapt to new situations, the convergence time diminished its value in practical deployment given how fast wireless environments change. To address this shortcoming, researchers investigated combining a GA with other decision architectures. CBR possessed many of the desirable characteristics for CR. The fundamental algorithm is computationally straightforward, can make decisions faster than a GA and incorporates long-term learning. This experiential-based decision maker founds itself on the human decision-making principles that a solution to a problem can be found by utilizing or modifying solutions to past problems that are close in similarity [6]. While simple conceptually, the implementation requires mechanisms for case definitions, quantification of similarity, case search, and case addition. Hybrid combinations of CBR and heuristics were designed for use with 802.22 white space transmissions where the most similar cases from a library were then optimized using a hill climbing search and a GA [1, 7]. This engine uses the configuration of the most similar retrieved case if it falls within a defined similarity threshold, otherwise the top retrieved cases are used as part of the initial parent population of the GA.

3. Hybrid Architecture

3.1. General Process Flow. Figure 1 illustrates the general decision cycle of the cognitive architecture. The process flow includes five parts: (1) observation, (2) orientation, (3) decision, (4) action, and (5) learning. The first part of the decision cycle focuses on system observations. Typically, observations include meters and environmental conditions, such as noise level. This is implemented by feeding back collected meters from the receiver to the transmitter via a dedicated 802.11 link. Predefined thresholds for the performance determine when the engine moves out of the observation cycle into the orientation and decision cycles. Currently, the CE is triggered when the packet error rate (PER) goes over a certain threshold.

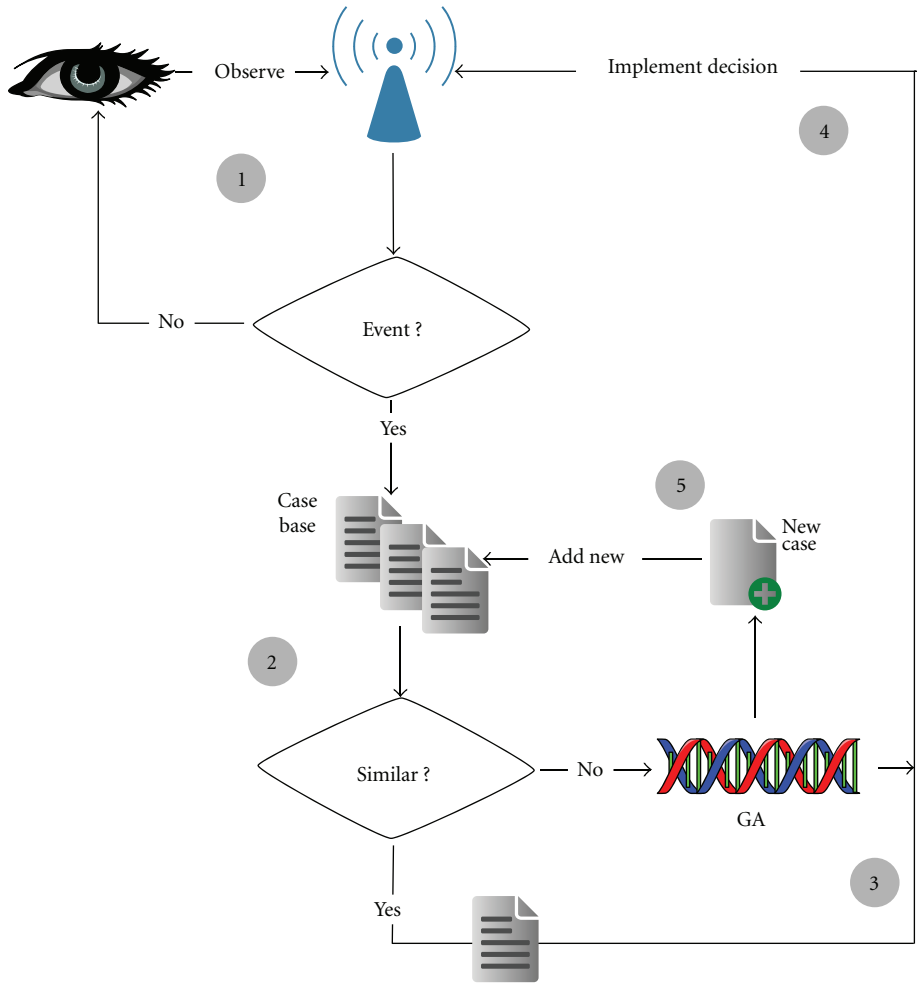

Figure 1: Hybrid CBR-GA cognitive engine process flow.

If an event has been detected, the engine moves onto an orientation phase where it determines which decision-making module best suits the situation. This engine is based on a hybrid architecture of a CBR and a GA. The goal is to first identify if a past decision is similar to the current situation. If similarity falls within a defined threshold, then the configuration settings from the most similar past case are selected and implemented on the radio. This is preferred, as the time-to-action for a CBR is typically much faster than the heuristic GA. However, if there is no past experience that falls within a defined similarity threshold, then the GA is engaged.

The GA is a heuristic search optimization algorithm described in Section 3.2. Once it identifies a solution, the decision is implemented by changing the configuration inputs of the SDR to match the solution. The last part of the decision cycle involves learning whether or not this solution is worth remembering later. This is accomplished by checking the system metrics for improvement after implementing the solution. If this new solution resulted in improved performance, then solution is added as a new case to the library. Details on the GA process are discussed next, followed by the CBR.

3.2. GA. GAs fall underneath the classification of heuristic search. This section briefly reviews their operation. The reader is referred to [8] for more details. Inspiration for the GA came from the evolutionary processes of organisms. Here, organisms or animals that possess genetic traits that are more favorable for a given situation have a higher chance for survival. These traits are passed on from parents to children with the goal of passing on the best traits from each parent. Furthermore, random mutation provided the capability to adapt over time to new situations. Adapting these concepts to cognitive radio requires defining performance goals into computational functions and encoding radio configuration parameters into a string. Fitness functions quantify the success of specific set of configuration parameters. For example, a function that was a factor of packet error, throughput, and spectral efficiency could define a radio's performance. A second set of functions, called utility functions, is implemented to normalize each performance measure onto similar scales.

These functions provide a computational equivalent to an organism's chances of survival. The combination of configuration parameters that leads to the largest value of

the fitness functions is most desired. Similarly, encoding the parameters into a form equivalent to a cellular chromosome enables manipulation using genetic concepts such as gene crossover and mutation. The iterative operation of the GA starts by identifying an initial population. Each individual in the population is a unique set of encoded configuration parameters that factor into an individual's fitness function. The weakest individuals are removed and the remaining individuals are used as parents for a new population. The individuals in this next generation are created by combining, or crossing over, the best traits from a set of parents. Additionally, during each generation, random mutations occur in some individuals. This process is repeated until a predefined maximum number of generations is replaced. Overall, the key configuration parameters of a GA that drive its operation are population size, cross over rate, mutation rate, and maximum generations.

The GA eventually converges towards a good, though not necessarily optimal solution. Like any random-based search, the initial seeds, or starting point of the search are a key aspect of reducing convergence time. The architecture presented here attempts to provide stronger starting points for the GA by using entries in the case history as initial seeds.

3.2.1. Utility Functions and Fitness. Utilities are metrics that give the system a way to measure the desirability of a configuration parameter or meter. They are normalized between 0 and 1, where 1 indicates most desirable and 0 least desirable. Each utility function will either be monotonically increasing or decreasing depending on whether the desirability of the parameter follows a higher-is-better or a lower-is-better goal. The general equation that was used to generate the utility functions are based on previous work [9]. The plots of each utility function can be seen in Figure 2, where the x-axis represents the range of the configuration parameter and meters, and the y-axis is the utility value. Note that for transmit power, on the x-axis, the range goes from 0 to 100. This is because here transmit power is represented as a percentage, where 0 corresponds to minimum output power and 100 represents maximum output power.

Fitness is a metric that combines all utilities into one number. It is also normalized between 0 and 1. Several different methods for calculating fitness were considered:

$$F = \frac{\sum(u_i \cdot w_i)}{N}, \tag{1}$$

$$F = \sqrt[N]{\prod(u_i^{w_i})}, \tag{2}$$

$$F = \frac{\sum(u_i^{w_i})}{N}. \tag{3}$$

Equation (1) shows the fitness calculations through a weighted sum, (2) shows the calculation through a weighted product, and (3) shows a summation of utilities raised to their weights, where u_i are the utilities, w_i are the weights associated to each individual utility and N is the total number of configuration parameters and meters. The purpose of the weights is to give a different significance to each utility for the overall fitness calculation, defining what tradeoffs make when deciding what configuration parameters to select.

Out of the three possibilities, the product fitness was used, because the value of the fitness will only be desirable (close to one) if all the utilities are desirable, and if one utility value is undesirable (close to zero) then the overall fitness will also be undesirable. Figure 3 shows an example of what the fitness space would be for two utilities, one with a weight of 0.8 and the other with a weight of 0.2, for each of the three methods. The product fitness approach is the only one that fulfills the goals. This means that if a configuration parameter or meter is especially poor, then it will get strongly penalized in the fitness calculation; so only a solution that has good combination of configuration parameters and meters will have a good fitness value.

3.2.2. GA Process Flow. At a high level view, the basic GA process flow is described as follows.

(1) Each row of the population is a chromosome defined as a combinations of potential genes. Each available gene corresponds to a unique combination of configuration parameter values that the radio could be set to. Typically each gene is encoded into a defined number of bits.

(2) The initial population is generated by seeding one-third of it with the most similar cases in the CBR if list if it has more than two cases stored; else it seeds it with the current case. The other two-thirds are randomly generated.

(3) Then, for each generation, the following process is followed, until a new population is formed:

  (a) the utilities and fitness are calculated for each individual in the population,

  (b) to generate the next population, parent chromosomes are randomly selected, where the ones with a higher fitness are more likely to be chosen, and they are crossed over,

  (c) Then each bit a gene is randomly mutated with a certain fixed probability.

(4) This process is repeated for a fixed number of generations.

3.2.3. Estimation Methods. For the GA to estimate the meters, the following process is carried out.

(1) First, the new SNR is estimated from the current SNR, the current transmit power, and the new transmit power, where the new SNR is the current SNR less the current transmission power added to the new transmission power in dB.

(2) To calculate throughput, we know that the system uses a constant symbol rate (R_S). Therefore, we can calculate the new throughput ($R_{U_{\text{New}}}$) from the symbol rate, the new t-error correcting code (n_{New}, k_{New}), where t is the number of bits it can correct, modulation order (MO_{New}) and payload length (PL_{New}),

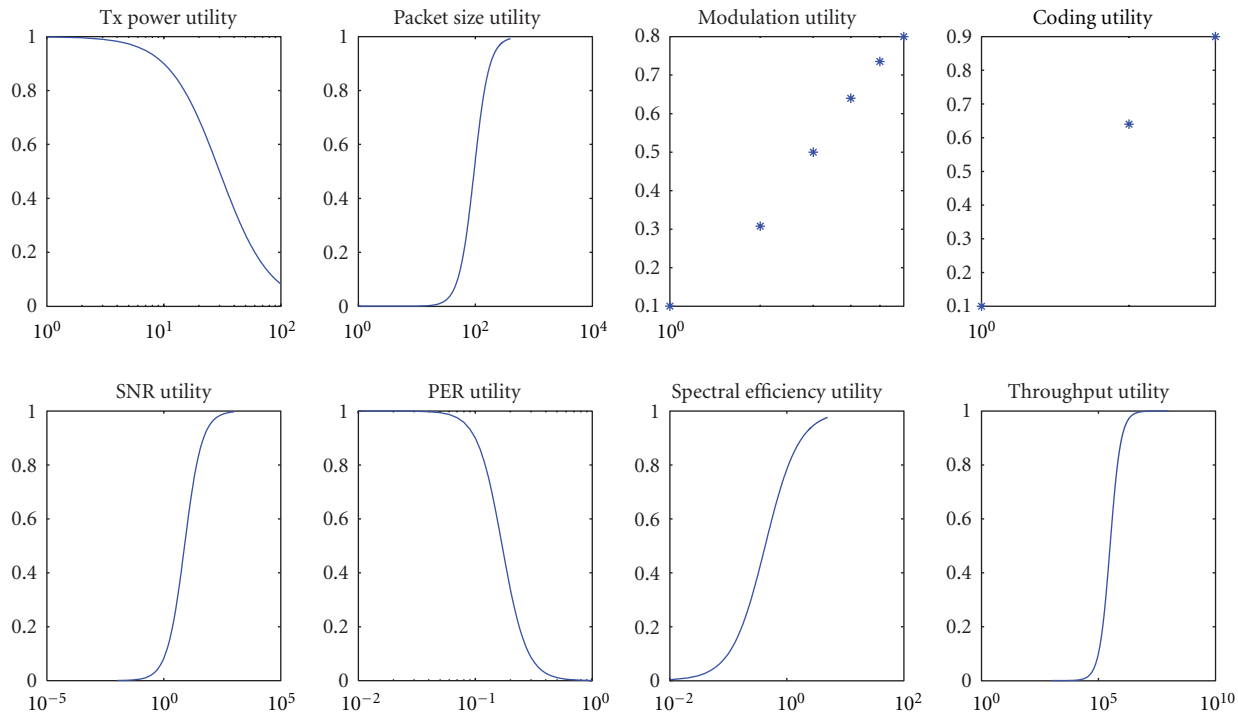

FIGURE 2: GA Utility functions— utility functions map the configuration parameters and meters onto a common scale between $(0, 1)$. A value of 0 is considered undesirable, while a value of 1 is considered most desirable. These utilities are adapted from previous work [1].

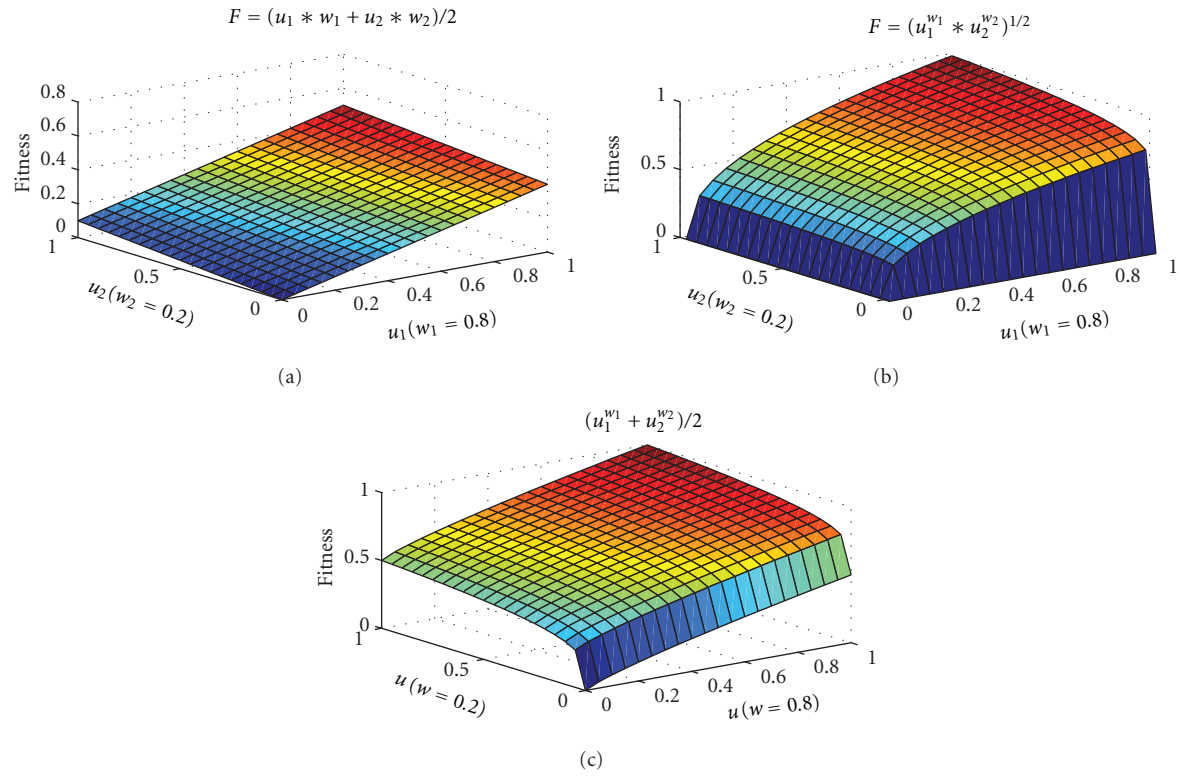

FIGURE 3: Fitness space— three methods for calculating overall fitness from utilities and weights were considered. These figures show the fitness with $w_1 = 0.8$ and $w_2 = 0.2$. The goal is for fitness to only be close to one, or highly desirable, when all of the utilities are also closer to 1. If anyone utility value's desirability drops, then the overall fitness value should drop as well. The product method met these criteria best.

the header length (HL), the number of subcarriers (NC), and the length of the cyclic prefix (CP). This is shown in (4):

$$R_{U_{\text{New}}} = R_S \cdot \frac{k_{\text{New}}}{n_{\text{New}}} \cdot \frac{\text{PL}_{\text{New}}}{\text{PL}_{\text{New}} + HL} \cdot \frac{\text{NC}}{\text{NC} + \text{CP}} \cdot \text{MO}_{\text{New}}. \quad (4)$$

(3) To calculate the BER for a t-error correcting code (n, k), refer to [10]. Assuming that the throughput for both the coded and uncoded data stream is the same, the relationship between the probability of error between the coded and uncoded data is shown in (5):

$$P_{e_{\text{Coded}}} = \binom{n-1}{t} \left[P_{e_{\text{Uncoded}}} \left(\frac{k}{n} \cdot \frac{E_b}{N_0} \right) \right]^{t+1}. \quad (5)$$

However, for the system's case, what remains constant is the symbol rate and not the throughput. Therefore, for coded data, the throughput (R_U) is calculated from the symbol rate (R_S) as described in step (3). Then a tilda symbol rate (R'_S) is calculated as if this throughput were that of uncoded data.

(4) Now we can calculate E_b/N_0 from the new SNR, the tilda symbol rate (R'_S), the new modulation order (M) and the bandwidth (BW) as shown in (6):

$$E_b/N_0 = \text{SNR}_N + 10 \log_{10} \left(\frac{\text{BW}}{R'_S \cdot \log_2(M)} \right). \quad (6)$$

(5) To estimate the new BER, the system uses the formulas from [16] for Additive White Gaussian Noise (AWGN) channels.

(6) The PER can be estimated from the BER and the PL and HL (in bytes) through (7):

$$\text{PER} = 1 - (1 - \text{BER})^{8(\text{PL}+\text{HL})}. \quad (7)$$

(7) Finally, the new spectral efficiency is estimated by simply dividing the estimated throughput by the bandwidth.

3.3. CBR. The CBR keeps a list where it stores previous situations encountered in the past and what solution it came up with for that particular situation. A vector distance is calculated that quantifies how close the current situation is to the past situations within the case-base. We define similarity as a combination of this distance and the effectiveness of the solution, known as fitness, when it was originally applied. The cases are ranked by similarity and are filtered by a defined similarity threshold. The top case that meets this threshold is applied to the radio front end. If none falls in this threshold, then the top cases are seeded into the GA as initial parents as described in Section 3.2.

3.3.1. Case Structure. For each case, the CBR stores the following.

(i) ID: Memory is preallocated for the CBR list. Each case is initialized to dummy values. The ID indicates if valid values are stored in that entry: 0 for when nothing is stored there and 1 for when a there is a case.

(ii) Old configuration parameters store the values of the parameters before they were changed.

(iii) Old meters store the values of the meters that triggered the CE.

(iv) New configuration parameters store the value of the parameters after they were changed.

(v) Utility stores the new utilities and fitness after the configuration parameters were changed and the meters measured.

3.3.2. Retrieval. To decide whether or not a previous case should be used for the current situation, two metrics are calculated: distance and similarity. In general, a case from the library can be considered a certain vector distance away from the current situation. While this alone is sufficient to identify past experience that could provide a solution to the current situation, more resolution in the retrieval is required.

(a) Distance is a metric that shows how close or far a current situation is from the old configuration parameters and meters stored in the CBR list. This value is normalized between 0 and 1, where 0 represents two identical cases, and 1 represents completely opposite cases (if the values of the configuration parameters and meters of the current case and of the stored case are at opposite sides of the range values). To calculate this metric, the euclidean distance was used in (8):

$$d = \sqrt{\frac{\sum \left((\text{CurCase}_i - CB_i) / (\text{Range e}_{\max_i} - \text{Range e}_{\min_i}) \right)^2}{N}}, \quad (8)$$

where CurCase_i is the value of the configuration parameters and meters of the current case, CB_i is the value of the old configuration parameters and old meters stored in the CBR list, $\text{Range e}_{\max_i}$ and $\text{Range e}_{\min_i}$ are the maximum and minimum values of each configuration parameter and meter, respectively, and N is the total number of configuration parameters and meters.

(b) Similarity is a metric that combines distance (how close the current case is to the stored ones) and new fitness (how good the stored solution is). Several different approaches for this combination were considered where smaller distances and higher fitnesses led to higher similarities. Equation (9) shows a product of distance and fitness, (10) shows the distance raised to the fitness, (11) shows the fitness raised to the distance, and (12) shows the inverse distance raised to the fitness

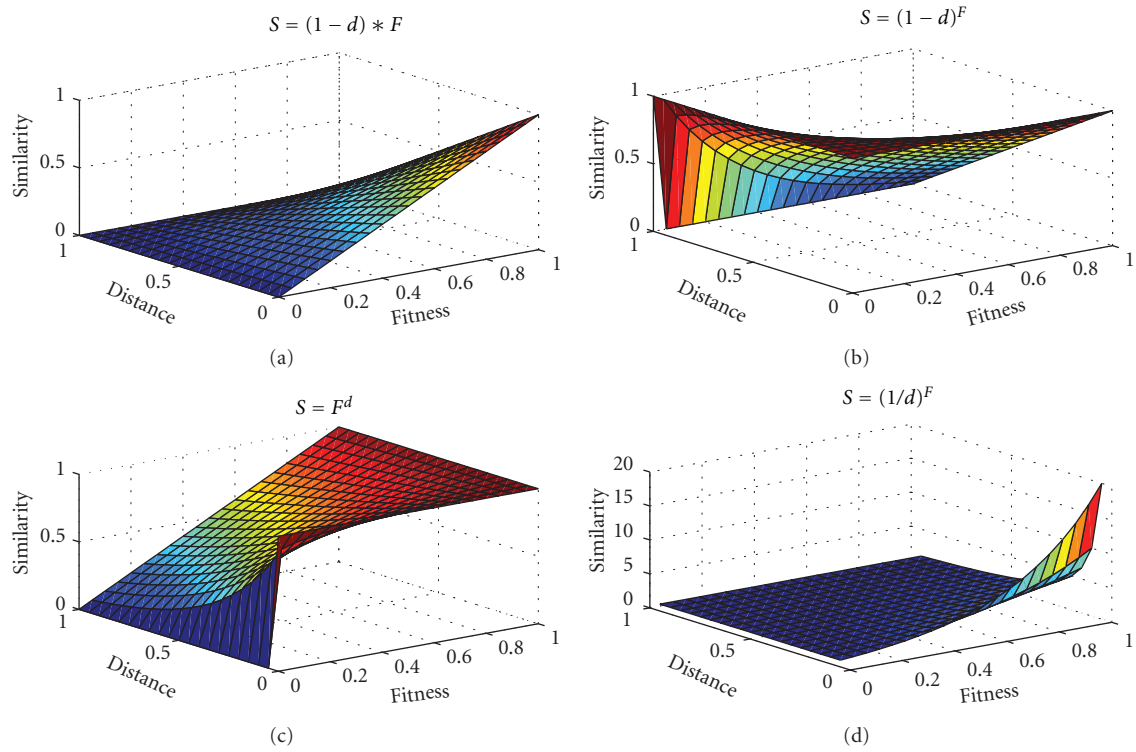

Figure 4: Similarity space— the similarity spaces of the four approaches of combining distance and fitness are shown. The goal is to achieve a high similarity when distance is small and fitness is high. Currently, the engine implements $S = (1 - d) * F$.

$$S = (1 - d) \cdot F, \tag{9}$$

$$S = (1 - d)^F, \tag{10}$$

$$S = F^d, \tag{11}$$

$$S = \left(\frac{1}{d}\right)^F, \tag{12}$$

where d and F are the distance and fitness metrics, respectively. In Figure 4 a comparison of the four possible similarity spaces are compared. Similarity (10) and (11) were discarded because the similarity metric should only have a high value when fitness is high and distance is low. Equation (12) was not used because it would present problems when distance was zero. It was also more complicated to normalize. Therefore, (9) was finally used for calculating similarity.

4. Configuration Parameters of the Cognitive Engine

The CE requires initialization of several elements before operations can begin. The GA requires definition of crossover rate, mutation rate, population size, and maximum generations. Similarly, the CBR requires definition of the the maximum case base size and similarity threshold for case retrieval. Finally, the defined PER threshold that will trigger engine engagement as well as the weightings of the configuration parameters used in calculating fitness are required. These are described below and listed in Table 1.

Table 1: Default configuration parameters of the CE.

Type	Parameter	Value
GA	Xover rate	0.7
	Mutation rate	0.01
	Population size	100
	Max generations	25
CBR	Case size	100
	Similarity threshold	100
Configuration parameter weights	PER	0.1
	Tx power	0.7
	Packet size	0.3
	Modulation	0.4
	Coding	0.5
Meter weights	SNR	0.5
	PER	0.9
	Spectral efficiency	0.3
	Throughput	0.3

(i) GA crossover rate: it is the probability that two parents, after being selected from the population in the GA, will crossover.

(ii) GA Mutation Rate: It is the probability that each bit of the GA population will get modified (changed from one to zero or from zero to one).

(iii) GA population size: it is the amount of chromosomes that the GA has in each generation.

(iv) GA Max generations: it is the maximum amount of iterations that the GA is allowed to make before coming up with a solution.

(v) Case-base size: its is the maximum amount of cases that will be stored.

(vi) Similarity threshold: it is a metric for the CE to decide whether to use the GA or the CBR. If the current case's similarity with any of the ones stored in the CBR is higher than this threshold, then it uses the CBR, and if it is lower, then it will use the GA.

(vii) Current PER threshold: if the measured PER is over this threshold, then the CE will get called.

(viii) Configuration parameter and meter weights: they are used for the calculation of fitness. The relative value of each weight with respect to the others will give each parameter more or less significance in the calculation of the value of fitness. This allows the GA to know how to compromise configuration parameter and meter values to try to find an optimum solution based on the goals.

5. System Model Implementation

The system is designed around the transfer of binary picture data from one node to the other under different environment scenarios. In order to accomplish the data transfer, a Universal Software Peripheral Device (USRP) was used in combination with the *liquid-DSP* software suite for software-based DSP [9]. The USRP is a flexible and affordable SDR platform often used in academic research. To extend this functionality, we implemented a feedback network on which to send control messages which collects real-time data. This section will describe, at a high level, the elements involved in the design of the parameter changes, the feedback collection, as well as certain design tradeoffs that must be made.

5.1. RF Hardware and SDR Interfacing. Ettus Research [11] is well known for producing the USRP which provides a flexible RF hardware front end on which to send and receive data. Among the different types of USRPs, there exists a distinction in the generations of these devices, each with a different bus speed for user data processing. For our system we chose to use the USRP 1 generation which is defined by the types of daughter cards supported along with its universal serial bus (USB) interface. Interfacing with the USB is a challenge and mechanisms for addressing this are discussed later. The USRP contains a single-core processor, however two threads from a multicore controlling laptop can share and interact with it. There is overhead for switching the USRP between threads as well as synchronization issues to consider. For this application, there is one dedicated thread from each USRP node and its accompanying laptop. In addition, there are other threads from the master controlling laptop that performance collection of meters, issues commands to start the receiver, and turns on or off the interference.

On top of the USRP board itself, a daughter card must be used to specifically define the RF parameters that it supports. Different daughter cards support different frequencies and bandwidths. For our system we chose the WRX daughter cards to support frequencies in the unlicensed TV bands. These higher frequencies are more susceptible to environmental conditions which provides a rich testing environment.

When implementing a CR system, one is limited by the amount of parameters supported by the DSP library. We feel that *liquid-DSP* [9] meets the requirements and is confirmed by [12] that it provides the most effective aspects of a communications system including a wide spectrum in each parameter. *liquid-DSP* provides many functionalities, however, we chose a subset of these to trade-off reducing the selection complexity of our algorithms while supplying a diverse solution set.

When our engine is used in combination with a lightweight DSP library, we are able to focus on accurate metric collection of the system. To facilitate ease of implementation, we used an 802.11 feedback network which is usually supported through an internal wireless network interface controller (NIC) in most recent laptops. By threading the processes of the radio applications, we are able to have the radio controller perform two essential tasks; data processing for the radio front end, as well as message parsing and taking the appropriate action. One thread is responsible for computing data to either go to or come from the USRP, while the other processes control messages to carry out the desired action. The most used commands for this system are meter collection, start-up and shut-down commands, parameter reconfiguration, and environmental control among others. Passing these messages around a light weight, custom, brokered architecture provides a reliable base for data collection, both on- and offline, in a multinode ad hoc network.

5.2. Software Control and Signal Processing. To interface with these messages at high level, a command structure was built around MathWork's MATLAB program. By defining MATLAB compatible functions, we make use of the lower level, C++ control code. Because C++ code cannot be used naturally by MATLAB, the use of the *MEX* interfaces was used to compile the system code into MATLAB usable functions. This way, complex matrix processing can be done efficiently in MATLAB, while low level socket code is still used to send and receive messages between separate programs. Different communication methods exist that send information between programs, such as file sharing, signals, and sockets. Socket communication was chosen for the ease of designing a single socket to be used in multiple instances, where the only redefinition needed would be changing the address and port number of the listening process. The network uses an ad hoc network, thus all nodes on the network have the potential to send information to one another, however, any given node only needs to send their messages to the *Broker*. This also provides the same interface for programs that are on the same computer, such as the transmitting program and the MATLAB control process.

The *Broker*'s main job is to accept messages from all nodes on the network and distribute them accordingly. This eliminates the need for an address included in every message as there are a relatively small number of messages that need to be sent throughout the system. Once these messages are initially defined, there is little need for extension, thus a more static approach to message passing. Using the *Broker* object, however, always for an easily extended network to add more nodes for further testing. Through the MATLAB/*MEX* interface, C++ code was used to interact with the *Broker* object as the CE. This is similar to other architectures such as CORBA, or the CROSS platform [13]. By using a properly layered and scalable control structure to handle back-end data processing, we are able to develop a high-level testing framework contained within MATLAB.

The initialization parameters for communications hardware are usually predefined and must be negotiated before the actual data transfer takes place. *liquid-DSP* offers support for real-time parameter augmentation in user payloads allowing us to focus on the CE in terms of optimizing data throughput at any point during the data transfer (bounded by at least every packet). This is possible by having a relatively short, robustly coded, and modulated header that contains the necessary information to demodulate and decode the user payload. Our system uses OFDM to transfer data which also incurs the need to consider the number of subcarriers and their frequency bandwidth allocations as listed in Table 5. This system is used instead of a single carrier signal due to its wide applicability in real world applications, such as long-term evolution as well as reporting more accurate network metrics for the type of noise we inject into the environment.

5.2.1. Observing the Meters. The meters provide the system with a means of classifying the transmitter's performance throughout the data transfer. By choosing appropriate meters we can aptly describe our system at any given point in time. The engine itself considers the following meters at the receiver node: received signal strength indicator (RSSI), signal-to-noise ratio (SNR), windowed packet error rate (PER), throughput, and spectral efficiency. Here, throughput and spectral efficiency are measured at the receiver and are used in contrast to the PER to measure performance.

5.2.2. Configurable Parameters. Based on each decision the engine makes, the engine needed an avenue to push new parameter settings to the radio front end. By adding the CE as a node on the ad hoc control network, we are able to effectively let the MATLAB engine communicate to the radios for metric collection, parameter adjustment, and other control messages. The engine considers parameters and their associated values listed in Table 2. We present just the minimum and maximum values here due to the discrete and static search space allowed in the system. Packet size and power are a continuous value within these ranges, while modulation and coding are discrete values. This distinction must be accounted for in the selection algorithms used, as our model has the possibility of coming up with a floating-point value for the discrete parameters. By properly segmenting a continuous search space, we can represent these results in a way that is transparent to mechanisms that rely on either a continuous (such as GA processing) or discrete (actually application of a new scheme to the radio) parameter.

Table 2: Ranges of reconfigurable SDR parameters.

Adjustable parameter	Min	Max
Transmission power	−20	0
Modulation	1 bps	6 bps
Coding	None	Reed-Solomon
Packet size	20	340

5.3. CE Triggers. The CE uses raw transmission data and collected metric data in a utilitarian style of abstraction. By considering the utility (i.e., usefulness) of the metric or configuration parameter value when making decisions we are able to consider not the raw value presented, but the usefulness of that value to the system. By measuring utility instead of the raw value themselves, we are optimizing each parameter's usefulness within the system, allowing for a more natural style of comparison. The engine, as of now, triggers on a predefined threshold of metric value, namely PER. For example, we implemented one trigger as a rise in PER above a rate of 10%. This can be changed to use its utility instead of a raw value to better represent the crossing of PER into an unusable area of operation. This is important to CE design and should be accounted for when considering case-base usage [9].

5.4. Metric Considerations. When collecting performance metrics, the system expects the data to reflect the current status of the transmitter's effectiveness for transmitting a file. In order to present a more instantaneous snapshot of the current situation, PER is presented on a 50 packet window. That is, for the last 50 received packets, the engine records the number of packets that failed the cyclic redundancy check (CRC). Given that a payload has failed this check, we can effectively discard the packet as incorrect data, recording the error. This is in contrast to the measured data rate, which is constantly averaged. Here, we allow the data rate to be averaged at the receiver as a measure of how effectively the transmitter is sending data. Thus, if the transmitter uses a high modulation, this will be reflected in the calculated data rate, however, if the power is too low, or it is simply too noisy an environment, then the PER should also reflect this in stark contrast to the amount of data being pushed through.

Measuring on an overall average, as well as a shorter window of considered metric samples has pros and cons as discussed above and are provided in a mix here for those reasons. Depending on the type of testing pursued, different methods for collecting performance meters are required. For example, a probing technique inspired by traditional design of experiments methodology required sending a specific number of packets repeatedly [14]. This is difficult in the engine's implementation due to the decoupling of the metric requests by the engine, and the amount of data, that is, an unspecified number of packets. By measuring the data

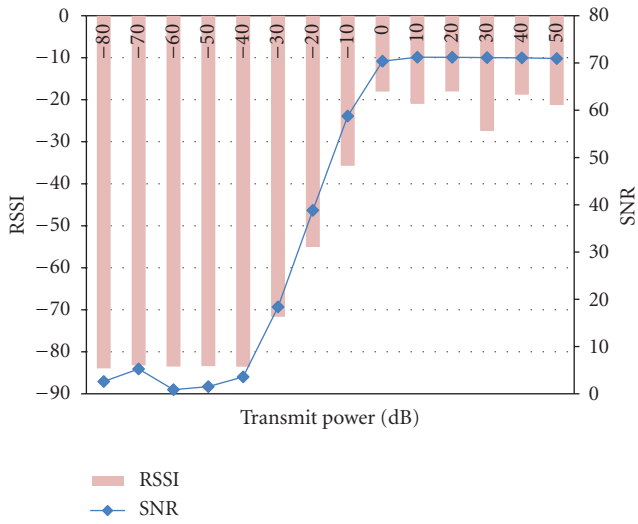

Figure 5: RSSI and SNR as the software gain is varied. RSSI is on the left axis and SNR is on the right axis. This illustrates the usable range of the transmit power parameter as between −40 dB and 0 dB.

sent over a specified number of packets on a whole, we can accurately provide results to the profiling mechanism. This is not intuitive for an instantaneous observation at any given time in the transmission in the case of the engine.

5.4.1. Configurable Parameter Considerations. Calibration of transmit power range is an important step prior to deployment. While the USRP allows one to set transmit power between −80 dB and 50 dB the radio does not operate well across this entire range. We need to define a more usable range that the CE can set the power to. A test was performed where transmit power gain was set and RSSI and SNR were measured during a data file transfer.

Because this range may be affected by many different things, including the environment itself, we thought it would be useful to test the effective range of powers available to the system within our context of a no-noise environment. The results, shown in Figure 5, illustrate that usable range is between −40 dB and 0 dB.

Note that there are actually two transmitter gains settable in the USRP. Typically one considers the software transmit gain setting as a tunable parameter of the USRP. There is also a hardware gain setting implemented by the Universal Hardware Drivers (UHD) alongside of the liquid interfaces. Due to the higher difficulty in setting the UHD gain setting, it is not a parameter that the CE has access to. It is set to a high level and all transmit power change are performed through the *liquid*-DSP interface.

Currently the engine selects from six defined modulation and three coding schemes. Packet size and transmit power have a much finer resolution. Overall, there are 56 potentially available modulation schemes in the *liquid* library. This limitation placed on available modulations was driven by the GA's need use of estimation models. The models used in the GA to estimate the fitness of potential solutions needed to account for all the available modulations. Therefore, to reduce complexity a select few modulations were used for each given bit per symbol range. These ranges are displayed in Table 3. A large number of coding schemes are also presented by *liquid*, but are not all used within the system. Two different codings are used for our GA's model, thus the system is limited to Hamming coding and no coding at all. Packet size is variable within the system to a predefined limit. Packet size is defined by header size and payload length. The payload length is user definable. We keep the size of the packets at least as long as the encoded header information, which is 33 bits and within the range of average packet size which usually does not exceed more than a few hundred bytes.

Table 3: Modulation schemes used for each bit per symbol setting.

Modulation depth (bps)	Scheme used
1	BPSK
2	QPSK
3	8-PSK
4	16-QAM
5	32-SQAM
6	64-QAM

5.5. Hardware Considerations. While there is great advantage to using a flexible USRP hardware board, there are still drawbacks in the interface. Previous work explored problems with the USRP 1′s USB interface and showed a poor performance benchmark for a USB connection. The USB interface limited the USRP's maximum output to 8 MSamples per second instead of the theoretical limitation of 128 MSamples per second [15]. The boards upper bound is limited by the digital to analog converters (DACs).

5.6. Experimental Test Environments. Data is sent over the air between two USRPs, sourcing data from a common picture file. A picture is used for demonstration purposes, but did not have to necessarily be used. Testing under different environments could possibly require a large amount of data thus we impose the requirement that the data sent should contain the payload length and the file offset in the header information. Should the header CRC fail, we cannot trust any data within the packet and is treated as a dropped packet. Given that more data is required, the transmitter starts sourcing the data from the beginning of the file, given that the end of file character is reached. This setup allows for variable payload sizes as well as a variable amount of packets to be sent.

Three different scenarios are created within our system to test it under different conditions. These signals are generated by varying the center frequency, the bandwidth, and overall power output of a third USRP. While the noise-generating node of this network is different in that it is a USRP 2, it generates junk data which we model as noise. These environments are modeled in three ways: no noise, a close by jamming signal, and a raise in the noise floor. The ambient environment lets the engine maximize performance as much as the environment will let it. The jamming signal uses a high peak power with low bandwidth to simulate a nearby signal causing interference, whereas the noise increase is simulated

Table 4: Interference environments.

Parameter	Narrow-band	Wide-band
Power (dB)	−10	−10
Bandwidth (kHz)	600	65
Center frequency (kHz)	910000	910150

Table 5: Static parameters within the transmission.

Parameter	Value
Header modulation	BPSK
Header coding	Hamming 128
Subcarriers	28
Cyclic prefix length	4
Bandwidth (kHz)	200
Hardware gain (dB)	0

through a wide-band, low powered signal across the center frequency we are transmitting.

Table 4 shows the differences in the two types of generated interference while Table 5 shows the configuration elements that we used for the transmitted signal.

6. Performance Results

6.1. Methodology and Results. The goal of the experimentation was to compare the performance of the CE against a noncognitive (no-CE) radio that is incapable of changing its initial configuration parameters. The no-CE configuration is equivalent to a traditional wireless devices that lack capability to adapt and learn. The wireless link is incapable of making a change to its initial configuration in reaction to interference.

It is acknowledged that adaptive communications does exist today, however most use rule-based decision making that follow the same course of action each time. A purely adaptive operation is easily exploited by malicious users. An anecdotal example is swatting a common house fly. Flies have adapted the capability to jump backwards before flying upwards in reaction to movements. This makes them difficult to swat, until one understands this behavior. One can exploit this adaptation by simply aiming the swatter slightly behind the fly. Similarly, if it is known that a radio simply increases transmit power in reaction to interference, it can still be easily jammed. However, a cognitive system that employed dynamic spectrum access may identify a new channel based on past experiences on which ones were most vacant.

The methodology consisted of first defining configuration parameter initial conditions, as listed in Table 6. Once defined, a data file was sent across the link in the presence of interference, wide-band interference, and narrow-band interference signals. For the tests, a total of 2000 packets are transmitted. However, because the packet size changes for the CE system, the exact amount of transmitted bits changes for each run.

The cognitive radio follows the decision cycle described in Section 3.1. By following this decision cycle, the CE identifies when packet error has fallen below a defined threshold.

Table 6: Configuration parameter initial settings.

	TX power (dBm)	Packet size	Modulation	Coding
CE	−20	400	64-QAM	No coding
No-CE	−15	300	32-QAM	No coding

Table 7: Mean values of the meters.

		SNR (dB)	PER	Spec. Eff.	Txput. (kbps)
Ambient	CE	20.8	0.0162	3.2	637.1
	No-CE	23.4	0.0111	3.6	718.9
Wide-band	CE	10.6	0.0147	1.0	191.4
	No-CE	5.2	1.0000	0.0	0.0
Narrow-band	CE	12.5	0.0076	1.8	367.8
	No-CE	7.5	1.0000	0.0	0.0

At this point, the engine engages either the CBR or the GA depending on the availability and similarity of past cases. The solution identified from either decision-making module is then implemented to the radio. An example of these decisions are shown in Figure 6 where transmit power, packet size, and modulation change. Results tabulated in Table 7 indicate that the cognitive engine is capable of mitigating interference conditions while the no-CE performance degrades.

6.1.1. Testing Environments

(i) Interferer off: the noise floor is simply that of the lab in which the test took place.

(ii) Wide-band noise floor increase: the overall noise floor, centered at the transmitted signal carrier frequency and with a bandwidth that is wider than the transmitted signal's, is raised.

(iii) Narrow-band noise spike: a high power noise spike with a much narrower bandwidth is inserted into the transmitted signal bandwidth.

To compare the CE system versus the no-CE system, it is assumed that the no-CE case is designed for the noise environment "Interferer off."

6.1.2. Configuration Parameter Initialization Values. The initial values of the transmitter configuration parameters (transmit power, packet size, modulation, and coding) need to be determined. For the case of the CE system, they will be set to values that are close to the most ideal case, that is, close to minimum power, close to maximum packet size, highest modulation order and no coding. For the case of the no-CE system, different tests were run with different combinations of configuration parameters to find a good set of them for the case of "Interferer off." This set of configuration parameters will also be used for the other types of environments to be tested. The initial parameter values for both systems can be seen on Table 7. For the CE system, the configuration parameter ranges are as the following.

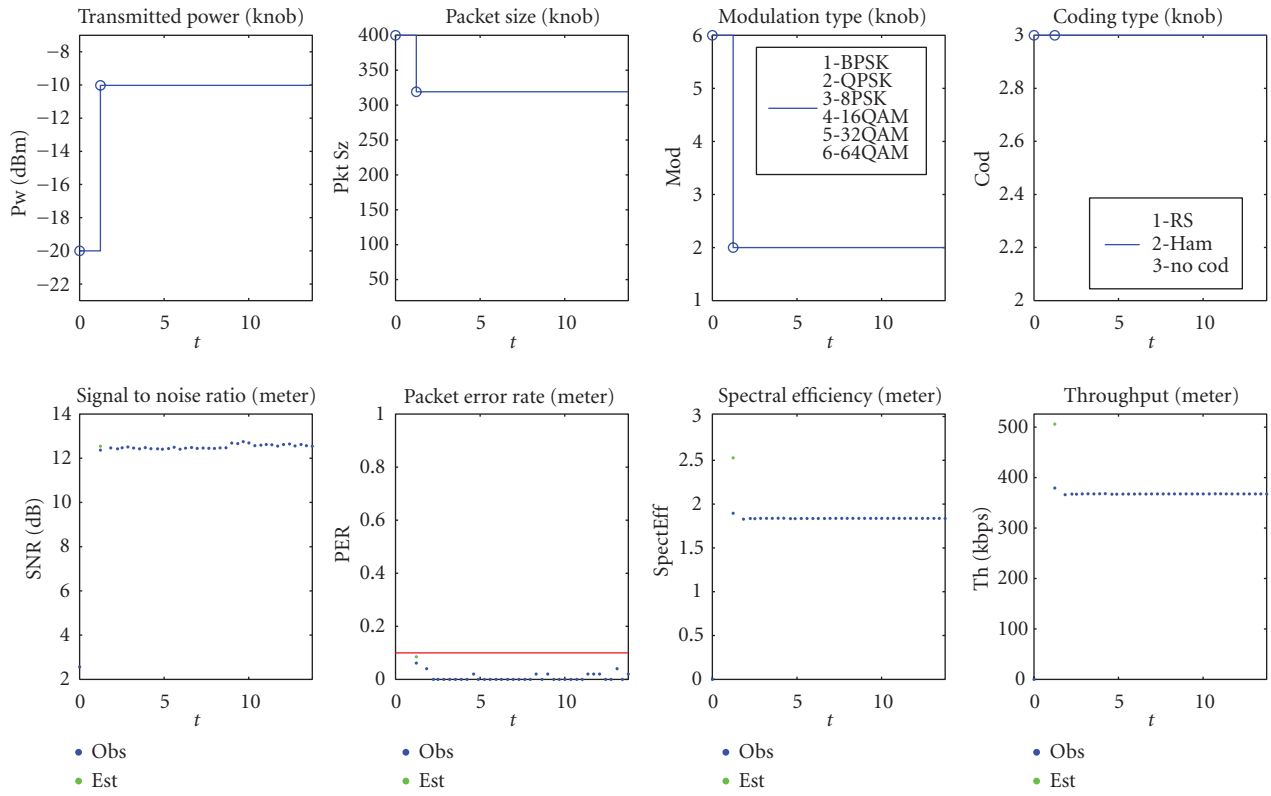

Figure 6: CE with narrow-band interference—in the presence of the narrow-band interference, the engine again raise transmit power and changed modulation to a more robust method. Packet size was able to remain higher than in the wide-band environment. Additionally, error coding was not required. This enabled a higher overall throughput to be achieved.

(i) Transmit power: (−20 dBm, −10 dBm).

(ii) Packet size: (20 bytes, 400 bytes).

(iii) Modulation: (BPSK, QPSK, 8-PSK, 16-QAM, 32-QAM, 64-QAM).

(iv) Coding: (hamming (7, 4), no coding).

Figure 6 shows how the configuration parameters and meters change during a run over time (in seconds) for the narrow-band interference environment. The results for the three environments, ambient, wide-band interference, and narrow-band interference are tabulated in Table 7. There are eight subplots in the figure.

(i) The top four show what the different values of the different configuration parameters are and what they are changed to when the CE gets called. For the case of no-CE, these values will remain constant over the whole run.

(ii) The bottom four show the values of the different meters at the time instances when they are measured. For this reason they are represented by dots. The blue dots are the meters the radio measured, while the green ones are what the GA estimated these values should be. On the PER graph, there is also a red line that represents the threshold for when the CE should get called. Therefore, if there is a blue dot in the PER graph that is over the red line, then the CE will get called (for the CE system).

On Table 7, the mean value of the meters for the CE system once it made its final decision versus the mean value of the meters over the entire run of the no-CE system are compared. As can be seen from the results, the performance of the CE system and the no-CE system for the case with the interferer off is similar. However, the CE system was able to find its solution on its own, while for the no-CE system it had to be designed and tested first. The no-CE system has a higher throughput and spectral efficiency at the cost of also having a higher transmission power than the CE system. For the other two scenarios (wide-band noise floor increase and narrow-band noise spike), the CE system was able to find a solution that allowed it to get data across the link, while the no-CE system could not operate under the new channel conditions, and therefore the PER was one. Note that the throughput for the no-CE system under the unfavorable channel conditions is 0 because the receiver could not synchronize with the received signal and could not measure it.

7. Current Limitations

7.1. Case-Base Searching. Case-base reasoning has been introduced in [16] for CR and has been used in different applications such as [15, 17] studies the impact that USRPs have on timing considerations for given networks

such as 802.11 and IEEE 802.15.4 sensor networks. The latency in these networks must be considered for a number of reasons, one of which is the clear to send/request to send protocol of 802.11. [15] shows that the USB transfer of information from the controlling computer introduces nonnegligible latency causing possible packet collisions. Similarly, given that a network has a relatively large number of nodes begin managed by a cognitive entity, an efficient cognition scheme is key. If the cognition for a wireless network introduces nonnegligible latencies, certain timing deadlines may not be met, thus causing problems within the system, such as the one described above. While this is not the only application, it is a simple example of why latency is an important issue and can be applied to a number of wireless systems that depend on computational deadlines to follow the protocol effectively.

By investigating further into the indexing schemes used for the case-base, we can improve performance of the searching algorithm used to find similar cases the engine has encountered in the past. Traditionally, the current case's similarity is calculated against each case in the case base, which can be done using the methods described in earlier sections. This scheme of similarity may be required for more structurally complex cases, but here, we can define a few simple, yet pivotal aspects of each case for fast access within the case-base. The approach being investigated eliminates the exponential dependency of the case-base size and the lookup time, allowing the case-base to grow large for more complex networks, and retain a faster access time throughout. The approach that is being investigated uses predefined thresholds for similarity relative to each parameter to eliminate the need for a similarity calculation, and uses these thresholds to index different cases within the data structure. By using the appropriate threshold for each parameter value, we can define what we determine to be similar enough in terms of distance on the vector's available search space. This is similar to [18] in that it separates the search space into binary tree decisions, however, we extend this to allow for more than two children and allow each node to index entries in the next dimension based on past cases seen. We also do not require any computation on deciding where to split the search space, as it is predefined before any case even enters the database.

To demonstrate the effectiveness of this indexing structure, Figure 7 demonstrates some preliminary results for average access times for both the traditional computation method along with a customize tree data structure to store cases. It is clear that traditional methods depended exponentially on the size of the case-base.

7.2. Estimation Methods. Currently, to estimate the BER for the GA, theoretical formulas for AWGN channels are used. However, it is well known that most real world environments do not follow this model, and that wireless signals will experience other effects such as fading. Therefore, the AWGN formulas will not accurately predict the performance of the system when changing its parameters to a different configuration.

The proposed solution to this problem is to implement a blind channel estimator, at the receiver, and to send this information back to the transmitter through the dedicated feedback channel. This new information would tell the transmitter what type of channel the system is in, so it could make better estimations of what the meters would be. this would enable the engine to find a more accurate solution for different types of coding.

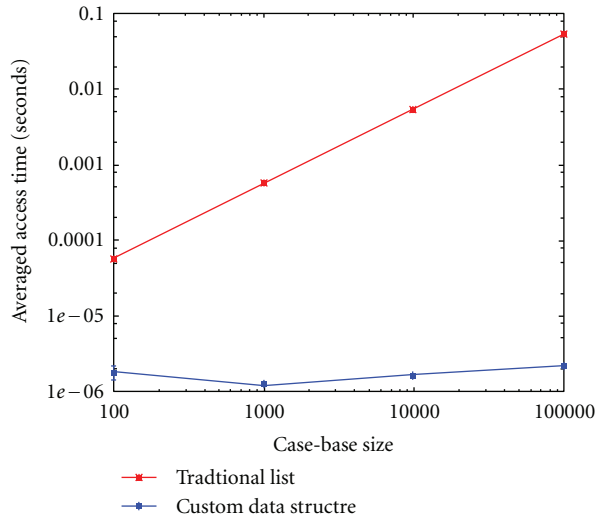

Figure 7: Average access time for the traditional storage approach versus a custom approach.

The designed system is essentially a way to perform link adaptation. In [19, section 2.2] an overview can be found of different techniques to adapt data rate and packet size. For data rate adaptation techniques, most of the described rely on some form of success rate or failure rate, a statistical approach to determine whether or not it should be changed. Other techniques use a measured SNR approach or a hybrid mechanism between the two. The described methods for adjusting packet size are based on estimating BER, using a Kalman filter or based on the success rate.

A method of adapting modulation and power is presented in [20]. It is a simple algorithm where if the target BER is not achieved, then the modulation order is progressively reduced. If the minimum modulation order still does not enable the BER to reach its desired target, then power is adjusted. It decides how much to increase the power by estimating the interference power and SINR, and then it increases the power to reach a target SINR. In [21] they adapt the modulation order of M-QAM for a Rayleigh block-fading channel. To do so, they estimate the channel; this channel estimation is not blind, so they have to use a training phase and a data phase. In [22–25], a CE is used to determine what MIMO technique and what modulation and coding to use based on feedback from the receiver sent back to the transmitter. However, their system is based on empirical observations, where a trial-and-error method is used and in which they balance exploration versus exploitation. This system would be different in two ways: an analytical model would be derived from the estimated channel information, and the GA would be used to find a close to optimal solution. To the best of our knowledge, the combination of a blind

channel estimator and a CE to find a close to optimal solution to an analytical model to fine-tune multiple configuration parameters has not yet been implemented.

8. Summary

This paper presented the implementation of a hybrid CBR-GA CR engine designed for link adaptation. The discussion included architecture, process flow, CBR similarity-based case retrieval, GA estimation methods, GA fitness definitions, and hardware/software lessons learned. The system was implemented on a USRP platform and tested in three interference environments. Performance results show that the engine is able to mitigate around interference when a non-CE fails. Limitations in the current architecture are discussed and new solutions to case searching and estimation methods were proposed.

We plan on extending this work in several ways to improve the engine's performance, such as expanding available transmission parameter support, using utility thresholds for engine triggering, simulating more accurate environments, as well as a more comprehensive study of proper case-base usage and a more accurate and dynamic channel model estimation for the GA. Most importantly, by implementing dynamic environments, we will be able to observe and tune the engine to react to dynamic spectrum access. While a frequency selection protocol has not been considered thus far in the system, we can at least expect to observe the engine's natural optimization. For example, if high spikes of power interfere with our transmission, by shortening packet length, the engine can observe better throughput in that only data sent at the time of the spike fails, instead of large packets that have error during the spikes, but good data otherwise. This provides one example of the engine reacting to the environment.

Acknowledgments

The research presented in this investigation was partially supported by the Federal Railroad Administration, Office of Research and Development, FRA Grant no. DTFR53-09-H-00021. Any opinions, findings, and conclusions or recommendations expressed in this publication are those of the author(s) and do not necessarily reflect the view of the Federal Railroad Administration and/or US DOT. This work was also partially supported by the Institute for Critical Technology and Applied Science (ICTAS) of Virginia Tech.

References

[1] A. He, J. Gaeddert, K. Bae et al., "Development of a case-based reasoning cognitive engine for IEEE 802.22 wran applications," *ACM SIGMOBILE Mobile Computing and Communications Review*, vol. 13, no. 2, pp. 37–48, 2009.

[2] J. Mitola, *Cognitive radio—an integrated agent architecture for software defined radio*, Ph.D. dissertation, Royal Institute of Technology (KTH), 2000.

[3] A. Amanna and J. H. Reed, "Survey of cognitive radio architectures," in *Proceedings of the IEEE SoutheastCon Conference: Energizing Our Future*, pp. 292–297, Charlotte, NC, USA, March 2010.

[4] C. J. Rieser, *Biologically inspired cognitive radio engine model utilizing distributed genetic algorithms for secure and robust wireless communications and networking*, Ph.D. dissertation, Virginia Tech, Blacksburg, Va, USA, 2004.

[5] Y. Zhao, J. Gaeddert, L. Morales, K. Bae, J.-S. Um, and J. H. Reed, "Development of radio environment map enabled case- and knowledge-based learning algorithms for IEEE 802.22 wran cognitive engines," in *Proceedings of the 2nd International Conference on Cognitive Radio Oriented Wireless Networks and Communications (CrownCom '07)*, pp. 44–49, Orlando, Fla, USA, August 2007.

[6] A. Aamodt and E. Plaza, "Case-based reasoning: foundational issues, methodological variations, and system approaches," *AI Communications*, vol. 7, no. 1, pp. 39–59, 1994.

[7] A. MacKenzie, J. Reed, P. Athanas et al., "Cognitive radio and networking research at virginia tech," *Proceedings of the IEEE*, vol. 97, no. 4, pp. 660–686, 2009.

[8] D. Goldberg, *Genetic Algorithms in Search Optimization, and Machine Learning*, Addison-Weslet Publishing, 1989.

[9] J. D. Gaeddert, *Facilitating wireless communications through intelligent resource management on software-defined radios in dynamic spectrum environments*, Ph.D. dissertation, Virginia Polytechnic Institute & State University, Blacksburg, Va, USA, 2011.

[10] B. P. Lathi, *Modern Digital and Analog Communication Systems*, Oxford University Press, 3rd edition, 1998.

[11] M. Ettus, "Ettus research," 2010, http://www.ettus.com.

[12] T. Newman and J. Evans, "Parameter sensitivity in cognitive radio adaptation engines," in *Proceedings of the 3rd IEEE Symposium on New Frontiers in Dynamic Spectrum Access Networks (DySPAN '08)*, pp. 1–5, Chicago, Ill, USA, October 2008.

[13] B. Hilburn, "Cognitive radio open source system," 2010, http://cornet.wireless.vt.edu/trac/wiki/Cross.

[14] A. Amanna, D. Ali, M. Gadhiok, M. J. Price, and J. H. Reed, "Statistical framework for parametric optimization of cognitive radio systems," in *Proceedings of the Software Defined Radio Forum Technical Conference and Product Exposition (SDR '11)*, 2011.

[15] T. Schmid, O. Sekkat, and M. B. Srivastava, "An experimental study of network performance impact of increased latency in software defined radios," in *Proceedings of the 2nd ACM International Workshop on Wireless Network Testbeds, Experimental Evaluation and Characterization (WinTECH '07)*, pp. 59–66, ACM, New York, NY, USA, 2007.

[16] T. W. Rondeau, *Application of artificial intelligence to wireless communications*, Ph.D. dissertation, Virginia Polytechnic Institute & State University, Blacksburg, Va, USA, 2007.

[17] A. He, J. Gaeddert, K. K. Bae et al., "Development of a case-based reasoning cognitive engine for ieee 802.22 wran applications," *SIGMOBILE Mobile Computing and Communications Review*, vol. 13, pp. 37–48, 2009.

[18] S. Wess, K. Dieter Althoff, and G. Derwand, "Using k-d trees to improve the retrieval step in case-based reasoning," in *Proceedings of the Selected papers from the 1st European Workshop on Topics in Case-Based Reasoning (EWCBR '93)*, S. Wess, K. Dieter Althoff, and M. M. Richter, Eds., pp. 167–181, Springer, London, UK, 1993.

[19] N. C. Tas, *Link adaptation in wireless networks: a cross-layer approach*, Ph.D. dissertation, University of Maryland, College Park, Md, USA, 2010.

[20] K. Jayanthi, *Some investigations on quality improvement using link adaptation techniques in cellular mobile networks*, Ph.D. dissertation, Pondicherry University, 2010.

[21] A. Soysal, S. Ulukus, and C. Clancy, "Channel estimation and adaptive m-qam in cognitive radio links," in *Proceedings of the IEEE International Conference on Communications (ICC '08)*, pp. 4043–4047, Beijing, China, May 2008.

[22] H. Volos, C. Phelps, and R. Buehrer, "Initial design of a cognitive for mimo systems," in *Proceedings of the SDR Forum Technical Conference and Product Exposition (SDR '07)*, 2007.

[23] H. Volos, C. Phelps, and R. Buehrer, "Physical layer cognitive engine for multi-antenna systems," in *Proceedings of the IEEE Military Communications Conference (MILCOM '08)*, pp. 1–7, San Diego, Calif, USA, November 2008.

[24] H. Volos and R. Buehrer, "Cognitive engine design for link adaptation: an application to multi-antenna systems," *IEEE Transactions on Wireless Communications*, vol. 9, no. 9, pp. 2902–2913, 2010.

[25] H. Volos and R. Buehrer, "Robust training of a link adaptation cognitive engine," in *Proceedings of the IEEE Military Communications Conference (MILCOM '10)*, pp. 1442–1447, San Jose, Calif, USA, November 2010.